

**CYTOSKELETON ASSEMBLY AT ENDOTHELIAL
CELL-CELL CONTACTS IS REGULATED BY
 α II-SPECTRIN/VASP COMPLEXES**



DISSERTATION ZUR ERLANGUNG DES
NATURWISSENSCHAFTLICHEN DOKTORGRADES
DER BAYERISCHEN JULIUS-MAXIMILIANS-UNIVERSITÄT WÜRZBURG

vorgelegt von

Peter Michael Benz

aus

Scherzingen

Würzburg 2007

Eingereicht am: _____

bei der Fakultät für Chemie und Pharmazie.

1. Gutachter: Prof. Dr. Ulrich Walter

2. Gutachter: Prof. Dr. Utz Fischer

der Dissertation.

1. Prüfer: Prof. Dr. Ulrich Walter

2. Prüfer: Prof. Dr. Utz Fischer

3. Prüfer: PD. Dr. Thomas Renné

des öffentlichen Promotionskolloquiums.

Tag des öffentlichen Promotionskolloquiums: _____

Doktorurkunde ausgehändigt am: _____

Die vorliegende Arbeit wurde in der Zeit von Februar 2004 bis Mai 2007
in der DFG Nachwuchsgruppe von PD. Dr. Thomas Renné am
am Institut für Klinische Biochemie und Pathobiochemie
der Bayerischen Julius-Maximilians-Universität Würzburg angefertigt.

Teile der im Rahmen dieser Arbeit erzielten Ergebnisse sind bereits veröffentlicht worden:

Publikationen

Benz, P.M., Blume, C., Moebius, J., Oschatz, C., Schuh, K., Sickmann, A., Walter, U., Feller S. M., and Renné, T. (2007) Cytoskeleton assembly at endothelial cell-cell contacts is regulated by α II-spectrin/VASP complexes. *J Cell Biol.* In revision.

Benz, P.M., Feller S.M., Walter, U., and Renné, T. (2007) Prostaglandin-induced VASP phosphorylation controls α II-Spectrin break down in apoptotic cells. *Int Immunopharmacol.* In press.

Blume, C., Benz, P.M., Walter, U., Ha, J., Kemp, B.E., and Renné, T. (2007) AMP-activated Protein Kinase Impairs Endothelial Actin Cytoskeleton Assembly by Phosphorylating Vasodilator-stimulated Phosphoprotein. *J Biol Chem*, 282, 4601-4612.

Johne, J., Blume, C., Benz, P.M., Pozgajova, M., Ullrich, M., Schuh, K., Nieswandt, B., Walter, U., and Renné, T. (2006) Platelets promote coagulation factor XII-mediated proteolytic cascade systems in plasma. *Biol Chem*, 387, 173-178.

Posterpräsentationen und Vorträge

Benz, P.M., Blume, C., Schuh, K., Feller, S. M., Sickmann, A., Walter, U., and Renné, T.

The cAMP-dependent Interaction of Vasodilator-stimulated phosphoprotein (VASP) with alpha-II Spectrin Regulates Cortical Cytoskeleton Formation in Endothelial Cells. Poster bei der 3. Jahrestagung der Deutschen Vereinten Gesellschaft für Klinische Chemie und Laboratoriumsmedizin, Mannheim, Germany, October 1-4.2006.

Benz, P.M., Blume, C., Schuh, K., Feller, S. M., Sickmann, A., Walter, U., and Renné, T.

Interaction of VASP with α II-Spectrin is Crucial for the cAMP-Dependent Regulation of Cortical Actin Dynamics. SFB 688 Symposium, Würzburg, Germany, Mai 18th 2006.

Benz, P.M., Schuh, K., Blume, C., Feller, S.M., Sickmann, A., Walter, U., and Renné, T.

Interaction of Vasodilator-stimulated phosphoprotein (VASP) with α II-Spectrin is Crucial for the cAMP-Dependent Regulation of Cortical Actin Dynamics. Poster at the 100th Annual Meeting of the American Society for Biochemistry and Molecular Biology, San Francisco, U.S.A., April 1-5.2006. Abstract in *FASEB J.* 2006; 20:A103.

Blume, C., Schuh, K., Benz, P.M., Walter, U., and Renné, T.

In vivo modulation of vasodilator stimulated phosphoprotein functions by phosphorylation. International Conference of cGMP Generators, Effectors and Therapeutic Implications, Potsdam, Germany. June 10–12. 2005. Abstract in *BMC Pharmacol.* 2005; 5 (Suppl 1), P4.

Blume, C., Schuh, K., Benz, P.M., Walter, U., and Renné, T.

Differential phosphorylations of the vasodilator stimulated phosphoprotein (VASP) regulate actin-dynamics and subcellular targeting. 46th Spring Meeting of the German Society of Experimental and Clinical Pharmacology and Toxicology, Mainz, March 15-17.2005. Abstract in *Naunyn-Schmiedeberg's Archives of Pharmacology.* 2005; 371, R50.

I would like to thank ...

Prof. Dr. Ulrich Walter for giving me the possibility to do my PhD research in his institute, for his constant interest in my work, and the opportunity to present my results at the "Centennial Meeting of the American Society of Biochemistry and Molecular Biology (ASBMB)" in San Francisco, April 2006.

Prof. Dr. Utz Fischer who as a member of the Faculty of Chemistry and Pharmacology kindly accepted to examine this thesis.

PD. Dr. Thomas Rennè for his continuous support of my project, the excellent working conditions, and the freedom to develop my own ideas and solutions to a problem.

Prof. Dr. Kai Schuh for his patience answering all my "hypothetical" questions, the helpful discussion of experimental problems and results, and the legendary meetings at Burger King.

Constanze Blume for the never-ending supply of VASP-mutants and her logistic skills, which made the daily lab-life so much easier.

Dr. Albert Sickmann and Dr. Jan Moebius for the mass spectrometry-based identification of VASP-binding proteins.

Dr. Stephan Feller for his help with all SH3-related problems, the peptide scan arrays, and the critical and time-consuming discussion of our manuscript.

All members of the institute who assisted me and who contributed to the very pleasant working atmosphere. In particular I thank Monika Kuhn for help with VASP affinity columns, Melanie Ullrich for help with FACS-analyses, Chris Oschatz for the skin vascular leakage assay, Evi Reichert for taking care of my mice, and Elfi Walter for always being around to help as a good fairy.

My parents for their advice, encouragement, and financial support.

... and especially my wife Katrin and my daughter Sarah for their support, patience, and never-ending love. You are my light if it is dark and my rock in stormy times.

To Katrin and Sarah

TABLE OF CONTENTS

I INTRODUCTION	1
1. Actin Dynamics and Actin-Binding Proteins	1
2. cAMP/PKA Signaling Pathways	5
3. Endothelial Cells and Interendothelial Junctions.....	8
4. Cytoskeletal Organization in Sparse and Confluent Endothelial Cells	10
5. Ena/VASP Proteins	11
6. Spectrins	13
7. SH3 Domains	16
8. Aims of the Study	18
II MATERIALS AND METHODS	19
1. Plasmids.....	19
2. Protein Purification, Coupling, and Phosphorylation	21
3. Antibodies and Fluorescent Phalloidin	22
4. Cell Culture.....	23
5. 2D-PAGE Proteome Analysis of VASP-AAA- and VASP-DDE-Binding Proteins.....	24
6. Immunoprecipitations and GST Pull-Down Assays.....	25
7. Immunocytochemistry	26
8. Peptide and Alanine Substitution Scans	26
9. Endothelial Permeability Assays	28
10. Skin Vascular Leakage Assay.....	28

III RESULTS.....	30
1. α -Spectrin (SPCN) is a New VASP-Binding Protein in Endothelial Cells	30
2. VASP Interacts with SPCN at sites of Interendothelial Adhesion.....	33
3. The SPCN SH3 Domain Specifically and Directly Interacts with VASP	35
4. The SPCN SH3 Domain Binds to the Triple GP ₅ Motif of VASP	37
5. VASP Prolines 177, 178, and 179 are Crucial for the SPCN/VASP Interaction.....	38
6. PKA-Mediated Phosphorylation of VASP at S157 Inhibits its Interaction with SPCN	40
7. Phosphomimetic Substitution of S239 and T278 does not Influence the SPCN/VASP Interaction.....	40
8. SPCN Colocalizes with S157 VASP but not with Phospho-S157 VASP in Contacting Endothelial Cells.....	43
9. Ectopic Expression of SPCN_SH3 Recruits VASP and Promotes Cortical Actin Formation	47
10. Function of SPCN/VASP Complexes for Endothelial Barrier Function.....	51
IV DISCUSSION.....	54
1. Spectrin/VASP Assemble Perijunctional Multi-Protein Complexes	54
2. SPCN SH3 Domain Mediates Interaction with VASP.....	57
3. Regulation and Functional Importance of SPCN/VASP Complexes	59
4. Concluding Remarks and Future Perspectives	62
V SUMMARY	63
VI ZUSAMMENFASSUNG.....	64
VII ABBREVIATIONS	65
VIII REFERENCES	66
IX CURRICULUM VITAE	74

I INTRODUCTION

1. Actin Dynamics and Actin-Binding Proteins

Actin is an essential component of the cytoskeleton and the most abundant protein in virtually all eukaryotic cells. The actin cytoskeleton functions in highly diverse processes such as cell division, generation and maintenance of cell morphology and polarity, cell motility and contractility, and cell-cell and cell-matrix adhesion. Many of actin's cellular roles revolve around its ability to polymerize and depolymerize rapidly in response to extracellular signals. Therefore, understanding the molecular mechanisms and signaling pathways underlying cellular actin dynamics remains a major focus of ongoing research (Nicholson-Dykstra et al., 2005).

Actin is a 43 kDa monomeric globular protein (G-actin) that can polymerize into thin, double-helical actin filaments (F-actin). The initial step in actin filament assembly, the formation of di- and trimers (nucleation), is unfavorable and occurs slowly. Subsequent filament elongation is favorable and fast, resulting in a polar actin filament, in which all monomers are oriented into the same direction. Monomers are polymerized faster to the "barbed" or "plus" end of the filament than to the "pointed" or "minus" end. Actin is an ATPase. Actin monomers bind ATP tightly and hydrolyze the nucleotide upon addition to the filament. However, ATP hydrolysis is not essential for fiber formation and occurs with considerable lag after polymerization. Dissociation of the γ -phosphate group (Pi) is even slower than ATP hydrolysis, so that the ADP-Pi-actin is a relatively long-lived intermediate in freshly assembled actin filaments. ATP hydrolysis and Pi release affect filament stability, as ADP-actin subunits dissociate faster from the barbed end than ATP-actin subunits. These kinetics lead to a very slow treadmilling of actin subunits from the barbed to the pointed end. ATP hydrolysis and Pi dissociation in the filament are essential to maintain treadmilling and appear to be an internal timer that indicates the age of the actin filament (Nicholson-Dykstra et al., 2005; Pollard and Borisy, 2003) (Figure I-1, central image).

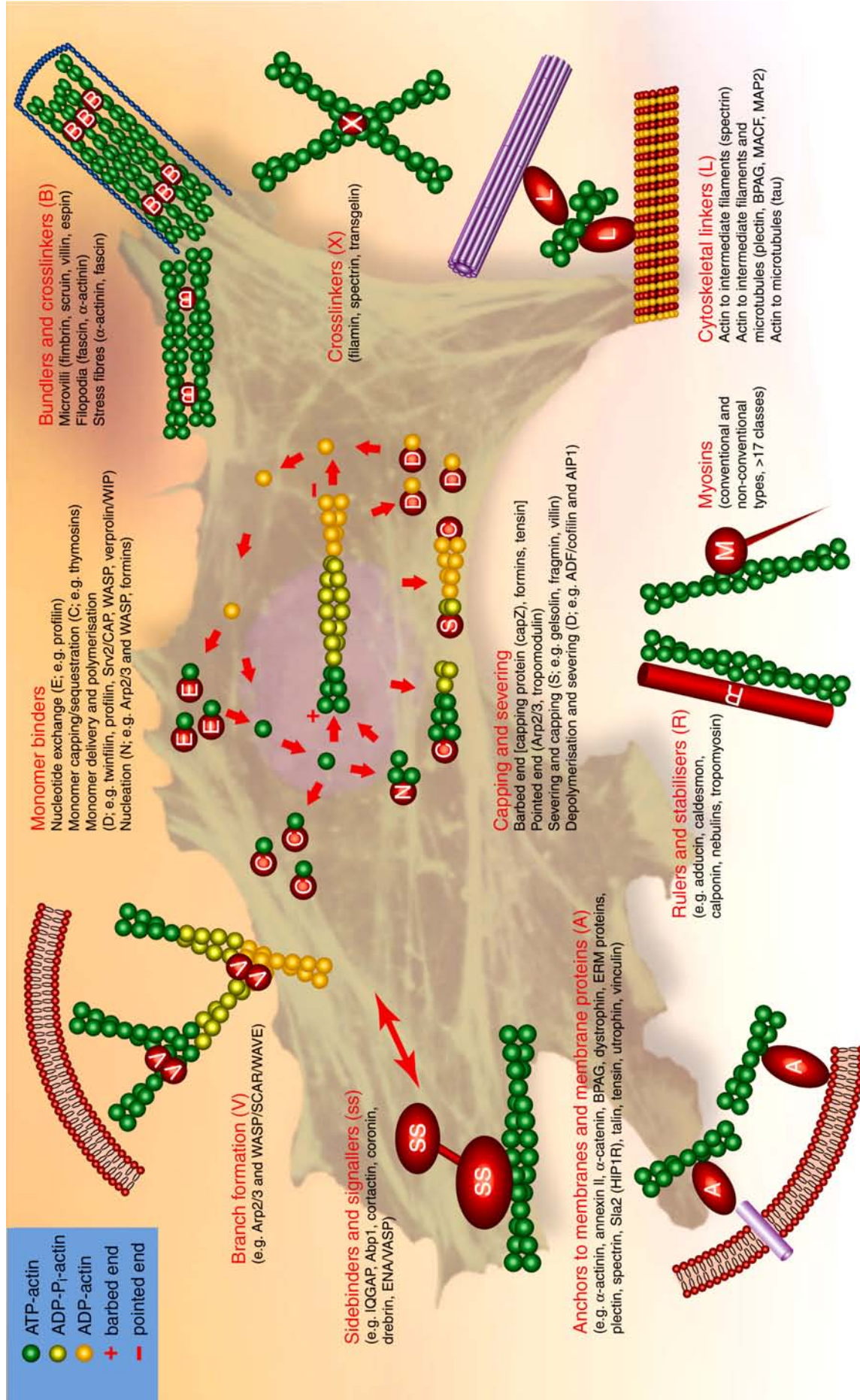
In cells, dynamic assembly and spatial organization of actin filaments is precisely regulated by a large repertoire of over 100 actin-binding proteins (ABPs, Revenu et al., 2004; Winder and Ayscough, 2005) (Figure I-1, peripheral images). These can be grouped into three classes. The first class of ABPs is comprised of proteins that regulate F-actin assembly and disassembly.

The actin-related protein (Arp) 2/3 complex and formins promote actin filament nucleation and generate short branched or long unbranched actin fibers required for cell movement and cell polarity, respectively. The capping proteins capZ and tropomodulin seal the barbed or pointed ends of actin filaments, thereby controlling filament length. Binding of actin-depolymerizing factor (ADF)/cofilin to ADP-actin promotes filament severing and dissociation of ADP-actin from the pointed end of the filament. In contrast, binding of tropomyosin and nebulin along the filament protects F-actin against spontaneous or ADF/cofilin-mediated depolymerization and determines its length. By simultaneous binding to F-actin and components of the actin polymerization machinery and adhesion complexes, respectively, vasodilator-stimulated phosphoprotein (VASP) and cortactin link signaling pathways to actin fiber remodeling. G-actin binding proteins profilin and cyclase-associated protein (CAP) facilitate the nucleotide exchange of ADP for ATP after release of ADP-actin from the fiber's pointed end and deliver the monomer to the barbed end for a new round of actin treadmilling. In contrast, thymosins sequester and cap G-actin thereby preventing incorporation into actin filaments. This results in a large pool of actin monomers that can be released to allow rapid filament extension. The second class of ABPs are proteins that regulate higher-order F-actin structures. The organization of actin into networks and higher-order structures is crucial for specialized cellular functions such as adhesion and locomotion. Except for the dendritic branches in lamellipodia, which are formed by the Arp2/3 complex, all other higher-order F-actin structures are formed by actin bundling and actin crosslinking proteins. Actin bundling is the parallel or antiparallel alignment of F-actin into linear arrays (stress fibers, bristles, microvilli, stereocilia, and filopodia). It is mediated by proteins that either contain two or more discrete actin-binding domains within their sequence (e.g. fimbrin) or by multimeric proteins that contain only a single actin-binding site per subunit (e.g. α -actinin). Depending on the spacing between the actin-binding motifs, tight or more loosely ordered F-actin bundles are formed, which are found in microvilli or filopodia and stress fibers, respectively. The arrangement of actin filaments into orthogonal arrays is mediated by mono- or multimeric actin crosslinking proteins that also contain multiple actin binding domains. However, as in dimeric filamin or tetrameric spectrin complexes, these motifs are separated by

long flexible spacers, which allow perpendicular organization of actin fibers. The third class of ABPs are proteins that utilize F-actin as structural framework to produce movement, force, and cell integrity. Myosins, ATP-dependent motor proteins, use actin as track to move other proteins (including actin filaments) and vesicles. Annexin and vinculin link actin fibers to the plasma membrane, either directly or by binding to cell adhesion receptors, respectively. Interaction with other cytoskeletal elements is mediated by plectin, which links actin fibers to microtubules and intermediate filament. Among the plethora of ABPs, spectrins accomplish diverse actin-related functions. Spectrin-multimers crosslink actin fibers thereby creating a higher-order two-dimensional network (class II). However, they also link actin filaments to the plasma membrane and intermediate filaments and may therefore be considered class III ABPs (Revenu et al., 2004; Winder and Ayscough, 2005) (Figure I-1, peripheral images).

Figure I-1. Actin Dynamics and Actin-Binding Proteins (see next page)

(Central image) Actin Dynamics. After slow filament nucleation, the actin filament elongates rapidly when ATP-actin monomers are incorporated at the barbed end. As the filament matures, actin subunits hydrolyze their nucleotides gradually and release the phosphate group Pi with even more delay. ADP-actin monomers dissociate from the pointed end and undergo nucleotide exchange to generate ATP-actin monomers that can be added to the filament's barbed end for a new round of polymerization. In the steady state, actin monomers are added at the barbed end (+) and released from the pointed end (-), but there is no net change in filament length (actin treadmilling). (Peripheral images) Actin-binding proteins. *In vivo*, dynamic assembly and spatial organization of actin filaments is tightly regulated by a plethora of actin-binding proteins that promote G-actin nucleotide exchange and/or delivery and polymerization (E), actin filament nucleation (N), stabilization and sizing (R), capping (C), severing (S), and depolymerization (D). Sidebinders and signallers (SS) link actin dynamics to signaling pathways. ABPs that regulate higher-order F-actin structures include actin filament branching (V), bundling (B), and crosslinking (X) proteins. Myosins (M), cytoskeletal linkers (L), and membrane anchoring proteins (A) utilize F-actin as structural framework to produce movement, force, and cellular integrity. Figure taken from (Winder and Ayscough, 2005).



2. cAMP/PKA Signaling Pathways

The cAMP signaling pathway is one of the most extensively studied signal transduction cascades. Typically, signal transduction begins when an extracellular first messenger (neurotransmitter, hormone, or drug) binds to its cognate G-protein coupled receptor (GPCR). GPCRs are a seven-helix transmembrane proteins that are associated with a heterotrimeric guanine nucleotide-binding protein (G protein) composed of an α -, β -, and γ -subunit. Whereas $G\beta$ and $G\gamma$ form a stable complex, $G\alpha$ is part of the complex only in its inactive, GDP-bound form. When $G\alpha$ is activated by the catalytic GDP-GTP exchange activity of the ligand-bound receptor, $G\alpha$ dissociates from the $G\beta\gamma$ dimer. Both complexes dissociate from the GPCR and initiate or inhibit intracellular signaling cascades, while the receptor is able to activate the next G protein. $G\alpha$ -subunits of the stimulatory subtype ($G\alpha_s$) activate the membrane-bound adenylyl cyclase (AC), which converts ATP to cAMP. GPCR-mediated downstream signalling is terminated by the intrinsic GTPase activity of the $G\alpha$ subunit, which hydrolyses GTP to GDP and the overall effect is the generation of cAMP at the cytoplasmic face of the plasma membrane. cAMP binds to and activates cyclic-nucleotide-gated channels and guanine nucleotide-exchange proteins activated by cAMP (EPACs). cAMP, which is not bound to signal transduction proteins, is rapidly hydrolyzed by phosphodiesterases (PDEs). The principal intracellular target for cAMP, however, is the cAMP-dependent protein kinase (PKA). The PKA holoenzyme is a tetramer that consists of two catalytic (C) subunits, which are kept in an inactive conformation by a homodimer of regulatory (R) subunits. When cAMP binds to the regulatory PKA subunits, the holoenzyme dissociates. This liberates the catalytic subunits. Active PKA is a protein kinase with broad substrate specificity, which phosphorylates serine/threonine residues in the consensus sequence K/R-R-X-S/T- Φ (where Φ tends to be a hydrophobic residue). Prominent PKA substrates are the actin-binding protein vasodilator-stimulated phosphoprotein (VASP) or the transcription factor cAMP response element binding protein (CREB) (Kennelly and Krebs, 1991; Sechi and Wehland, 2004; Shaywitz and Greenberg, 1999; Wong and Scott, 2004) (Figure I-2).

Because cAMP-elevating stimuli may trigger diverse physiological processes, it is necessary to control cAMP/PKA signaling in a precisely spatially and temporally confined manner. The molecular basis of cAMP signaling compartmentalization is the organization of cAMP-signal transduction components in specific subcellular microdomains and the differential activation of these proteins (Colledge and Scott, 1999; Schwartz, 2001). The most important mechanism, which regulates cAMP signaling specificity, involves targeting of PKA-holoenzymes to distinct intracellular compartments through association with A-kinase-anchoring proteins (AKAPs). AKAP-mediated PKA targeting brings the enzyme in proximity to defined physiological substrates and thereby triggers specific phosphorylation events. Perhaps the most biologically significant property of AKAPs is their ability to colocalize PKA with other protein kinases, phosphatases, and PDEs that counterbalance kinase activity. This regulates the phosphorylation of distinct cellular targets and integrates diverse signaling pathways within a single multivalent signal transduction complex (Wong and Scott, 2004). Today, increasing evidence argues for a particularly important role of AKAP-based complexes in cytoskeletal signaling events (Diviani and Scott, 2001; Scott, 2003). One example for such AKAPs is WAVE-1, a member of the Wiskott-Aldrich syndrome protein (WASP) protein family that simultaneously binds to PKA and Abl tyrosine kinase, and coordinates cytoskeleton dynamics by coupling the small GTPase Rac to the actin filament nucleation activity of the Arp2/3 complex (Diviani and Scott, 2001; Westphal et al., 2000) (Figure I-2).

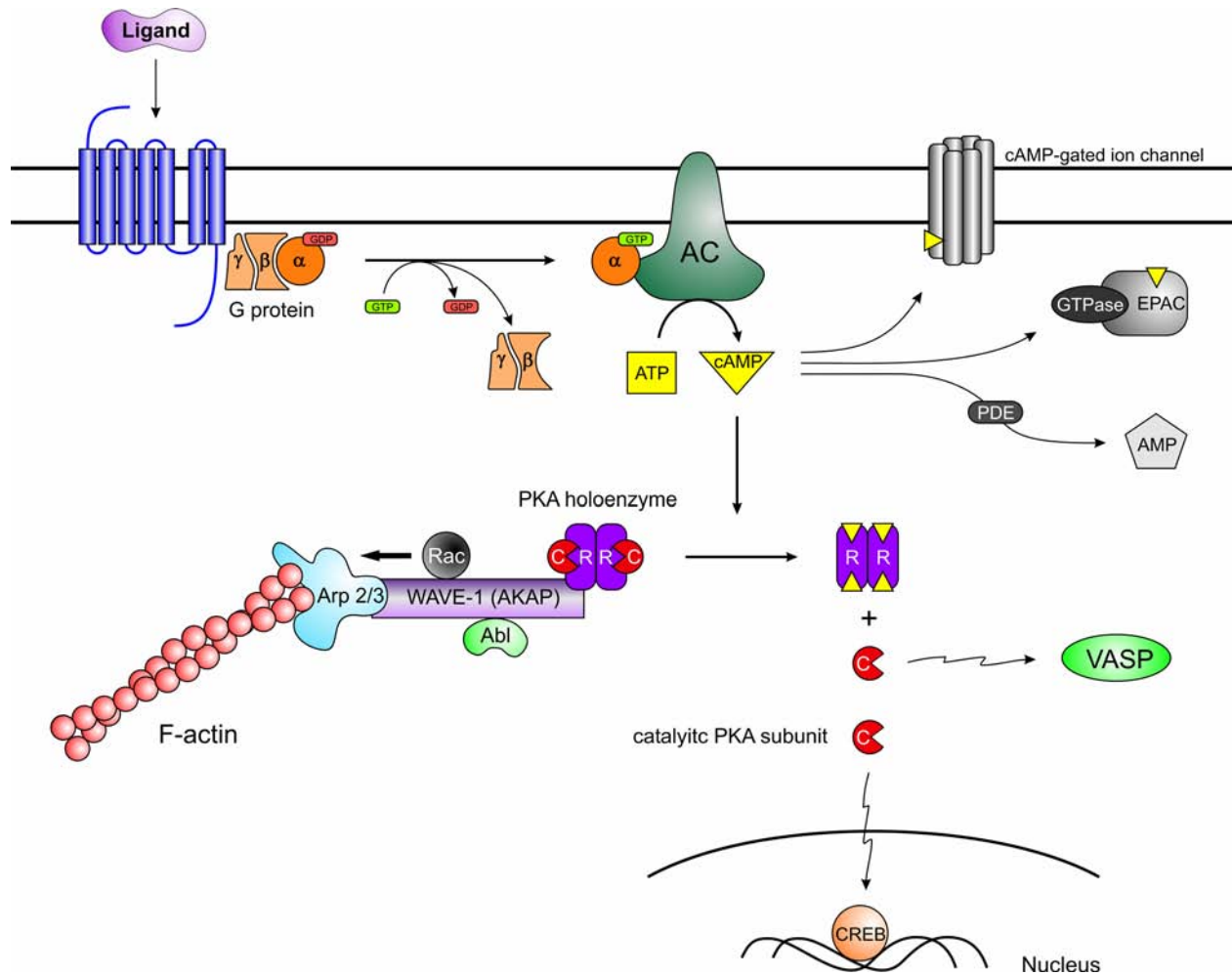


Figure I-2. cAMP/PKA Signaling Pathways

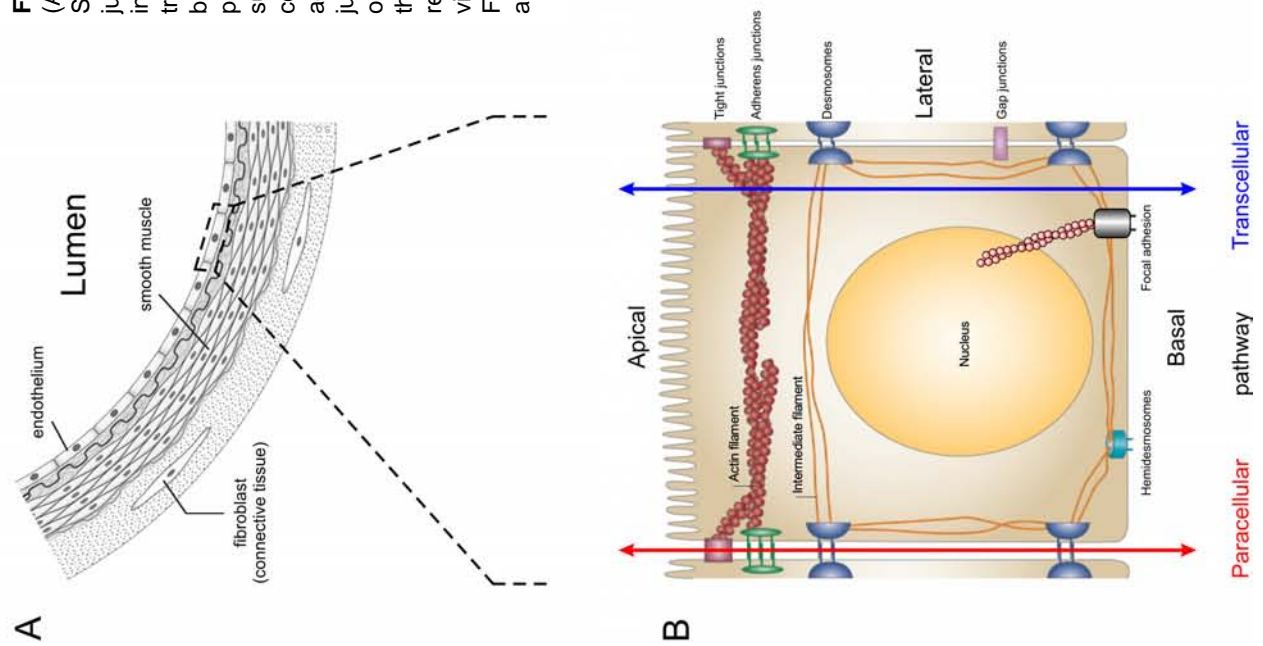
Binding of extracellular ligands to their cognate G-protein coupled receptors liberates GTP-bound $G\alpha$, which activates the adenylyl cyclase (AC) to convert ATP to cAMP. cAMP binds to cAMP-gated ion channels and guanine nucleotide-exchange proteins activated by cAMP (EPACs), or is hydrolyzed by phosphodiesterases (PDEs). The main target for cAMP is the cAMP-dependent protein kinase (PKA). cAMP binding to the regulatory PKA subunits (R) of the PKA holoenzyme liberates the catalytic subunits (C). Active PKA subunits phosphorylate serine/threonine residues of vasodilator-stimulated phosphoprotein (VASP), the cAMP response element binding protein (CREB), and other proteins. Subcellular targeting of PKA holoenzymes by A-kinase-anchoring proteins (AKAPs) such as WAVE-1 triggers specific phosphorylation events.

3. Endothelial Cells and Interendothelial Junctions

Endothelial cells (ECs) line vessel walls and form a semipermeable barrier between blood and the underlying tissue. They function as gatekeepers and control the luminal to abluminal movement of water, plasma proteins, and circulating cells. Material can penetrate endothelial monolayers either via the passive paracellular pathway or by active vesicular transport via the transcellular pathway (Figure I-3). Endothelial barrier function is regulated by a complex interplay of adhesive forces generated by interendothelial junctions (IEJs), counteradhesive forces generated by actinomyosin molecular motors, and integrin receptor binding to the extracellular matrix (ECM), which stabilizes the closed configuration of IEJs. Inflammatory mediators such as thrombin, bradykinin, histamine, and vascular endothelial growth factor disrupt the organization of IEJs and integrin-ECM complexes. This opens the junctional barrier and allows the uncontrolled passage of plasma proteins and liquid (Dejana, 2004; Mehta and Malik, 2006). Tight junctions (TJs) and adherens junctions (AJs) are the two major forms of IEJs. Although formed by different molecules, they share a common tripartite organization: (I) Transmembrane proteins (claudins, occludin, and junctional adhesion molecules in TJs and VE-cadherin in AJs), which mediate the adhesion of opposing cells by the formation of homophilic interactions arranged in zipper-like structures. (II) Adapter and scaffold proteins (zonula occludens-1 in TJ and β -catenin in AJ) that bind to the cytoplasmic domains of the adhesion molecules. (III) Actin-binding and actin-modulating proteins (spectrin and α -catenin in TJ and α -catenin, α -actinin, vinculin, and formin in AJ), which associate with the adapter proteins thereby linking the IEJs to the actin cytoskeleton (Dejana, 2004; Mehta and Malik, 2006; Tsukita et al., 2001) (Figure I-3). Directed cortical actin assembly and coupling of transmembrane adhesion molecules to the actin assembly machinery are essential for the integrity and stability of IEJs and for intercellular adhesion (Adams et al., 1998; Ermert et al., 1995; Lai et al., 2005; Vasioukhin and Fuchs, 2001; Waschke et al., 2005). Members of the Ena/VASP protein family are critically involved in cortical actin dynamics and blocked Ena/VASP function prevents actin polymerization at cell-cell contacts and adjacent cell membranes cannot seal (Scott et al., 2006; Vasioukhin et al., 2000). However, molecular mechanisms involved have remained obscure.

Figure I-3. Endothelial Cells and Interendothelial Junctions

(A) Schematic cross section of a blood vessel, comprised of endothelium, smooth muscle, and connective tissue. (B) Schematic representation of a polarized endothelial cell with cell-cell and cell-matrix adhesions. Tight and adherens junctions and focal adhesions are linked to the actin cytoskeleton, desmosomes and hemidesmosomes are linked to intermediate filaments. Gap junctions allow the rapid exchange of the second messengers Ca^{2+} and inositol 1,4,5-trisphosphate (IP_3) between contiguous cells. Material can cross the intact endothelial monolayer by passive movement between adjacent cells (solutes with molecular radii of up to 3 nm, mostly inorganic ions and glucose; paracellular pathway) or by active vesicular transport through the endothelial cells (macromolecules with molecular radii over 3 nm, such as albumin or immunoglobulins; transcellular pathway). (C) Electron micrograph of an endothelial junctional complex. (D) Structural organization of tight and adherens junctions (cell-cell adhesion) and focal adhesions (cell-matrix adhesion). Occludin, claudins, and junctional adhesion molecules (JAMs) are the backbones of the impermeable tight junctions, whereas VE-cadherin is required for formation of adherens junctions. While the extracellular domains of occludin, claudins, and VE-cadherin maintain cell-cell contact, intracellular domains provide junctional stability through their linkages with the actin cytoskeleton via catenins or members of the zona occludens (ZO) protein family. Integrin receptors link endothelial cells to the ECM (basal lamina) through association with the matrix proteins fibronectin or vitronectin, either alone, or by interaction with actin (focal adhesion), or the intermediate filaments (hemidesmosomes). Figures modified from www.wikipedia.org/wiki/Endothelium, (Matter and Balda, 2003), (Tsukita et al., 2001), or (Mehta and Malik, 2006), respectively.



4. Cytoskeletal Organization in Sparse and Confluent Endothelial Cells

ECs form monolayers in vessels but may also function as individual cells during angiogenesis and wound healing. ECs behave differently in confluent and sparse condition. In mature blood vessels, endothelial cells have a typical "cobblestone" morphology with an epitheloid phenotype. Formation of intercellular junctions inhibits cell growth and cell motility, and protects cells from apoptosis. Actin microfilaments are arranged to form an perijunctional ring, cells establish apical-basal polarity, and are in full control of paracellular permeability (Dejana, 2004) (Figure I-4). In contrast, when ECs are growing and proliferating, e.g. during angiogenesis or wound healing, they display a fibroblastoid-like morphology and lack intercellular junctions. They are elongated, highly motile, sensitive to growth-factor stimulation, and display an increased number of vinculin-positive focal adhesion sites and actin stress fibers, which are aligned in direction of cell migration (Dejana, 2004) (Figure I-4). The differences between sparse and confluent endothelial cells suggest that intercellular junctions are not only attachment sites between adjacent cells. But they can also function as signaling structures, which regulate cell growth, apoptosis, shape and polarity, cytoskeletal organization, and vascular homeostasis in general (Dejana, 2004; Rousseau et al., 2000; Tang et al., 1997; Yeaman et al., 1999).

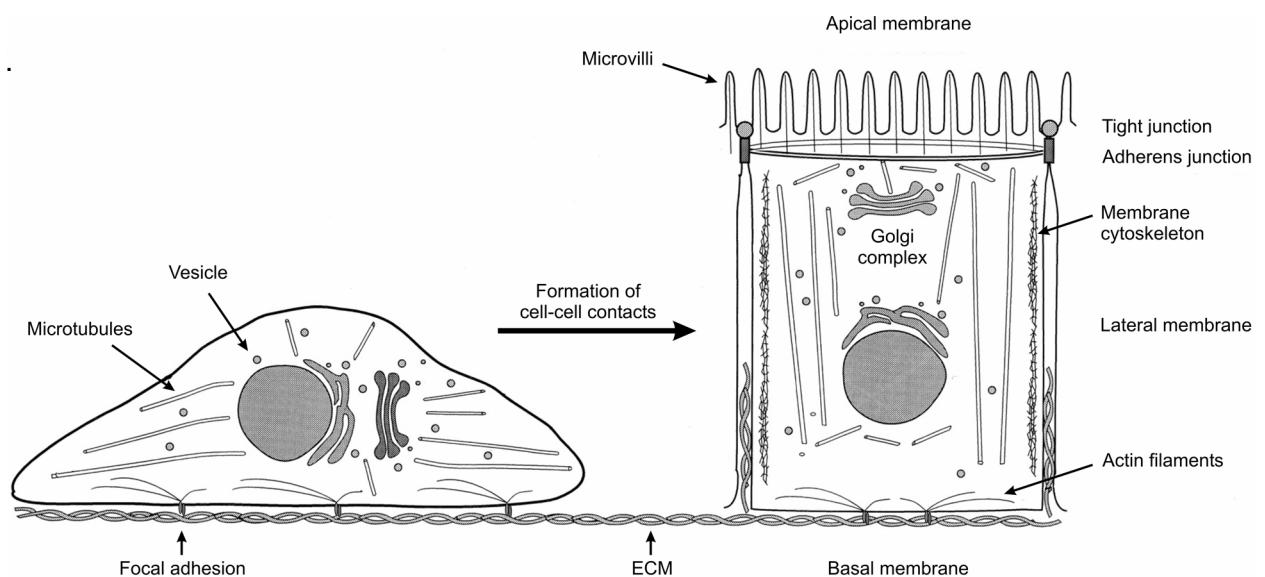


Figure I-4. Cytoskeletal Organization in Sparse and Confluent Endothelial Cells

In sparse endothelial cells (left), actin filaments are primarily organized into focal contacts that arise from sites of cell-substrate interactions. In confluent cells (right), actin bundles form the core of long membrane protrusions at the apical membrane, termed microvilli. Actin filaments are also distributed in a ring around the apex of the lateral membrane at adherens junctions just beneath of tight junctions. Along the basolateral membrane, actin fibers are associated with the membrane cytoskeleton and focal adhesion sites. Figure modified from (Yeaman et al., 1999).

5. Ena/VASP Proteins

Regulation of actin cytoskeletal turnover is necessary to coordinate cell movement, cell adhesion, and cellular shape change. Proteins of the Enabled/vasodilator-stimulated phosphoprotein (Ena/VASP) family are important mediators in cytoskeleton control, linking cyclic nucleotide signaling pathways to different modes of actin organization including actin filament assembly, cross-linking, and bundling (Sechi and Wehland, 2004). Recently, Ena/VASP proteins have also been shown to promote the formation of long, unbranched actin fibers, by protecting actin filament barbed ends from capping (Barzik et al., 2005; Bear et al., 2002). In mammals, the Ena/VASP family consists of the three proteins mammalian Enabled (Mena), VASP, and Ena-VASP-like (EVL). The family members share a tripartite domain organization of an N-terminal Ena/VASP homology 1 (EVH1) domain, a central proline-rich region (PRR), and an Ena/VASP homology 2 (EVH2) domain at the C-terminus (Sechi and Wehland, 2004). The EVH1 domain mediates binding to proteins that harbor one or multiple copies of the F/LPPPP motif including the surface protein ActA and iActA of *Listeria monocytogenes* and the cytoskeletal and adapter proteins vinculin, zyxin, Fyb/SLAP, and WASP (Ball et al., 2000; Niebuhr et al., 1997) (Figure I-5). The PRR contains multiple copies of the GPPPPP (GP₅) motif and interacts with the actin monomer-binding protein profilin (Reinhard et al., 1995a). Later studies have shown that it can also associate with Src homology 3 (SH3) domains of the non-receptor tyrosine kinases Abl, Src, and Lyn and the insulin receptor tyrosine kinase substrate IRSp53. However, functional consequences of these PRR-driven interactions, as well as binding to the WW domain of the neuronal protein FE65, have remained illusive (Ahern-Djamali et al., 1999; Ermekova et al., 1997; Krause et al., 2002; Krugmann et al., 2001; Lambrechts et al., 2000) (Figure I-5). The EVH2 domain consists of three modules: a G-actin-binding site, an F-actin-binding site, and a coiled-coil motif required for tetramerization (Bachmann et al., 1999; Kuhnel et al., 2004).

Both the EVH1 and EVH2 domain target Ena/VASP proteins to sites of high actin dynamics such as focal adhesions, cell-cell contacts, lamellipodia, filopodia, and comet tails on the surface of bacteria. In these locations, Ena/VASP proteins promote actin polymerization and

assembly, thereby modulating cell migration and cell-cell or cell-matrix interactions (Drees et al., 2000; Grosse et al., 2003; Loureiro et al., 2002; Rottner et al., 1999; Vasioukhin et al., 2000).

VASP harbors three phosphorylation sites: S157, conserved among all vertebrate family members and located N-terminally to the central PRR, and S239 and T278, located in the EVH2 domain, adjacent to the G- and F-actin binding sites, respectively (Butt et al., 1994; Gertler et al., 1996; Lambrechts et al., 2000) (Figure I-5). Phosphorylation of VASP at S157, the primary target of the cAMP-dependent protein kinase (PKA), leads to a shift in apparent molecular mass from 46 to 50 kDa in SDS-PAGE (Butt et al., 1994; Halbrugge and Walter, 1989). In contrast, VASP phosphorylation at S239 or T278, the preferred phosphorylation site of the cGMP-dependent protein kinase (PKG) or AMP-activated protein kinase (AMPK), respectively, does not shift the apparent molecular weight of VASP (Blume et al., 2007; Butt et al., 1994; Halbrugge et al., 1990). Functionally, phosphorylation of VASP at S239 and T278 decreases its ability to bind and bundle actin filaments and also reduces its barbed end anti-capping activity (Barzik et al., 2005; Harbeck et al., 2000; Walders-Harbeck et al., 2002). Phosphorylation at the conserved site common to all Ena/VASP proteins (S157 of VASP) is implicated in promoting Ena/VASP function during cell motility, filopodia formation, and correlates with fibrinogen receptor inhibition in platelets (Horstrup et al., 1994; Lebrand et al., 2004; Loureiro et al., 2002). PKA-mediated phosphorylation of VASP at S157 correlates with cell spreading and cell detachment from their substrata whereas reattachment of suspended cells to fibronectin causes a transient dephosphorylation of this site (Howe et al., 2002). Importantly, PKA-mediated phosphorylation of EVL and VASP at the conserved site abrogates their interaction with the SH3 domains of Abl and Src *in vitro* (Howe et al., 2002; Lambrechts et al., 2000). In contrast, the EVH1-mediated interaction with vinculin and zyxin, the binding of profilin or the Lyn SH3 domain to the PRR, and the EVH2-mediated tetramerization of Ena/VASP proteins are insensitive to both PKA and PKG phosphorylation (Harbeck et al., 2000; Lambrechts et al., 2000; Reinhard et al., 1995a). Therefore, the interaction of Ena/VASP proteins with specific SH3 domains may constitute an important target in cAMP/PKA signaling pathways.

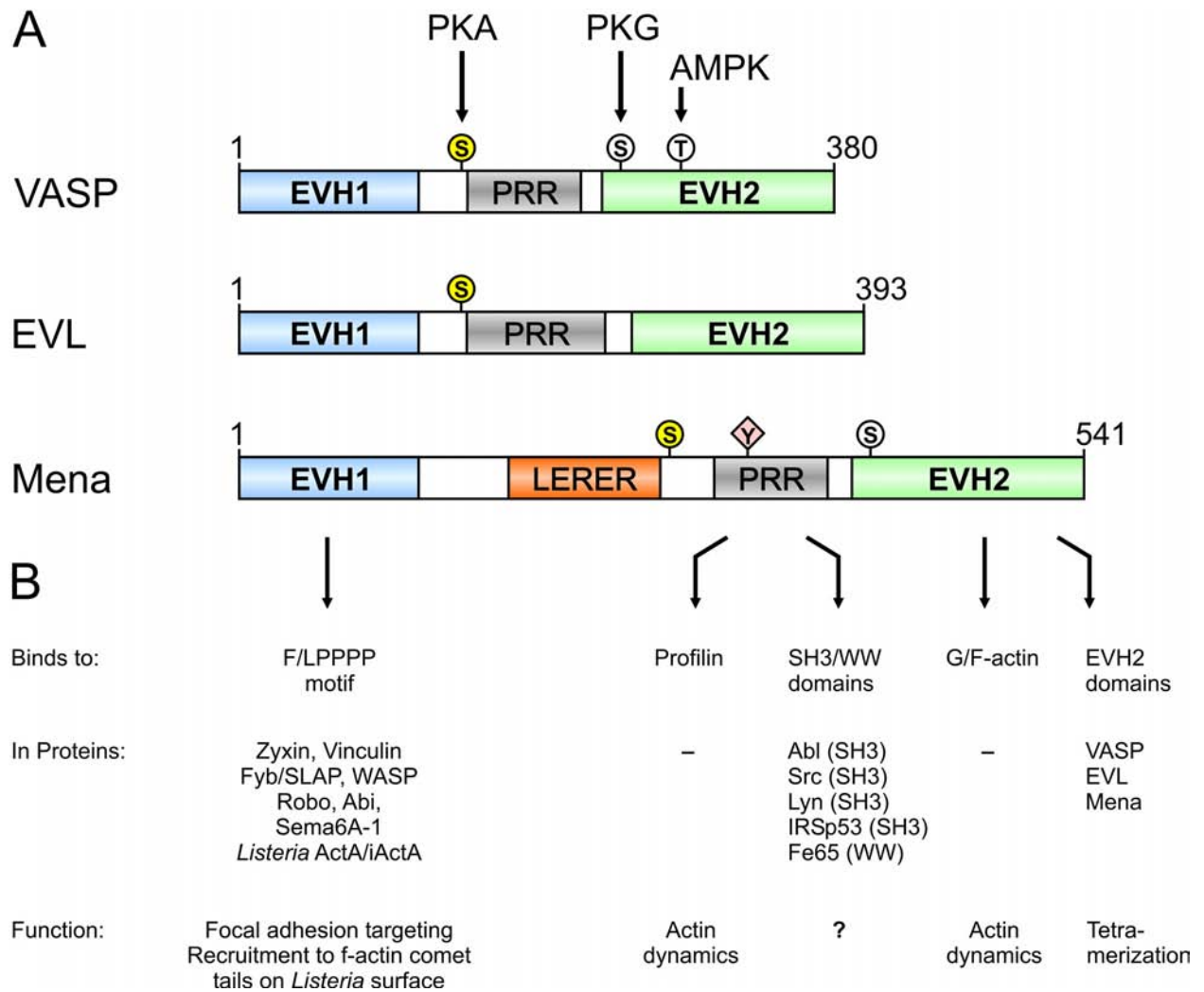


Figure I-5. Domain Structure of Ena/VASP Proteins along with their Binding Partners and Functions.

(A) Domain structure of the mammalian Ena/VASP proteins VASP, EVL, and Mena. EVH1: Ena/VASP homology 1, PRR: proline-rich region, LERER: low complexity region harbouring LERER repeats, EVH2: Ena/VASP homology 2. Serine and threonine phosphorylation sites are indicated as circles. In VASP, residues S157, S239, and T278 are preferentially phosphorylated by PKA, PKG, and AMPK, respectively. The VASP PKA phosphorylation site S157 (highlighted in yellow) is structurally and functionally conserved in all family members (Mena S236, EVL S156). The tyrosine phosphorylation site in Mena is indicated as pink rhombus. (B) Ena/VASP binding domains and motifs. Major interacting proteins for EVH1, EVH2, and PRR of Ena/VASP proteins and the associated functions are given below. The functional consequences of Ena/VASP interactions with SH3/WW domain-containing proteins are undefined. Amino acid numbering according to the human proteins.

6. Spectrins

Spectrins were originally identified as flexible, rod-shaped molecules that are part of the hexagonal, lattice-like skeleton underneath the erythrocyte membrane (Bennett and Baines, 2001; Bennett and Gilligan, 1993) (Figure I-6). They assemble into tetramers that are composed of two alpha (280 kDa) and two beta (245 - 460 kDa) subunits. Currently, two α - (α I, α II) and five

β -subunits (β I, β II, β III, β IV, and β V also termed β H) are known. Combinations of α - with various β -subunits yields α/β heterotetramers with distinct functions and patterns of expression (Bennett and Baines, 2001). In humans, the α I-subunit (also referred to as erythrocyte α subunit) is exclusively expressed in erythrocytes and in a subset of neurons where it assembles with the β I-subunit. In contrast, α II-spectrin (synonyms the non-erythrocyte or tissue-invariant α subunit, or α -fodrin) is expressed in most if not all mammalian tissues except for mature erythrocytes and mainly forms α II/ β II tetramers. In erythrocytes and most likely in all other cells, multiple spectrin molecules associate with actin filaments to form a polygonal, two-dimensional meshwork, which lines the cytoplasmic face of the plasma membrane. Either directly or through adapter proteins, spectrins bind simultaneously to integral membrane proteins and phospholipids on the one hand and cytosolic proteins on the other hand. This creates a multifunctional interface on which macromolecular complexes of membrane proteins, cytoplasmic signaling molecules, and structural elements are organized (De Matteis and Morrow, 2000) (Figure I-6). The role of the spectrin-based membrane skeleton in erythrocytes is to provide mechanical support for the membrane bilayer needed to withstand the high shear environment of the vascular system. Spectrins are not responsible for elasticity and rigidity of membranes, but rather affect their stability by controlling the lateral distribution of integral membrane proteins (Bennett and Gilligan, 1993; De Matteis and Morrow, 2000; Sleep et al., 1999). In adherent cells spectrin functions as "a protein accumulator", which sorts and collects adhesion proteins at specific sites of the plasma membrane, thereby stabilizing cell-cell and cell-matrix attachments after these structures have formed (Bennett and Baines, 2001; Nelson et al., 1990; Pinder and Baines, 2000; Yeaman et al., 1999) (Figure I-6). Mechanistically, coupling of cell adhesion molecules to the spectrin-based membrane skeleton promotes their interaction with molecules on neighboring cells by increasing the effective local concentration of these molecules. Moreover, mechanical coupling of adhesion molecules to the spectrin-actin network on both cytoplasmic sites of a cell-cell contact enhances adhesion and rigidity (Bennett and Baines, 2001) (Figure I-6).

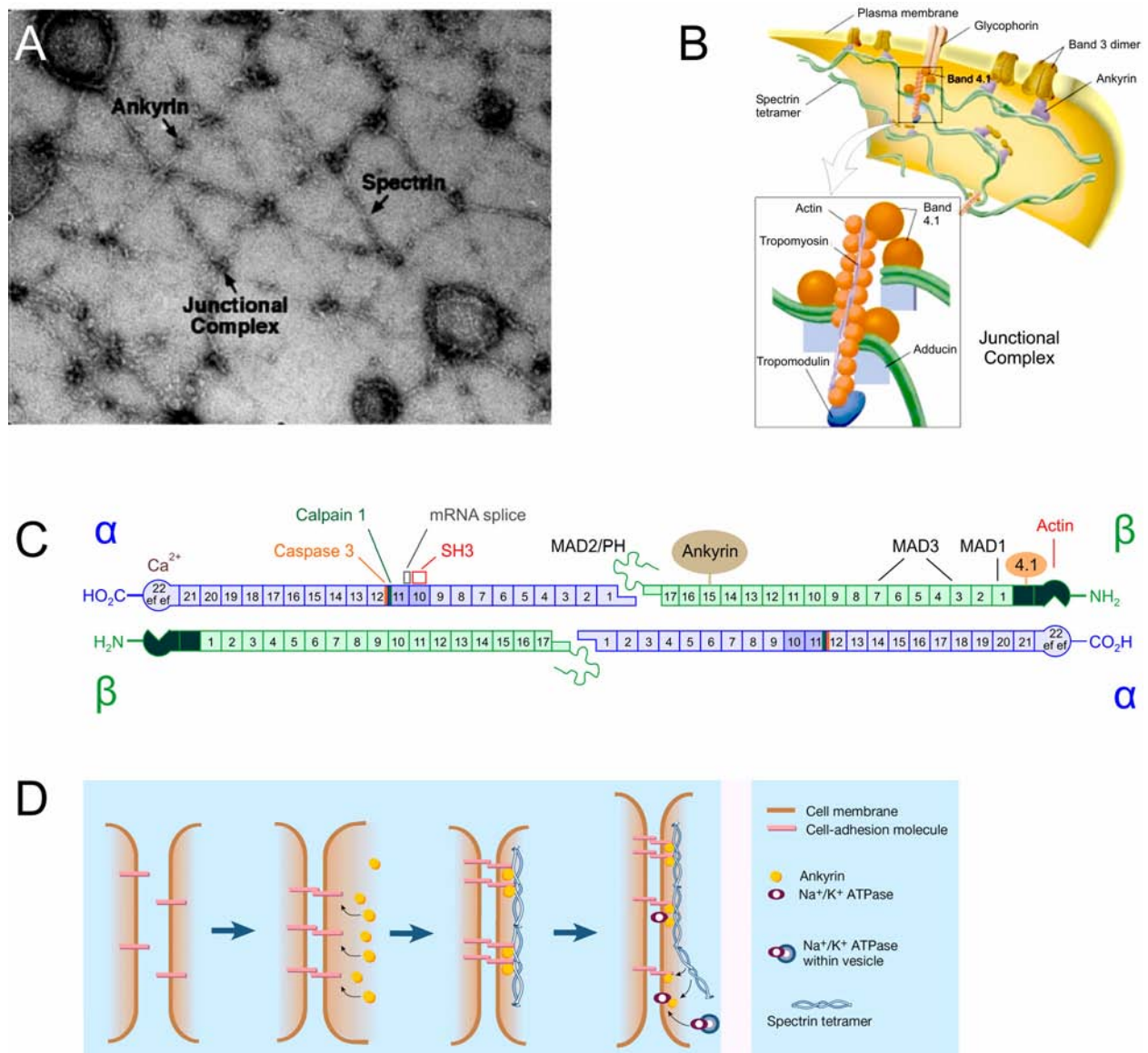


Figure I-6. The Spectrin-Based Membrane Skeleton, Spectrin Tetramer Structure, and Spectrin Function in the Organization of Cell-Cell Contacts.

(A) Electron microscopy image and (B) schematic representation of the erythrocyte membrane skeleton. Spectrin tetramers are cross-linked at junctional complexes by short actin filaments and band 4.1/adducin. Approximately six spectrins interact in each node to form a hexagonal, two-dimensional array. This network is attached to the plasma membrane by ankyrin, which simultaneously binds to the central region of spectrin tetramers and the transmembrane anion exchanger band 3, and by band 4.1-glycophorin C interactions at the junctional complexes. (C) Domain organization of α II/ β II spectrin tetramer. Each subunit is composed of multiple, approximately 106 residue, triple helical repeats. Non-homologous segments are shaded. The actin-binding, tandem calponin homology domains at the N-terminus of the β -spectrins are shown in dark green. The two ef-hand motifs at the C-terminus of the α -subunits are "calmodulin-like" structures that undergo Ca^{2+} -induced conformational changes. Sites for ankyrin, band 4.1, and actin binding, calpain 1 and caspase 3 cleavage, and mRNA splicing are indicated. Direct membrane association domains (MAD1-3), the pleckstrin homology (PH) domain, and the SH3 domain, located in the middle of the α -subunit, are also shown. α - and β -subunits associate laterally near the N-terminus of β and the C-terminus of α . "Head to tail" interactions bring two laterally associated $\alpha\beta$ -dimers together to form anti-parallel $(\alpha\beta)_2$ -tetramers. (D) Model for the strengthening of intercellular junctions by the spectrin/ankyrin accumulation machine. Two cells interact through transmembrane adhesion molecules, which then bind ankyrin, and in turn spectrin tetramers. The spectrins cross-link these complexes and stabilize the regions of cell-cell contact. Actin fibers cross-link spectrin tetramers and couple the transmembrane adhesion molecules to the actin cytoskeleton, which is essential for junctional integrity. Binding sites on spectrin and ankyrin trap further proteins, e.g. the Na^+/K^+ -ATPase, thereby promoting their incorporation into the plasma membrane microdomain. Images adapted from <http://www.jax.org/~slc/research.html>, <http://bioweb.wku.edu/courses/Biol22000/27Actin/default.html>, (Kreis and Vale, 1999), or (Pinder and Baines, 2000).

7. SH3 Domains

SH3 domains are the most abundant protein recognition motifs, comprising an estimated 409 copies in the human proteome alone (Li, 2005). Mostly found in signal transduction and cytoskeletal proteins, these 60-residue protein modules have a characteristic fold: a compact β -barrel, formed by five β -strands that are arranged as two tightly packed anti-parallel β sheets. The first four β -strands (β A- β D) are connected by the so-called RT, n-Src, and distal loop, respectively, while the last two (β D and β E) are connected by a 3_{10} helix. Characteristics of SH3 domains are the ALYDY motif in the RT-loop, the WW dipeptide in the β D strand, and the PXXY motif in the 3_{10} helix (Musacchio, 2002; Musacchio et al., 1992) (Figure I-7A). SH3 domains bind to two classes of proline-rich ligands: class I ligands have the general consensus sequence $+x\Phi Px\Phi P$ and class II ligands have the general consensus sequence $\Phi Px\Phi Px+$ (where x is any amino acid, P is proline, Φ is a hydrophobic amino acid, and + a positively charged amino acid, usually arginine). The ligands adopt an extended, left-handed helical conformation (termed polyproline-2 or PPII helix, Figure I-7C) and bind to three shallow pockets within the SH3 domain. Two of the three pockets are occupied by two hydrophobic-proline (ΦP) dipeptides, whereas the third "specificity" pocket is occupied by the positively charged residue, which is located N- or C-terminally in class I or class II ligands, respectively (Figure I-7B) (Kay et al., 2000; Li, 2005; Mayer, 2001).

SH3 domain-mediated interactions are commonly found in processes that require the rapid subcellular recruitment or interchange of proteins during initiation of signaling cascades and cytoskeletal rearrangements (Kay et al., 2000). Due to the insufficient inherent specificity in most SH3-mediated interactions, additional mechanisms exist *in vivo* to generate protein binding selectivity. These are temporal and cell-type specific gene expression, combination of multiple separate interactions between two binding partners, and the cooperative assembly of multiprotein complexes. Most common, however, is the compartmentalization of binding partners and the regulation of their interaction by posttranslational modifications such as phosphorylation (Kay et al., 2000; Mayer, 2001).

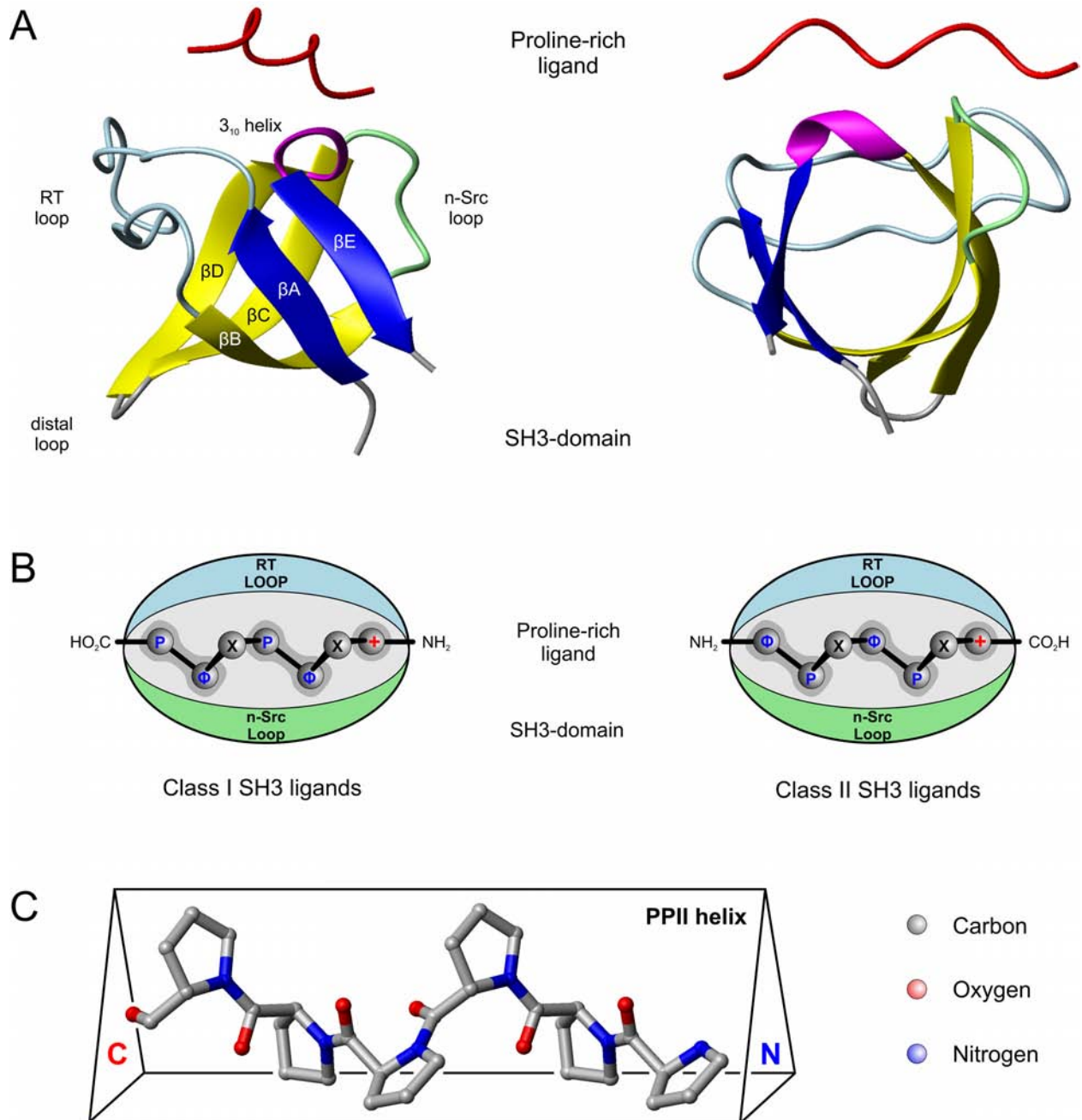


Figure I-7. SH3 Domain Structure and SH3-Mediated Interactions with Proline-Rich Ligands.

(A) Ribbon model of chicken α -spectrin SH3 domain as determined by X-ray diffraction (protein data bank ID: 1SHG) (Musacchio et al., 1992) in a hypothetical complex with a proline-rich ligand (PPPVPPRV, pdb ID: 1CKB). The SH3 domain is a compact β -barrel made of five antiparallel β -strands (β A- β E) that are connected (from N- to C-terminus) by the RT, n-Src, and distal loop, and by a 3_{10} helix, respectively. β -Strands β A and β E, and β -strands β B- β D form two tightly packed anti-parallel β sheets that are shown in blue or yellow, respectively. The β -barrel is shown in two different orientations related by a 90° rotation: side view of (left panel) and view into the β -barrel (right panel). (B) Diagram illustrating the binding of class I (left panel) and class II (right panel) ligands to the surface of a typical SH3 domain. The two hydrophobic grooves and the specificity pocket, which typically interacts with an arginine, are shown in grey. Approximate positions of the RT loop and the n-Src loop are indicated in blue and green, respectively. In class I (class II) SH3 ligands, the positively charged residue is located N-terminally (C-terminally) to the hydrophobic-proline (Φ P) dipeptides. In the ligands, x is any amino acid, P is proline, Φ is a hydrophobic amino acid, and + a positively charged residue, usually arginine). (C) Ball/stick model of a typical polyproline type II (PPII) helix as determined by X-ray diffraction (modified from pdb ID: 1FYN). PPII are left-handed helices that can be represented as triangular prism. Three consecutive prolines account for one turn of the PPII helix and occupy a different edge of the prism. Figures (A) and (C) were obtained with the program MOLMOL (Koradi et al., 1996), figure (B) is adapted from (Mayer, 2001).

8. Aims of the Study

Actin fiber assembly is crucial for a variety of cellular processes and tightly regulated by a plethora of actin-binding proteins. Originally identified in platelets, the actin-binding protein VASP participates in a variety of actin-based processes including cell-cell and cell-matrix adhesion, cell spreading, and cell migration in leucocytes, fibroblasts, smooth muscle, epithelial, and endothelial cells. Because of different VASP-functions in distinct subcellular locations, it is obvious that VASP activity and VASP distribution needs to be spatially and temporally regulated. VASP is a substrate for cAMP- and cGMP-dependent and the AMPK-activated protein kinase and VASP phosphorylations are involved in regulation and subcellular targeting of the protein. Therefore we asked for new VASP interaction partners, which bind dependent on the VASP phosphorylation states.

The goals of the presented work can be divided into three parts:

1. Identification of novel endothelial proteins, which bind to VASP dependent on its phosphorylation state by mass spectrometry. Characterization of the VASP/protein interaction and mapping of the relevant binding sites in both proteins.
2. Identification of the VASP phosphorylation site(s) and the corresponding kinase(s), which regulate VASP-binding to the novel protein interaction partner.
3. Functional analyses of the new interaction for the actin cytoskeleton in living endothelial cells and genetically altered mice.

II MATERIALS AND METHODS

1. Plasmids

Plasmids were prepared by standard PCR cloning techniques and subsequently confirmed by DNA sequencing. VASP point mutants were generated by site-directed mutagenesis using the “QuikChange Multi” kit according to the manufacturer’s instructions (Stratagene). With N-terminally His₆-tagged human VASP (Haffner et al., 1995) in the prokaryotic expression vector pQE-30 (Qiagen) as template, adequate primers (Table II-1) were employed to exchange S157, S239, and T278 with alanines (S157A, S239A, T278A) or acidic amino acids (S157D, S239D, T278E) and P177, P178, and P179 with alanines (P177A, P178A, P179A). For expression in eukaryotic cells, His₆-tagged full-length VASP was subcloned into pcDNA3 (Invitrogen). For eukaryotic expression of C-terminally truncated VASP mutants, DNA fragments coding for VASP amino acids 1-380 (VSV-VASP), 1-195 (VSV-EVH1/PRR), and 1-114 (VSV-EVH1) were generated by PCR adding a 5′ sequence encoding the VSV (vesicular stomatitis virus glycoprotein) epitope tag (YTDIEMNRLGK), and then cloned into pcDNA3.

Table II-1. Primers Used for the Generation of VASP Point Mutants by Site-Directed Mutagenesis.

Point mutation	Primer Sequence ¹
S157A	5′ – CG GAG CAC ATA GAG CGC CGG GTC GCC AAT GCA GGA GGC CCA CC – 3′
S157D	5′ – CG GAG CAC ATA GAG CGC CGG GTC GAC AAT GCA GGA GGC CCA CC – 3′
S239A	5′ – GGA GCC AAA CTC AGG AAA GTC GCC AAG CAG GAG GAG GCC TCA GGG – 3′
S239D	5′ – GGA GCC AAA CTC AGG AAA GTC GAC AAG CAG GAG GAG GCC TCA GGG – 3′
T278A	5′ – G CTG GCC CGG AGA AGG AAA GCC GCG CAA GTT GGG GAG AAA ACC – 3′
T278E	5′ – G CTG GCC CGG AGA AGG AAA GCC GAG CAA GTT GGG GAG AAA ACC – 3′
P177A	5′ – CA CCA CCA GGA CCT GCC CCT CCT CCA GGT C – 3′
P178A	5′ – CA CCA GGA CCT CCC GCT CCT CCA GGT CCC C – 3′
P179A	5′ – CA GGA CCT CCC CCT GCT CCA GGT CCC CCC C – 3′

¹Sequence variations with respect to the VASP cDNA are shaded in green.

For GST-fusion protein constructs, DNA fragments encoding amino acids 970-1025 of SPCN (SPCN_SH3; numbering according to GenBank accession no. AAH53521), and 595-659 (N-

VAV1_SH3) and 785-835 (C-VAV1_SH3) of VAV1 (acc. no. NM_005428) were generated by PCR and cloned into pGEX-4T3 (GE Healthcare) using the *EcoRI* and *XhoI* restriction sites (Table II-2). The SPCN cDNA clone was obtained from RZPD (IRAKp961A1733Q) and the VAV1 cDNA was a kind gift from Dr. A. Obergfell (Würzburg, Germany).

Table II-2. Primers Used for the Generation of GST-SH3 Fusion Proteins.

Primer	Domain	Primer Sequence ¹
SpecF1_ <i>Eco</i>	SPCN_SH3	5' – CCG AAT TCG GAG CTG GTC TTG GCT CTC T – 3
SpecR1_ <i>Xho</i>	SPCN_SH3	5' – CCG CTC GAG TTA GTC CAA TTT CTT CAC GTA CGC A – 3
VAV1_F1_ <i>Eco</i>	N-VAV1_SH3	5' – CCG AAT TCG CCC AAG ATG GAG GTG TTT CAG – 3'
VAV1_R1_ <i>Xho</i>	N-VAV1_SH3	5' – CCG CTC GAG TTA GAC ATA GGG CTT CAC CCT GTT A – 3'
VAV1_F2_ <i>Eco</i>	C-VAV1_SH3	5' – CCG AAT TCT GGC ACA GCC AAA GCC CGC T – 3'
VAV1_R2_ <i>Xho</i>	C-VAV1_SH3	5' – CCG CTC GAG TTA ATA ATC TTC CTC CAC GTA GTT GG – 3'

¹ *EcoRI* and *XhoI* restriction sites are indicated in blue and orange, respectively. Stop codons are shown in red.

Cloning of claudin-5 constructs: C-terminally VSV-tagged claudin-5 (CI-VSV) was generated by PCR using a reverse primer to replace the native stop codon with a VSV-tag and cloned into *BamHI/EcoRI* sites of pcDNA3 (Table II-3). The chimeric protein claudin-5-VSV-SPCN_SH3 (CI-VSV-SH3) was generated in two steps. Initially, the cDNA of claudin-5 was amplified excluding the native stop codon and inserted into the *BamHI/EcoRI* sites of pcDNA3. Subsequently, the SPCN SH3 domain was amplified including a 5'-located sequence coding for the VSV-tag, and this VSV-SPCN_SH3 construct was then inserted into the *EcoRI/XhoI* sites in the pcDNA3 vector, 3' to and in frame with claudin-5. The claudin-5 cDNA was obtained from RZPD (IRATp970A0452D, acc. no. BC032363).

Table II-3. Primers Used for the Generation of Claudin-5 Constructs.

CI-VSV	
Primer	Primer Sequence ¹
Cla5_F1 <i>Bam</i>	5' – TT GGA TCC ATG GGG TCC GCA GCG TT – 3
Cla5_R2VSV	5' – TG GAA TTC TTA TTT GCC TAG TCG GTT CAT CTC GAT GTC GGT GTA CGG GAC GTA GTT CTT CTT GTC GTA G – 3
CI-VSV-SH3 (step 1)	
Primer	Primer Sequence ¹
Cla5_F1 <i>Bam</i>	5' – TT GGA TCC ATG GGG TCC GCA GCG TT – 3
Cla5_R1 <i>Eco</i>	5' – T GGA ATT CGG GAC GTA GTT CTT CTT GTC GTA G – 3'
CI-VSV-SH3 (step 2)	
Primer	Primer Sequence ¹
SpecF2_VSV	5' – CGGAATTCC ATG TAC ACC GAC ATC GAG ATG AAC CGA CTA GGC AAA CCC GAG CTG GTC TTG GCT CTC T – 3'
SpecR1_ <i>Xho</i>	5' – CCG CTC GAG TTA GTC CAA TTT CTT CAC GTA CGC A – 3

¹ *Bam*HI, *Eco*RI, and *Xho*I restriction sites are indicated in magenta, blue, and orange, respectively. Start codons are shown in green, stop codons are shown in red. Nucleotides encoding the VSV epitope tag are shaded in yellow, codons for extra prolines, introduced to enhance VSV epitope recognition by VSV-specific antibodies, are shaded in grey.

2. Protein Purification, Coupling, and Phosphorylation

His₆-tagged wild-type and mutant VASP (VASP-AAA, -DDE, -DAA, -ADA, -AAE, -P177A, -P178A, and -P179A) was expressed in *E.coli* BL21 (DE3) and purified as described (Bachmann et al., 1999). GST-fusion proteins (SPCN_SH3, N-VAV1_SH3, and C-VAV1_SH3) or GST alone were expressed in *E.coli* BL21 (DE3), affinity purified on glutathione sepharose beads (GE Healthcare), and then covalently coupled to Affi-Gel 15 (Biorad). Purified proteins were

analyzed by SDS-PAGE and quantified by comparison with bovine serum albumin (BSA) as standard or from absorbance at 280 nm using molar extinction coefficients (E) as calculated from the amino acid sequence according to the formulas:

$$E (280\text{nm}) [M^{-1} \text{ cm}^{-1}] = (N_W \cdot 5,500) + (N_Y \cdot 1,490) + (N_C \cdot 125)$$

and

$$\text{Protein concentration [M]} = (\text{absorbance at } 280\text{nm [cm}^{-1}\text{]}) / E$$

where N equals the number of tryptophans (W), tyrosines (Y), or cysteines (C) (Pace et al., 1995). His₆-tagged wild-type VASP was phosphorylated *in vitro* with PKA catalytic subunit essentially as described (Butt et al., 1994). Briefly, 10 µg purified His₆-tagged VASP was incubated at 30°C for 15 min with 10 mM Hepes (pH 7.4), 5 mM MgCl₂, 1 mM EDTA, 0.2 mM DTT, and 0.5 µg porcine PKA catalytic subunit (Sigma, P8289) in a total volume of 180 µl. The reaction was started by addition of 20 µl 1 mM ATP to give a final concentration of 100 µM. VASP S157 phosphorylation was confirmed by Western blotting using total-VASP and phosphorylation-specific antibodies for this site (5C6).

3. Antibodies and Fluorescent Phalloidin

Antibodies were from the indicated sources and used at given concentrations: anti-VASP (M4, Immunoglobe, immunofluorescence (IF): 1/1000, Western Blot (WB): 1/2000, immunoprecipitation (IP): 1/125), anti-VASP (FITC-M4, IF: 1/30), anti-VASP (IE273, Immunoglobe, IF: 1/150, WB: 1/1000, IP: 1/25), anti-pS157-VASP (5C6, Nanotools or 3111, Cell Signaling Technology IF: 1/30, WB: 1/500. Note: as detailed by the supplier, anti-pS157-VASP antibodies unspecifically stain cell nuclei), anti-pS239-VASP (16C2, Nanotools, WB: 1/500), anti-pT278-VASP ((Blume et al., 2007), WB: 1/500), anti-SPCN (2122, Cell Signaling Technology, IF: 1/90, WB: 1/1000, IP: 1/20), anti-SPCN (MAB1622, Chemicon, WB: 1/1000, IP: 1/25), anti-ZO-1 (BD Transduction Laboratories, IF: 1/200), anti-His₆ (Novagen, WB: 1/1000), anti-VSV (Clone P5D4, Sigma, IF: 1/1000, WB: 1/2000), anti-GST (kindly donated by Dr. K.

Bundschu, University of Wuerzburg, Wuerzburg, Germany, WB: 1/2000), and anti-GAPDH (mAB 374, Chemicon, WB: 1/8000). Anti-plasma kallikrein antibodies, used as controls, were kindly provided by Dr. W. Muller-Esterl (University of Frankfurt, Frankfurt, Germany). Horseradish peroxidase-conjugated secondary antibodies were from Dianova (WB: 1/5000), fluorescence-conjugated antibodies (Alexa-fluor 488, 594, or 647, IF: 1/500) from Molecular Probes. TRITC-phalloidin (P1951, Sigma, IF: 1/350) was used to visualize F-actin.

4. Cell Culture

EA.hy926 cells and human umbilical vein endothelial cells (HUVEC, Cambrex Bioproducts) of passages 2-5 were cultivated as described (Profirovic et al., 2005; Renne et al., 2005). ECV304 and 293 EBNA cells were grown in Dulbecco's modified Eagle's medium (DMEM) containing 4.5 g/l glucose, 1 mM sodium pyruvate, and 10% FBS and split 1:10 or 1:20 every 3-4 days. Wild-type (EC-VASP^{+/+}, also named MyEnd^{+/+}) and VASP-deficient (EC-VASP^{-/-}, also named MyEnd^{-/-}) murine microvascular myocardial endothelial cells were generated, characterized, and cultured as described (Golenhofen et al., 2002). Briefly, every 7-10 days, cells were rinsed and detached with trypsin-EDTA and collected in DMEM medium containing 4.5 g/l glucose, 1 mM sodium pyruvate, and 10% FBS. Cells were then replated on gelatinized tissue culture plates (0.5% gelatine in PBS, incubated for 1h at room temperature) at a ratio of 1:2 or 1:3. 3-4 days after passaging, the culture medium was replaced with DMEM medium containing 4.5 g/l glucose, 1 mM sodium pyruvate, and 10% FBS following washing of the cells in the same medium. 293 EBNA and ECV304 cells were transiently transfected with Lipofectamine 2000 (Invitrogen) following the manufacturer's instructions and analyzed 10-24 h thereafter. To analyze whether VASP phosphorylation correlates with cell density, ECV304 cells were detached with trypsin-EDTA and collected into DMEM containing 10% FBS. Cells were then either maintained in suspension (Sp) for 15 min before lysis or immediately replated on tissue culture plates at a density of 7.5×10^4 cells/cm². 3, 6, 12, 24, 48, or 72 h after seeding, adherent cells were washed with prewarmed PBS and then immediately lysed in SDS-sample buffer

followed by Western blot analysis (loading per lane was normalized to equal cell counts) with anti-total-VASP (M4) and anti-phospho-VASP (5C6, 16C2, and, pT278) antibodies. As control for maximal PKA stimulation, ECV304 cells were treated for 10 min with 10 μ M forskolin 72 h after replating. The amount of S157-phosphorylation relative to total-VASP was quantified from M4 Western blots by densitometric scans (ImageJ, V. 1.34s).

5. 2D-PAGE Proteome Analysis of VASP-AAA- and VASP-DDE-Binding Proteins

1.2 mg of purified recombinant His₆-VASP-AAA or His₆-VASP-DDE, respectively, was covalently coupled to 1 ml Affi-Gel 10 (Biorad), each. Cytosolic proteins from 100 confluent dishes (10 cm diameter) of EA.hy926 cells in PBS were prepared as described (Herwald et al., 1996) and applied to His₆-VASP-AAA or -DDE affinity columns. After incubation for 2 h at 4°C, columns were washed with 12 volumes of PBS and bound proteins were eluted with 10 mM glycine/HCl pH 5, pH 4, pH 3, and pH 2. pH 2 fractions containing the established VASP interaction partner zyxin and vinculin were analyzed by 2D-PAGE and mass spectrometry. Electrophoresis equipment was from GE-Healthcare. For first dimension protein separation, immobilized pH gradient (IPG)-strip (24 cm) rehydration was performed using 450 μ l R-buffer (7 M Urea, 2 M Thiourea, 2% CHAPS and 2% IPG-buffer 3-10 NL) for 8 h at room temperature. Protein samples were dissolved in rehydration-buffer, resulting in approximately 300 μ g of protein for each strip, and then applied using the sample cup method according to the manufacturer's instructions. Isoelectric focussing was done with the IPG-phor system (GE-Healthcare) by application of a standard multi-step gradient resulting in a total of approximately 55 kVh. For second dimension SDS-PAGE, strips were equilibrated using E-buffer (6 M urea, 2% SDS, 30% glycerine, 50 mM Tris-HCl, pH 8.8) with 130 mM DTT for reduction and 280 mM iodoacetamide for alkylation of cysteine residues, each 15 min, respectively. The re-equilibrated strips were transferred onto 10% Tris-Glycine SDS-gels (20 cm x 24 cm) and electrophoretic separation was performed with an Ettan-Dalt-Six chamber (GE-Healthcare) at 15 W per gel. Thereafter 2D-gels were stained with colloidal coomassie (G-250) as described (Neuhoff et al., 1988). Gel

images were processed using the Proteomweaver software Vers. 2.2 (Definiens). Briefly, spot detection and gel-matching was performed on both gel groups. Afterwards, all differentially detected spots were excised manually. Gel plugs were washed, equilibrated, and treated with trypsin as described (Shevchenko et al., 1996). Generated peptides were extracted from gel plugs with 10 μ l 0.1% trifluoroacetic acid (TFA) solution. An aliquot of 1 μ l was spotted onto a MALDI-steel target (Bruker Daltonik) together with 1 μ l of saturated alpha-cyano-4-hydroxycinnamic acid-solution containing 50% acetonitrile and 50% of a 0.1% TFA solution. MALDI-PMF measurements were performed with an Ultraflex MALDI-TOF/TOF mass spectrometer (Bruker Daltonik). Acquired spectra were processed using the mascot algorithm (V. 1.9) and the current NCBI protein database.

6. Immunoprecipitations and GST Dull-Down Assays

For immunoprecipitations, confluent EA.hy926 cells (10 cm dishes) were lysed for 30 min at 4°C in 150 μ l lysis buffer per plate (50 mM Tris-HCl, pH 8.0, 500 mM NaCl, 1% NP40, and complete protease inhibitor cocktail tablets (Roche)). Lysates were cleared by centrifugation (21,000 x g, 30 min), supernatants diluted to final concentrations of 50 mM Tris-HCl, 150 mM NaCl, 0.3% NP40, and 1 x protease inhibitors (reaction buffer), and subjected to immunoprecipitation for 1.5 h at 4°C using VASP- and SPCN-specific antibodies or controls (see above). Subsequently, 60 μ l pre-equilibrated protein G-sepharose slurry (GE Healthcare) was added, incubated for 1 h at 4°C, and washed three times with ice-cold reaction buffer. Precipitates were resuspended in SDS sample buffer, resolved by SDS-PAGE, and analyzed by Western blotting. For GST pull-down assays, endothelial cells (EA.hy926, ECV304, EC-VASP^{+/+}, EC-VASP^{-/-}, and HUVEC) or 293 EBNA cells, transfected with full-length and C-terminally truncated VASP (VSV-VASP, VSV-EVH1-PRR, and VSV-EVH1), were grown to confluence in 6 cm dishes and then lysed for 30 min at 4°C in 250 μ l PD buffer (40 mM Hepes-NaOH, pH 7.4, 150 mM NaCl, 1% NP40, and protease inhibitors). Lysates were cleared by centrifugation and incubated for 1 h at 4°C with 5 μ g immobilized GST-fusion protein or a corresponding amount of GST. Precipitates were

washed in PD buffer, resolved by SDS-PAGE, and analyzed by Western blotting with VASP- or VSV-specific antibodies. GST pull-down assays with purified recombinant VASP were performed as above, using 1 μ g PKA-phosphorylated or unphosphorylated His₆-tagged wild-type VASP or 1 μ g of the following mutants: His₆-VASP-DDE, -AAA, -DAA, -ADA, -AAE, -P177A, -P178A, and -P179A. Precipitated material was analyzed with anti-His₆ antibodies. To analyze whether PKA activity regulates SPCN/VASP interaction in cells, His₆-VASP was overexpressed in 293 EBNA cells. 20 h after transfection, cells were either treated with 1 μ M okadaic acid (Sigma) and 10 μ M forskolin (Sigma) or 10 μ M Rp-8-Br-cAMPs (Biolog) for 30 min before cell lysis and GST pull-down experiments as described above.

7. Immunocytochemistry

IF studies were performed essentially as described (Blume et al., 2007). Briefly, ECV304 cells, either untransfected or transfected with CI-VSV or CI-VSV-SH3, were grown in chamberslides (Nunc), fixed in ice-cold 4% paraformaldehyde, permeabilized with 0.1% Triton X-100, and blocked with 10% goat serum. After overnight incubation with primary antibodies, cells were incubated with fluorescence-conjugated secondary antibodies and/or fluorescence-conjugated phalloidin (see above) for 1.5 h and mounted onto glass slides with Mowiol (Hoechst). All incubations were performed in 5% goat serum/PBS in a humid chamber at RT. Stained sections were investigated using a Nikon Eclipse E600 microscope equipped with a C1 confocal scanning head and a 100-fold oil immersion objective. Images were acquired and prepared for presentation using the EZ-C1 software (Nikon, V. 3.00).

8. Peptide and Alanine Substitution Scans

For peptide scans (Figure III-4C), 15-mer peptides with 14 amino acid overlap, spanning the VASP protein sequence from E114 to P224 (including the entire PRR), were synthesized in an array of 10 x 10 spots on a cellulose membrane. For the alanine substitution scan (Figure III-4D), the 15-mer VASP peptide P171-P185 or mutant peptides, in which each residue was

systematically substituted for alanine, were prepared accordingly. Arrays were assembled, one amino acid at a time by sequential coupling and deprotection, on a derivatised cellulose membrane using a Multiprep Synthesizer (Intavis). Briefly, fmoc-amino acids with appropriate side chain protection (Merck) were dissolved in a hydroxybenzotriazole/N-methylpyrrolidone (NMP) solution. For each cycle, an aliquot of this solution was activated by addition of diisopropylcarbodiimide (DIC) in NMP solution and spotted in a grid to generate the sequences previously programmed in. After coupling twice and washing with dimethylformamide and ethanol, any available reactive sites were capped with a solution of acetic anhydride/dimethylformamide followed by piperidine/dimethylformamide solution to remove the fmoc group. After extensive washing of the membrane, the next cycle of coupling began. Once peptides were assembled, the side chain protection groups were removed using TFA cocktail solution (trifluoroacetic acid, dichloromethane, triisopropylsilane, water). The membranes were washed extensively with dichloromethane, N-methylpyrrolidone, and ethanol, then air-dried and stored at -20°C until use.

For the peptide and alanine substitution scan, the corresponding membrane was rinsed in methanol, washed with Tris-buffered saline (TBS), and blocked for 2 h in 2% milk/TBS at RT. For GST and antibody background analysis, the membrane was incubated overnight with 1.6 µg/ml GST in 2% milk/TBS at 4°C. The membrane was washed with TBS-T (TBS with 0.05% Tween 20), incubated with an anti-GST antibody in 2% milk/TBS for 4 h at RT, washed with TBS-T, and incubated with horseradish peroxidase-conjugated secondary antibody in 2% milk/TBS for 2 h at RT. Following detection of bound GST and/or GST-specific antibody background signals using a chemiluminescence technique (ECL Plus, GE Healthcare), the entire procedure was repeated on the same membrane, but using 2 µg/ml GST-SPCN-SH3 instead.

9. Endothelial Permeability Assays

For calcium switch experiments, ECV304 cells were seeded at a density of 7.5×10^4 cells/cm² onto PET filters (Becton Dickinson) and transfected with cDNA coding for CI-VSV or CI-VSV-SH3 36 h afterwards. Equal expression of both proteins was confirmed by Western blot analyses and indirect immunofluorescence microscopy. 14 h later, cells were washed with PBS and maintained in phenol red-free DMEM medium (containing 10% FBS and 1.8 mM calcium) for 1 h before FITC-albumin (Sigma) to a final concentration of 4 mg/ml was added to the upper chambers. Following 2 h of pre-incubation, switch to low calcium was performed by supplementing the medium with EGTA to a final concentration of 4 mM in both the apical and the basal chambers (Citi, 1992). 100 μ l aliquots were collected from the lower chambers and assayed by absorbance at 492 nm (Tecan Spectra Rainbow). After subtracting the background absorbance of the medium alone, values without EGTA stimulation were used for normalization and set at 100%.

Calcium switch experiments with confluent EC-VASP^{+/+} and EC-VASP^{-/-} cells were done accordingly.

10. Skin Vascular Leakage Assay

Generation of VASP-deficient mice used in this study has been reported previously (Hauser et al., 1999). Animals were backcrossed for more than 8 generations to C57BL/6J background and their wild-type littermates were used as controls. All experiments and animal care were approved by the Regierung of Unterfranken.

Five- to seven-week-old male mice were employed for the leakage models. Mice were anesthetized with a single i.p. injection of ketamine/xylazine (80 mg/kg ketamine and 10 mg/kg xylazine), and a total of 200 μ l of sterile-filtered 0.25% Evans blue dissolved in sterile saline (0.9% NaCl) was injected intra venously in the retroorbital plexus. 10 min later, 50 μ l of bradykinin (Sigma, 100 μ M) or saline was injected intradermally in the dorsal region by using a tuberculin syringe. The animals were killed 10 min after the intradermal injections by

decapitation. The skin was removed, mounted, and photographed. Skin samples were removed by using a circular template, and the Evans blue dye was extracted by incubating them in *N,N*-dimethyl formamide overnight at 55°C. The following day, the Evans blue fluorescence from individual skin samples was measured at an excitation of 620 nm and an emission of 680 nm. The concentration of Evans blue was normalized by dividing with the value corresponding to skin samples injected with saline.

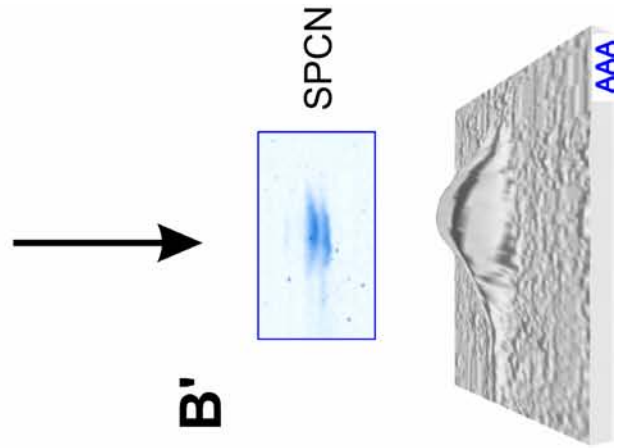
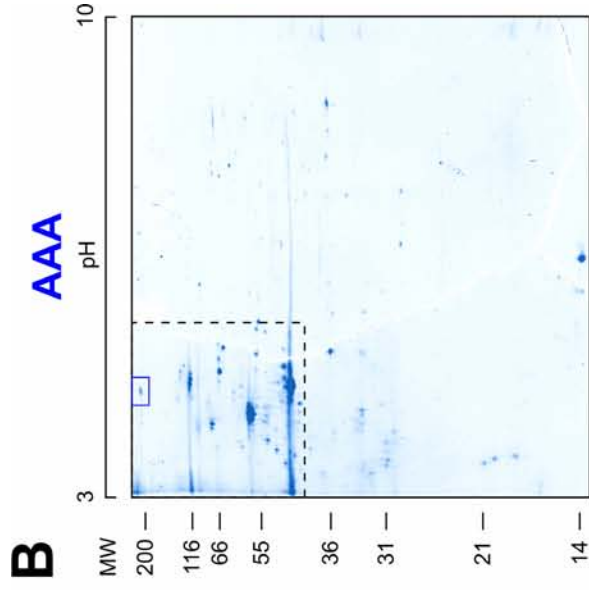
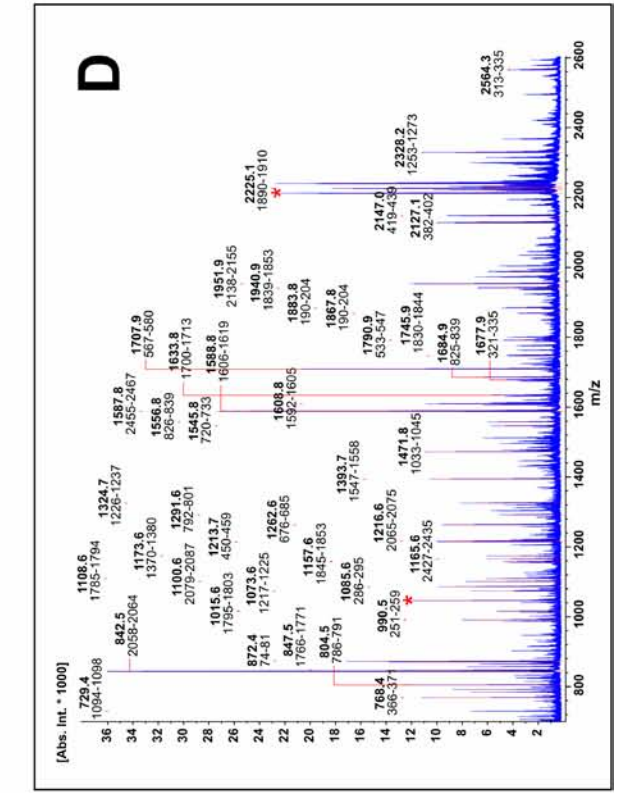
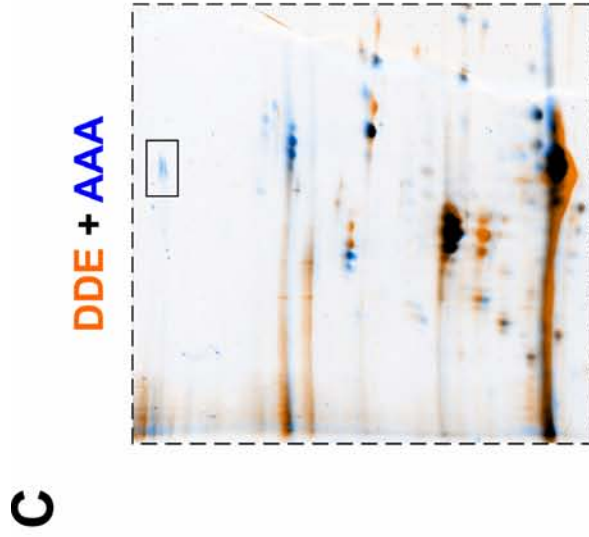
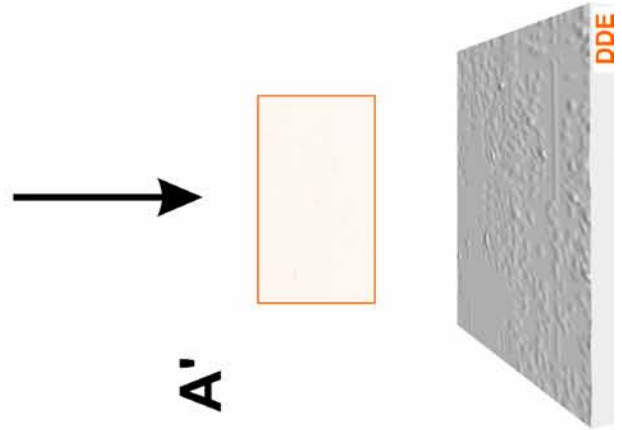
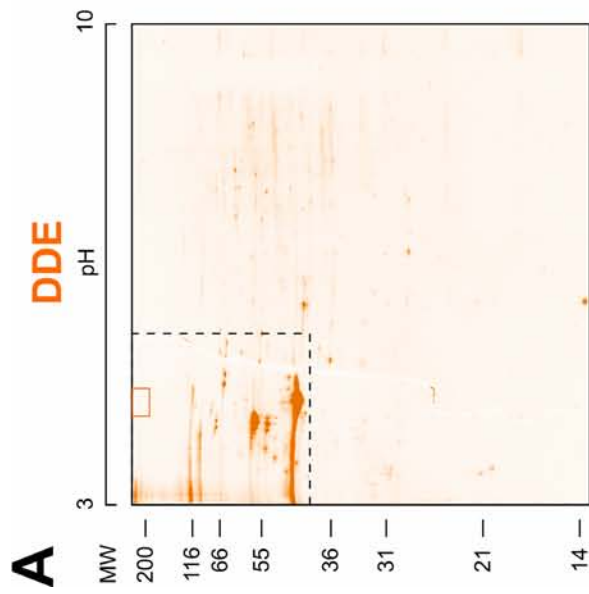
III RESULTS

1. α I-Spectrin (SPCN) is a New VASP-Binding Protein in Endothelial Cells

VASP is phosphorylated by PKA, PKG, and AMPK at residues S157, S239, and T278, respectively. We used differential proteomics to identify endothelial proteins that bind to VASP dependent on its phosphorylation status. VASP pseudophosphorylation mutants VASP-DDE and VASP-AAA (which mimic the completely phosphorylated or unphosphorylated protein, respectively) were cloned, recombinantly expressed in *E.coli*, purified, and covalently linked to an affinity chromatography matrix. To isolate VASP-DDE- or VASP-AAA-binding proteins by affinity chromatography, cytosolic proteins from confluent human EA.hy926 endothelial cells (Edgell et al., 1983) were prepared and applied to columns with immobilized VASP mutants. Specifically bound proteins were eluted by a stepwise pH-gradient. We probed the eluates for established VASP interacting proteins and detected zyxin (Reinhard et al., 1995b) and vinculin (Reinhard et al., 1996) in the pH 2 fraction by Western blotting. Proteins of this fraction were further analyzed using two-dimensional polyacrylamide gel electrophoresis (2D-PAGE). Colloidal coomassie blue staining detected >100 VASP-binding proteins in the eluates of VASP-DDE and VASP-AAA columns, respectively. The majority of spots was identical in both 2D gels, suggesting that these proteins bound to VASP independently of its phosphorylation state (representative 2D gels from n = 6, Figure III-1; compare A, B, and the merged image C). A protein spot with apparent MW of >200 kDa was found in eluates from VASP-AAA but not from VASP-DDE columns (Figure III-1A' and B'). Using matrix-assisted laser desorption ionization time-of-flight (MALDI-TOF) peptide mass finger printing (PMF), we identified the protein as α I-spectrin (SPCN, mascot score of 257, NCBI sequence identification number gi|31565122, Figure III-1D). In some experiments the α I-spectrin spot migrated as a doublet, probably due to limited separation capacity of high molecular proteins in the gel system. The calculated pI of 5.2 and MW of 240 kDa of SPCN is consistent with the observed migration behavior in the 2D gel.

Figure III-1. α II-Spectrin (SPCN) is a New VASP-Binding Protein in Endothelial Cells (see next page)

Proteins that bind to VASP dependent on its phosphorylation status were isolated from cytosolic fractions of EA.hy926 endothelial cells by affinity chromatography columns with coupled VASP-DDE (orange) or -AAA (blue). Eluted proteins were separated by 2D-PAGE and stained with colloidal coomassie G-250 (A, B). (C) Merged and magnified image of areas indicated by the dashed boxes in (A) and (B). Blue spots mark VASP-AAA- and orange spots mark VASP-DDE-binding proteins. Black spots (overlays of orange and blue spots) represent proteins that bind to both VASP forms. The boxed spot marks α II-spectrin (SPCN). (A', B') Magnifications of the SPCN spots in (B) and the corresponding gel area in (A) (upper panels) and three-dimensional densitograms of the spot intensities (lower panels). (D) MALDI-peptide mass fingerprint spectrum of the spot in (B') identified SPCN. Annotated peaks represent identified peptides, which are labeled with the exact mass (bold letters) and the amino acid positions of the protein. The peaks marked with asterisks represent trypsin-fragments, which originate from auto-digestion of the protease.

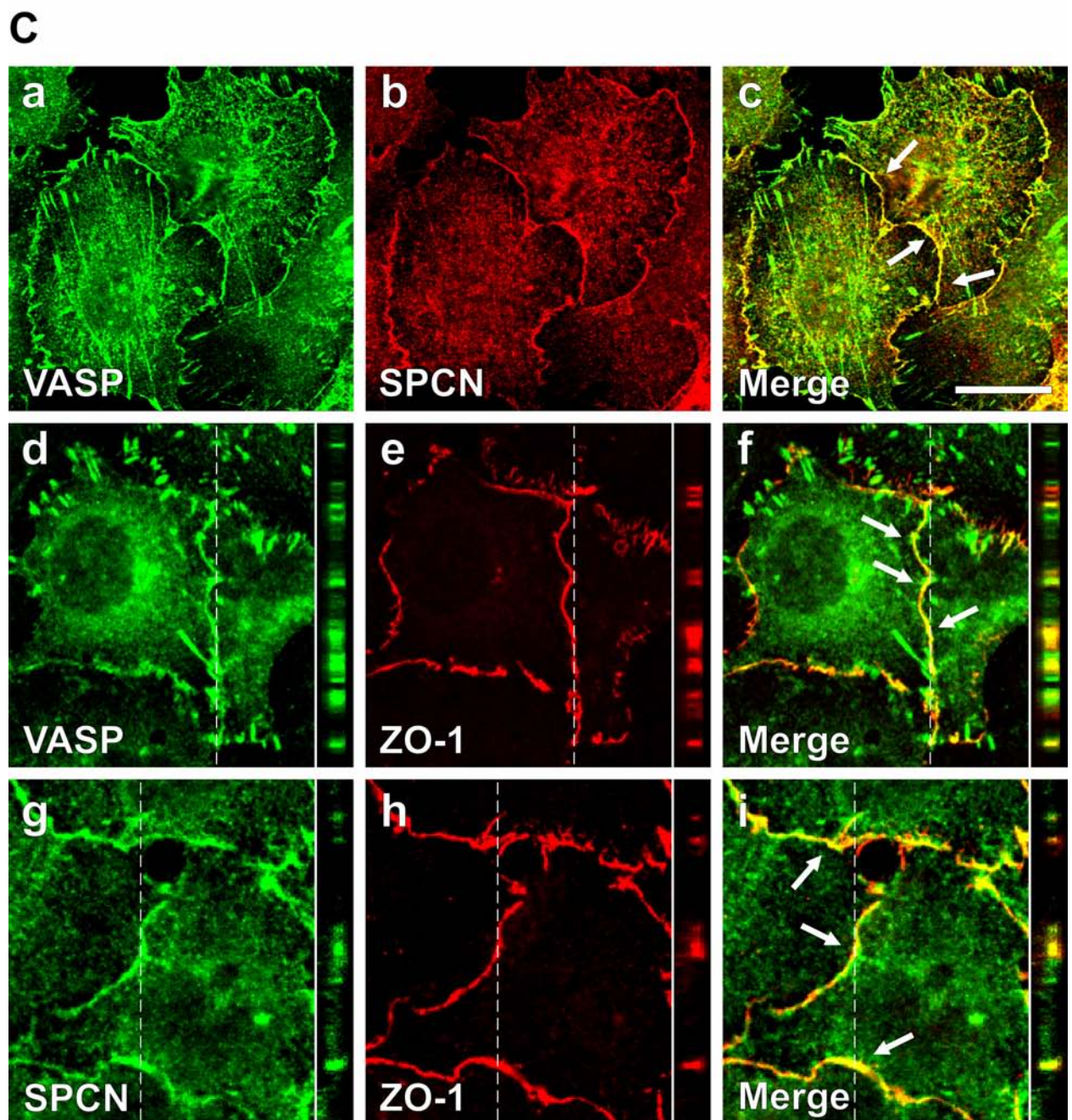
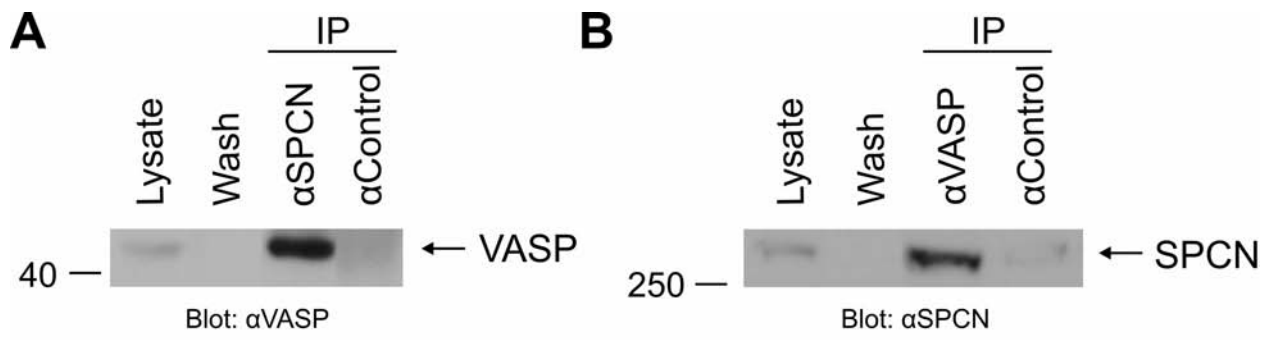


2. VASP Interacts with SPCN at Sites of Interendothelial Adhesion

To confirm the interaction of SPCN and VASP, confluent EA.hy926 endothelial cells were lysed, immunoprecipitated with antibodies against VASP, and precipitated material was probed with anti-SPCN antibodies or *vice versa*. Western blots indicated that SPCN and VASP mutually and specifically immunoprecipitated each other (Figure III-2A and B). The interaction of endogenous SPCN and VASP was further analyzed by immunofluorescence microscopy in confluent human ECV304 endothelial cells (Takahashi et al., 1990). Consistent with the subcellular localization of Ena/VASP proteins in endothelial and epithelial cell monolayers (Haffner et al., 1995; Vasioukhin and Fuchs, 2001), VASP was localized at cell-cell contacts, stress fibers, and focal adhesion sites. Notably, VASP colocalized with SPCN exclusively at cell-cell contacts but not at stress fibers or focal adhesions (Figure III-2C, panels a-c). To localize SPCN/VASP complexes in more detail, we employed confocal microscopy. In horizontal and vertical cell-sections, both VASP and SPCN colocalized with the tight junctions marker zonula occludens protein-1 (ZO-1) in its characteristic chicken wire-like staining pattern (Imamura et al., 1999) (Figure III-2C, panels d-i). SPCN and VASP colocalized at junctions in other ECs such as EA.hy926 and HUVEC (not shown). Together, these data demonstrate that VASP and SPCN interact at sites of interendothelial adhesion *in vivo*.

Figure III-2. VASP Interacts with SPCN at Sites of Interendothelial Adhesion (see next page)

(A, B) Confluent EA.hy926 cells were solubilized in lysis buffer and immunoprecipitated (IP) with antibodies against SPCN, VASP, or unrelated proteins (control). Lysate, wash fraction (Wash) and precipitated material was analyzed by Western blot with anti-VASP (A) or anti-SPCN (B) antibodies. (C) Confocal immunofluorescence images of fixed and permeabilized ECV304 cells. Cells were stained for VASP (a, d), SPCN (b, g), and the ZO-1 (e, h). The yellow color in the merged images indicates colocalized VASP and SPCN (c), VASP and ZO-1 (f), and SPCN and ZO-1 (i). Confocal immunofluorescence images were made with a 100 x objective on a Nikon Eclipse E600 microscope with a C1 laser scanning head. (d-i) 14 x 0.3- μ m sections were collected as Z-stacks. One image from the center of each stack is shown. Inserts on the right are confocal sections in the vertical plane of the Z-stacks, taken at the position of the dashed line. Arrows indicate sites of colocalization. Scale bar 15 μ m.



3. The SPCN SH3 Domain Specifically and Directly Interacts with VASP

SPCN is composed of 22 domains. Domains 1-9 and 11-21 are spectrin repeats, consisting of three α -helices, each. Domain 10 is an SH3 domain, and the C-terminal domain is a calmodulin-related domain (Bennett and Baines, 2001). Because VASP binds to the SH3 domain of Abl (Ahern-Djamali et al., 1999; Howe et al., 2002), we speculated that the SH3 domain of SPCN mediates binding to VASP. SPCN SH3 domain (SPCN_SH3, residues E970-D1025) was cloned, expressed as GST-fusion protein in *E.coli*, and employed in pull-down experiments. SPCN_SH3 (but not GST, which was used as a negative control in the same assay) precipitated VASP from cell lysates of confluent EA.hy926 and ECV304 (Figure III-3A). We immortalized endothelial cells from microvessels of VASP-null (EC-VASP^{-/-}) and isogenic wild-type mice (EC-VASP^{+/+}). A VASP signal was only detected in SPCN_SH3 precipitates from EC-VASP^{+/+}, confirming the specificity of the anti-VASP antibody (Figure III-3B). To exclude that VASP binding to SPCN_SH3 is indirect, mediated by bridging proteins in the cell lysates, we analyzed purified recombinant proteins in a cell-free system. In this setting, SPCN_SH3 specifically precipitated VASP, confirming a direct interaction of VASP with the SPCN SH3 domain (Figure III-3D, left lanes).

SH3 domains are versatile protein interaction modules, which bind to proline-rich ligands with moderate affinity and selectivity (Mayer, 2001). To analyze the specificity of VASP binding to the SH3 domain of SPCN, we compared VASP binding to SPCN-related SH3 domains. These domains were selected using the SH3-SPOT algorithm. This algorithm predicts complex formation of VASP with various SH3 domains based on a score ranging from 0 (no predicted affinity) to 1 (maximum affinity of the analyzed SH3 domain for VASP) (Brannetti et al., 2000). The N- and C-terminal SH3 domains of VAV1 (score 0.9075, 0.8375), and the SH3 domains of Abl (0.8992) and SPCN (0.8916) had the highest score for VASP binding. The interaction of VASP with the Abl SH3 domain has been confirmed previously (Howe et al., 2002). In addition to SPCN_SH3, we cloned the SH3 domains of VAV1, purified the GST-fused single domains (Figure III-3C), and analyzed them for VASP binding. In pull-down experiments, VASP

exclusively bound to the SPCN SH3 domain but not to VAV1 SH3 domains or GST alone (Figure III-3D). Taken together, our data demonstrate a specific and direct interaction of VASP with the SH3 domain of SPCN.

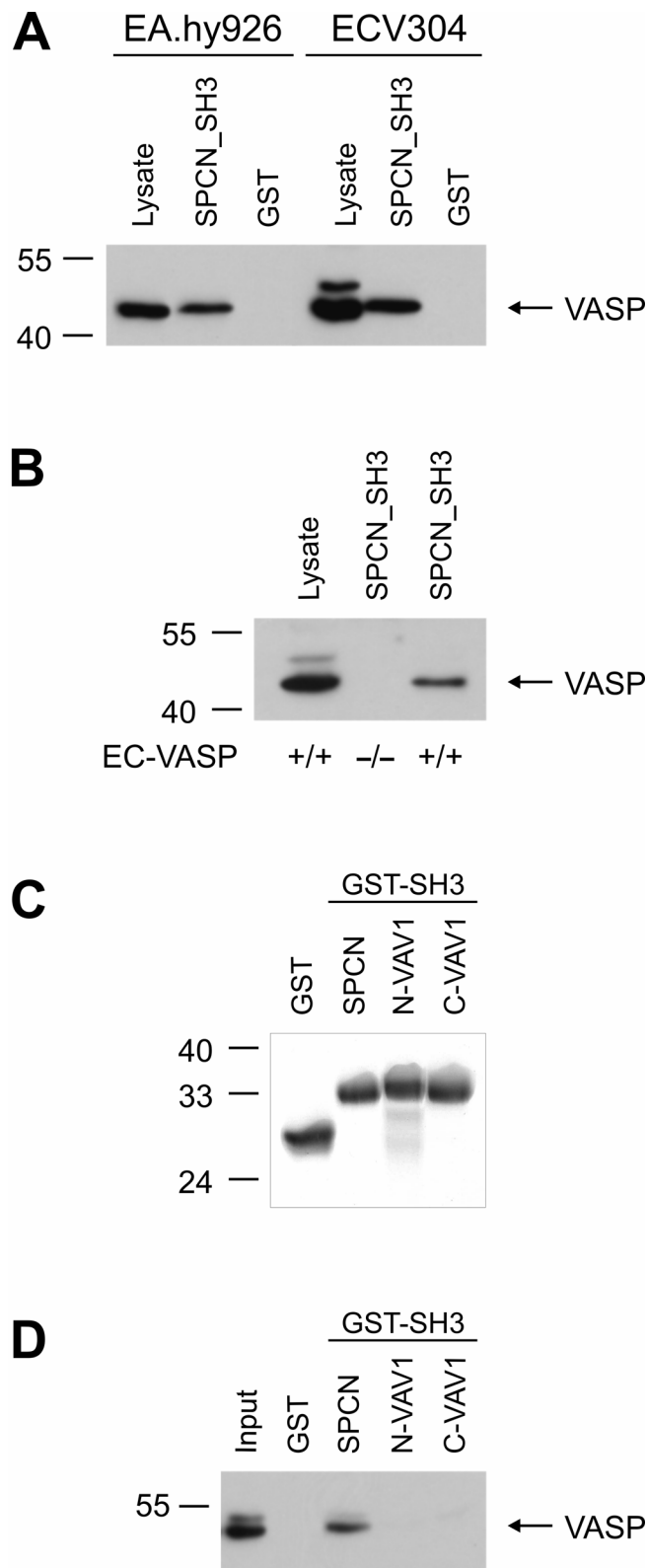


Figure III-3. The SPCN SH3 Domain Specifically and Directly Interacts with VASP

(A) Sepharose beads coated with GST-SPCN_SH3 fusion protein or GST alone were incubated with lysates from confluent EA.hy926 (left panel) or ECV304 (right panel) endothelial cells. Pulled-down proteins were separated by SDS-PAGE and probed with anti-VASP antibodies. For control, cell lysates (Lysate) were applied. (B) Lysates from wild-type (EC-VASP^{+/+}) and VASP-deficient (EC-VASP^{-/-}) murine microvascular myocardial endothelial cells, were precipitated with SPCN_SH3 and probed as in (A). (C) Coomassie-stained gel of purified SH3 domains of SPCN and VAV1 fused to GST or GST alone. (D) Sepharose beads coated with SH3 domains of SPCN and VAV1 fused to GST or GST alone were incubated with purified recombinant His₆-VASP. Precipitated protein was probed with His₆-specific antibodies in Western blots. As positive control His₆-VASP was run on the same gel (Input).

4. The SPCN SH3 Domain Binds to the Triple GP₅ Motif of VASP

To map the SPCN_SH3 binding site in VASP, two C-terminally truncated VASP mutants were generated. For Western blot detection, an N-terminal VSV-tag was added to the constructs. VSV-EVH1-PRR lacks the EVH2 domain. VSV-EVH1 is even shorter and lacks the central PRR and the EVH2 domain (Figure III-4A). The constructs were overexpressed in 293 EBNA cells and SPCN_SH3 precipitates from lysed cells were analyzed by Western blotting with anti-VSV antibodies. VSV-VASP and VSV-EVH1-PRR, but not VSV-EVH1, bound to SPCN_SH3 (Figure III-4B), suggesting that the PRR mediates the VASP/SH3 domain interaction. Although equal amounts of VSV-VASP and VSV-EVH1-PRR were employed, the amount of precipitated EVH2-truncated protein was lower (Figure III-4B), suggesting that the EVH2 domain contributes to the SPCN/VASP interaction. To identify the SPCN_SH3 binding motif in the PRR of VASP, we employed peptide scans (Figure III-4C). Overlapping, 15-amino acid-long peptides, spanning the entire VASP PRR (residues 114-224) were synthesized on a cellulose membrane and incubated with SPCN_SH3 fused to GST or with GST alone (60 nM each). Bound proteins were detected by Western blotting with an anti-GST antibody. GST did not bind non-specifically to the membrane (not shown). SPCN_SH3 interacted with peptides F2 (P¹⁶⁵PAGGPPPPPGPPPP¹⁷⁹) and, more prominently, with F8 (P¹⁷¹PPPGPPPPPGPPPP¹⁸⁵, Figure III-4C). Both peptides overlap with the VASP triple GP₅ motif (positions 169-186). Peptides E10, F3, F4, and F10, which are as proline-rich as F8, were negative for SPCN_SH3 binding, confirming the specificity of the interaction. Furthermore, peptides A1-A4, which cover the single GP₅ motif in the N-terminal portion of the PRR (G¹¹⁷PPPPP¹²²), did not bind to SPCN_SH3 (Figure III-4C). The data localize the SPCN_SH3 binding site to the VASP triple GP₅ motif and suggest that a single GP₅ motif is not sufficient to mediate VASP binding to SPCN.

5. VASP Prolines 177, 178, and 179 are Crucial for the SPCN/VASP Interaction

To pinpoint residues within the VASP triple GP₅ motif that are crucial for SPCN binding, residues in peptide F8 were systematically changed to alanine. Mutated peptides were analyzed for SPCN_SH3 binding (Figure III-4D). Substitution of the proline residues P171, P174, P182, P185, and both glycine residues G175 and G181 did not affect SPCN_SH3/VASP binding. Exchange of P172, P173, P183, and P184 by alanines moderately decreased SH3 binding to VASP. In contrast, proline residues from the central GP₅ motif (P176-P180) were critical for SH3 binding and exchange of any of the residues 177, 178, or 179 abrogated SPCN_SH3 binding (Figure III-4D). To evaluate the importance of the three prolines for SH3 binding of full-length VASP, we generated three VASP point mutation constructs (P177A, P178A, and P179A). In our pull-down experiments, P179A interaction to SH3 was weak as compared to non-mutated VASP. Substitution of P177 or P178 completely abrogated VASP interaction with the SPCN SH3 domain (Figure III-4E).

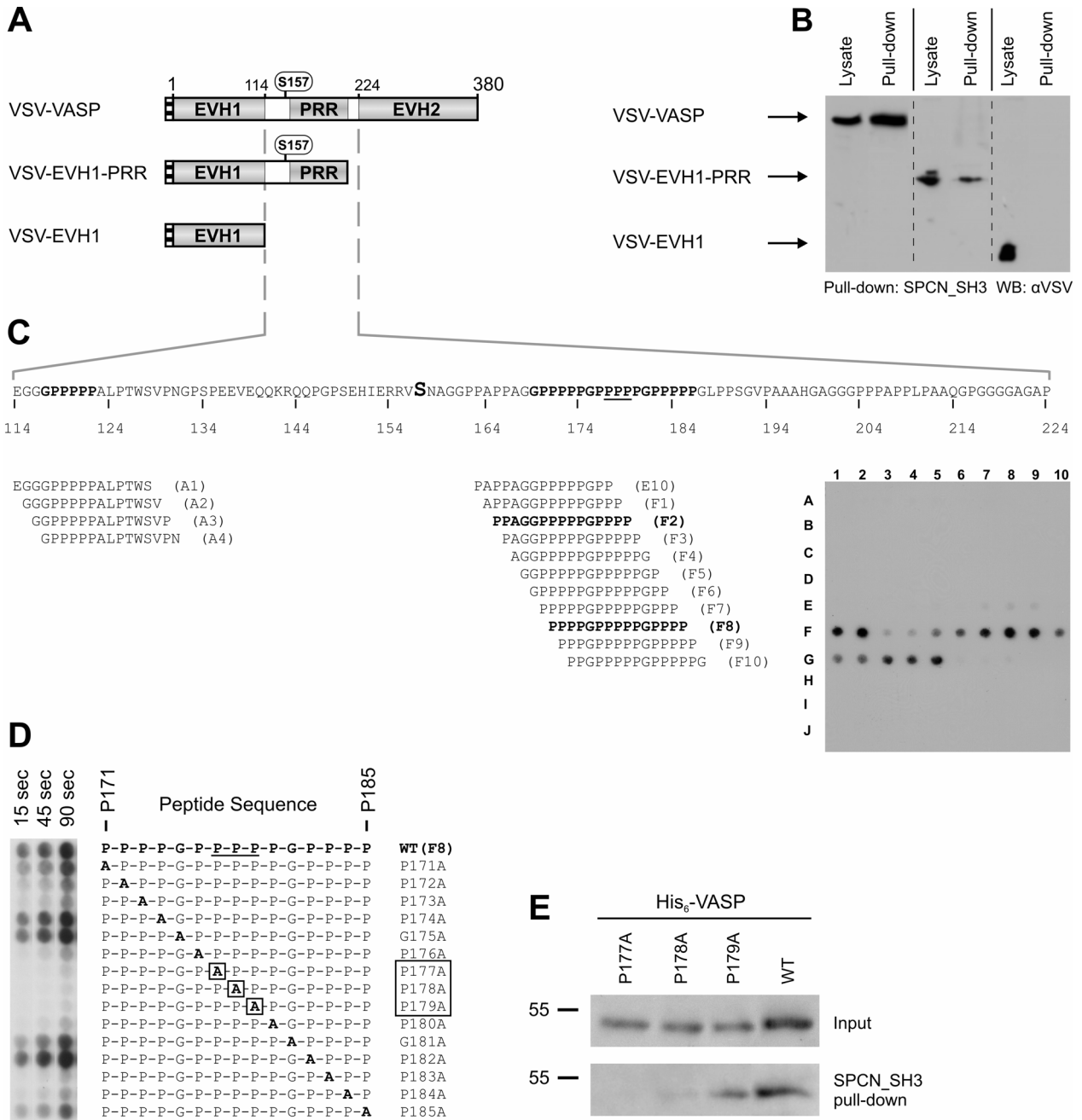


Figure III-4. The SPCN SH3 Domain Binds to the Triple GP₅ Motif of VASP

(A) Schematic representation of N-terminally VSV-tagged VASP and two C-terminally truncated VASP mutants. VSV-EVH1-PRR lacks the EVH2-domain and VSV-EVH1 lacks both the EVH2-domain and the central PRR. The PKA phosphorylation site S157 is printed in bold and highlighted in (C). (B) VSV-VASP, VSV-EVH1-PRR, and VSV-EVH1 were overexpressed in 293 EBNA cells and cell lysates were pulled-down with SPCN_SH3. Precipitated material and lysed transfected cells (Lysate, positive control) was probed with anti-VSV antibodies in Western blotting. (C) 15-mer peptides with 14 amino acid overlap, which span the VASP PRR, were synthesized in a 10 x 10 peptide spot array (lines A-J and rows 1-10) on a cellulose membrane. VASP-peptides were probed with purified recombinant SPCN_SH3 fused to GST (final concentration 60 nM) followed by Western blot detection with GST-specific antibodies. Sequences of peptides bound by SPCN_SH3 (dark spots) are shown in bold face. (D) The VASP peptide F8 (P171-P185) or mutants of this peptide, in which each residue was systematically substituted by an alanine, were synthesized on a cellulose membrane and probed with SPCN_SH3 as above. Alanine-substitution of P177-P179, underlined in peptide F8 and in (C), eliminates SPCN_SH3 binding. Film exposure times are given above each lane. (E) Sepharose beads coated with SPCN_SH3 were incubated with purified recombinant His₆-VASP (wt) or His₆-VASP mutants P177A, P178A, and P179A. Pulled-down material was analyzed by Western blotting with His₆-specific antibodies.

6. PKA-Mediated Phosphorylation of VASP at S157 Inhibits its Interaction with SPCN

SPCN bound to VASP-AAA but not to VASP-DDE (Figure III-1), suggesting that VASP phosphorylation controls the SPCN/VASP interaction. Because VASP residues P177-P179 are located in proximity to the preferred PKA phosphorylation site S157 (Figure III-4C), we analyzed the impact of S157 phosphorylation for SPCN/VASP binding. Phosphorylation of VASP at S157, but not at S239 or T278, induces an electrophoretic mobility shift of the protein from 46 to 50 kDa in SDS-PAGE (Krause et al., 2003). We incubated purified recombinant His₆-tagged VASP with active PKA *in vitro*. Anti-VASP antibodies detected the protein at 50 kDa revealing that VASP was completely S157-phosphorylated (pS157-VASP, Figure III-5A). Additionally, S157 phosphorylation was confirmed using a phosphorylation-status-specific antibody (5C6, (Blume et al., 2007), not shown). In our pull-down assay, SPCN_SH3 precipitated non-phosphorylated but not PKA-phosphorylated VASP (Figure III-5A). To investigate whether PKA-mediated VASP phosphorylation regulates SPCN/VASP interaction in cells, we treated His₆-tagged VASP-overexpressing 293 EBNA cells with Rp-8-Br-cAMPs (a PKA antagonist) or with forskolin (a PKA activator). Western blotting with 5C6 antibody indicated that PKA inhibition or activation clearly de- or increased VASP S157 phosphorylation status (not shown). Lysates from Rp-8-Br-cAMPs and forskolin treated cells were precipitated with SPCN_SH3, separated by SDS-PAGE, and probed with His₆-specific antibodies. SPCN_SH3 specifically pulled-down non-phosphorylated VASP but not the S157-phosphorylated protein (Figure III-5B). This demonstrates that PKA-mediated S157 phosphorylation impairs SPCN/VASP binding.

7. Phosphomimetic Substitution of S239 and T278 does not Influence the SPCN/VASP Interaction

To address the contribution of the two VASP phosphorylation sites S239 and T278 for the SPCN/VASP complex formation, we generated VASP pseudophosphorylation-mutants. The three phosphorylation sites are either exchanged to acidic amino acids or to alanines (mimicing

a constitutively phosphorylated or unphosphorylated residue, respectively). Figure III-5C gives a schematic representation of the five mutants VASP-DDE, -AAA, -DAA, -ADA, and -AAE. The VASP mutants allowed analyzing the effect of a negative charge at each of the three sites more specifically as compared to the protein kinase-phosphorylated protein. In addition to S157, PKA may also phosphorylate S239 and T278 (Butt et al., 1994). In pull-down experiments, SPCN_SH3 interacted with recombinant VASP-AAA, -ADA, and -AAE, but not with VASP-DDE or -DAA, demonstrating that a negative charge at position 157 abolishes SPCN/VASP binding, whereas pseudophosphorylation-state at positions 239 and 278, did not affect SPCN/VASP complex formation (Figure III-5D). This result is consistent with the observation that SPCN binds to VASP-AAA but not to VASP-DDE coupled to affinity-chromatography columns (Figure III-1) and with the loss of SPCN/VASP interaction following PKA-mediated VASP phosphorylation at S157 (Figure III-5A and B).

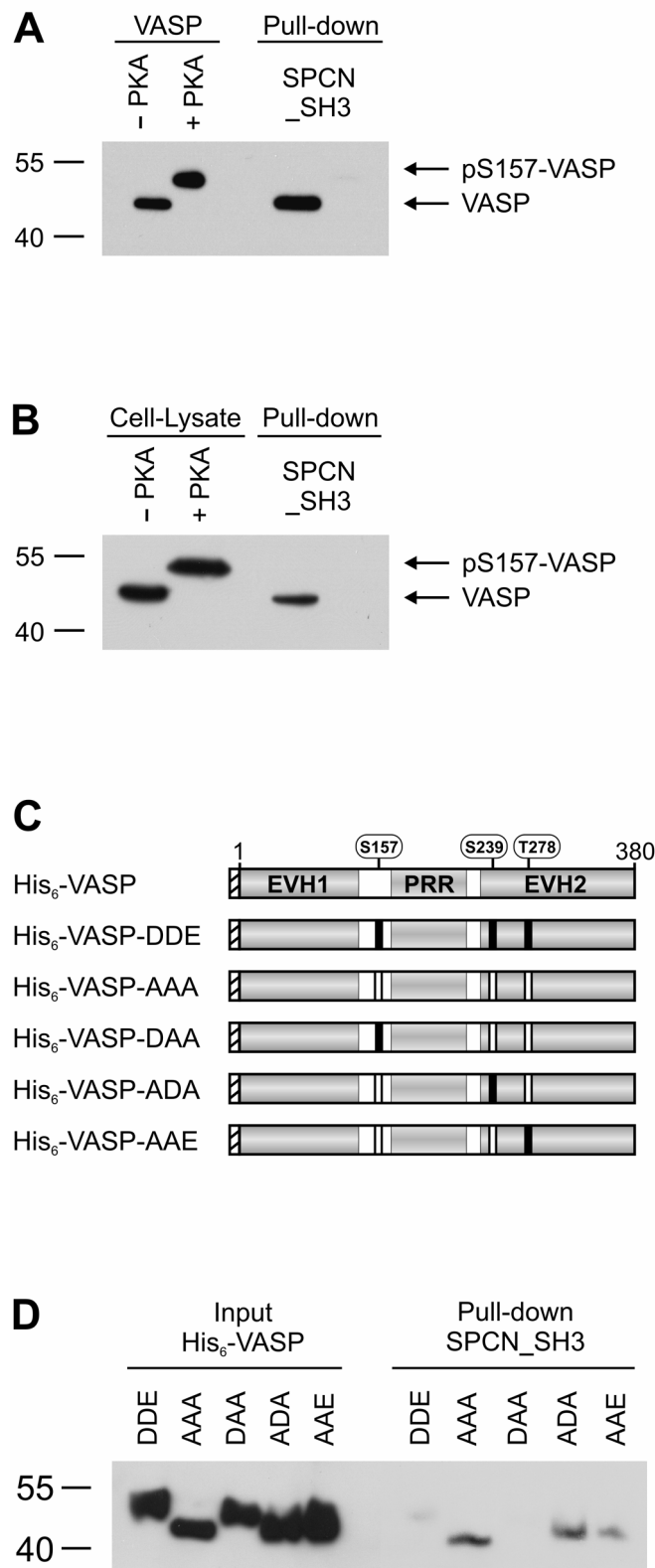


Figure III-5. PKA-Mediated Phosphorylation of VASP at S157 Inhibits its Interaction with SPCN

(A) Purified recombinant His₆-tagged VASP was S157-phosphorylated (pS157-VASP) *in vitro* by PKA (+PKA) or left untreated (–PKA) and pulled-down with immobilized SPCN_SH3. PKA-phosphorylated and non-phosphorylated VASP (VASP) and precipitated material (Pull-down) was analyzed by Western blotting with His₆-specific antibodies. (B) His₆-tagged VASP was overexpressed in 293 EBNA cells. 20 h after transfection, cells were either treated with a PKA inhibitor (Rp-8-Br-cAMPs, –PKA) or with a PKA stimulator (forskolin, +PKA). Cells were lysed, incubated with immobilized SPCN_SH3, and resulting complexes were analyzed with His₆-specific antibodies (Pull-down). For positive control, lysed cells (Cell-Lysate) was run on the same gel. (C) Schematic representation of His₆-tagged VASP and His₆-tagged mutants VASP-DDE, -AAA, -DAA, -ADA, and -AAE, mimicking different phosphorylation states of the protein. Positions of VASP phosphorylation sites S157, S239, and T278 are highlighted in the wild-type protein. In the mutants, phosphorylation sites were substituted by alanines („A“, open boxes, unphosphorylated state) or negatively-charged acidic amino acids („D“ or „E“, filled boxes, constitutively phosphorylated state). (D) Purified recombinant His₆-tagged VASP-DDE, -AAA, -DAA, -ADA, and -AAE was incubated with SPCN_SH3-coated sepharose beads and pulled-down proteins were analyzed with His₆-specific antibodies (right panel). Input shows the amount of each VASP mutant added to the immobilized SPCN SH3 domain probed with anti-His₆ antibodies. Please note that phosphorylation and phosphomimetic substitution of S157, but not S239 or T278, induces shift of VASP motility in SDS-PAGE.

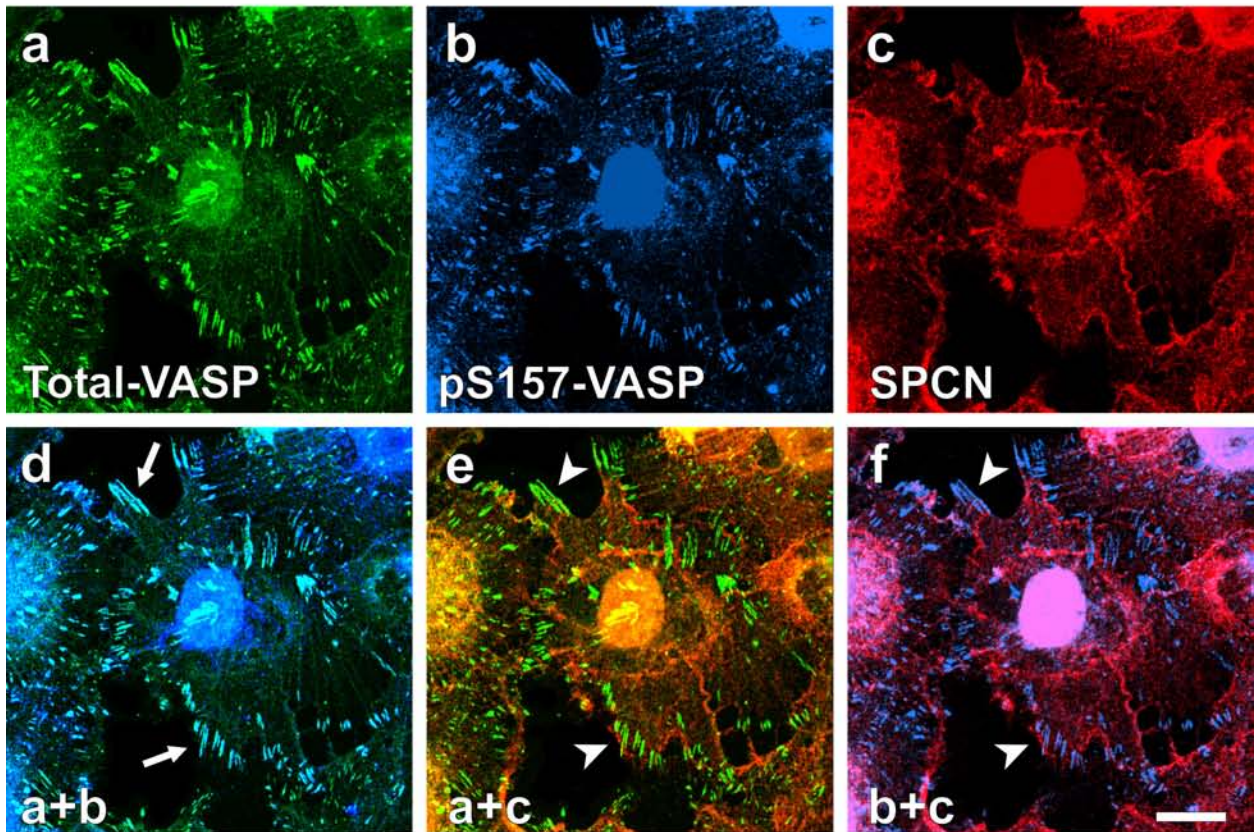
8. SPCN Colocalizes with S157 VASP but not with Phospho-S157 VASP in Contacting Endothelial Cells

To investigate the cellular function of PKA-mediated S157 phosphorylation for SPCN/VASP complex formation, we analyzed the subcellular distribution of total-VASP, S157-phosphorylated VASP (pS157-VASP), and SPCN in endothelial cells. Because pS157-VASP levels are dynamically regulated during actin-based processes (Howe et al., 2002), we analyzed the subcellular localization of the proteins dependent on cell density. We concentrated on two extremes, sparse (which are not in direct contact, Figure III-6A) and contacting cells (which form cell-cell junctions, Figure III-6B). In sparse cells, total-VASP and pS157-VASP were exclusively found at focal adhesions. Both proteins colocalized almost completely at these sites (Figure III-6A; panels a, b, and d). In contrast, SPCN was enriched at the cell periphery and did not colocalize with total-VASP (nor with pS157-VASP) (Figure III-6A; panels c, e, and f). In contacting cells, the subcellular VASP distribution was strikingly different. A portion of total-VASP was still localized at focal adhesions, but a second VASP pool at cell-cell contacts appeared (Figure III-6B, panel a). The membrane-associated VASP fraction colocalized with SPCN and was *not* S157-phosphorylated (Figure III-6B, panels a-e). In contacting cells, S157 phosphorylation was lower as compared to sparse cells. pS157 positive protein was exclusively found at focal adhesions and pS157-VASP did not colocalize with SPCN (Figure III-6B; panels b, c, and f). In confluent cells, total-VASP was completely located at cell-cell junctions and colocalized with SPCN, whereas pS157-VASP was no longer detectable (not shown).

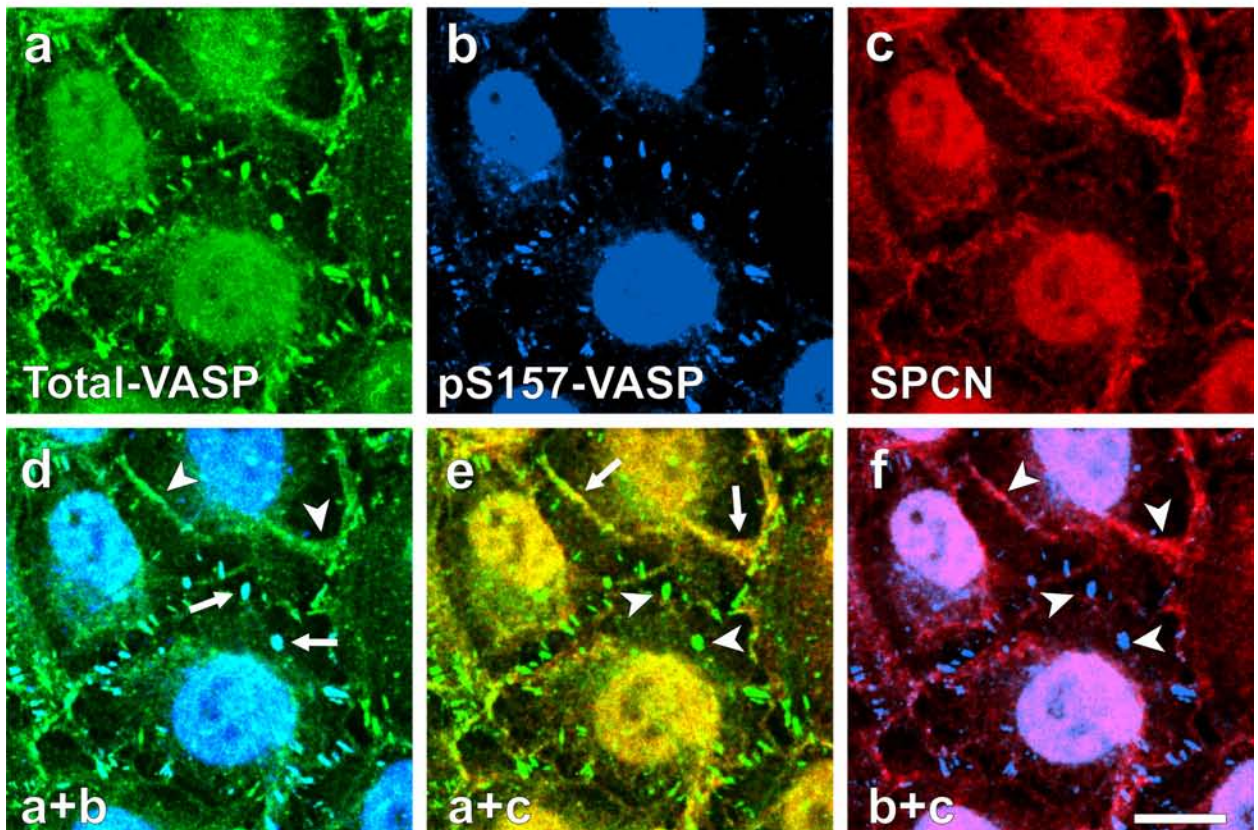
Figure III-6. SPCN Colocalizes with S157 VASP but not with Phospho-S157 VASP in Contacting Endothelial Cells (see next page)

Confocal immunofluorescence images of sparse (A) or contacting (B) ECV304 cells. Cells were fixed and stained for total-VASP (a), pS157-VASP (b), and SPCN (c). (A) In sparse cells, total-VASP and pS157-VASP pool was found at focal adhesions (d, arrows). SPCN was enriched at the cell periphery and did not colocalize with total-VASP or pS157-VASP (e and f, arrowheads). (B) In contacting cells, total-VASP was found at focal adhesions, where it colocalized with pS157-VASP, and at cell-cell contacts, where it colocalized with SPCN (d and e, compare arrows and arrowheads). pS157-VASP was exclusively seen at focal adhesions and did not colocalize with SPCN (f, arrowheads). Images were made with a 100 x objective. Arrows (arrowheads) indicate sites with (without) colocalization. Scale bars 15 μ m.

A



B



To confirm that VASP phosphorylation disappears with formation of cell-cell contacts, we quantified VASP phosphorylation by Western blotting using phosphorylation-status-specific antibodies directed to the sites S157, S239, and T278, respectively. ECV304 cells were detached, equal cell numbers seeded, and allowed to grow for various times before lysis. Consistent with high pS157 levels in detached cells (Howe et al., 2002) VASP phosphorylation at S157 was high in fresh seeded sparse cells. S157 phosphorylation level decreased time-dependently when cells grew to higher density and established cell-cell contacts. Only trace amounts of pS157-VASP were detected in confluent cells, 48 h after replating (Figure III-7A and B). In contrast, phosphorylation levels of S239 and T278 were not changed when cells grew to confluency. As control for intact PKA signaling, we stimulated confluent cells with forskolin (10 μ M, a PKA activator). Treatment largely increased S157 phosphorylation. These results demonstrate, that SPCN/VASP complexes are absent in sparse cells but form when cell-cell contacts develop. VASP S157 phosphorylation inhibits SPCN/VASP binding and disappears when cells form contacts. Taken together, these findings suggest that in response to PKA activity, SPCN/VASP interaction contributes to the formation of cell-cell junctions.

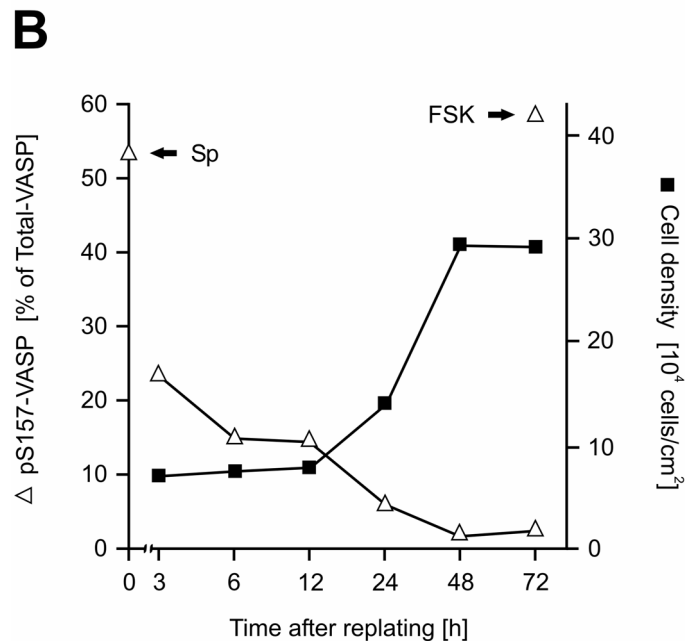
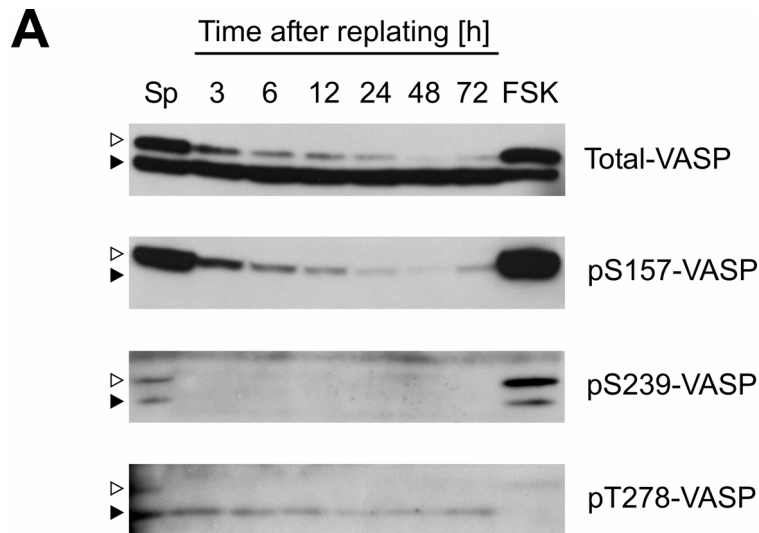


Figure III-7. VASP Phosphorylation at S157 is Inversely Correlated with the Formation of Cell-Cell Contacts

(A) Confluent ECV304 cells were detached and a constant number of cells (7.5×10^4 cells/cm²) was replated and grown for the indicated times before lysis. Western blot analyses with antibodies against total-VASP or phosphorylation-specific antibodies against pS157-, pS239-, and pT278-VASP, respectively. As control for maximal PKA stimulation, cells were either detached and incubated in suspension for 15 min (Sp) or treated with 10 μ M forskolin (FSK) 72 h after replating. Open triangles represent S157-phosphorylated VASP (apparent MW of 50 kDa), while filled triangles indicate S157 non-phosphorylated VASP form (apparent MW of 46 kDa). (B) Kinetics of VASP S157 phosphorylation levels (open triangles) dependent on density of ECV304 cells (filled squares). Magnitude of pS157-VASP (relative to the amount of total-VASP) was quantified from Western blots (in A) by densitometric scans. pS157-VASP level of suspended (Sp) or forskolin treated cells (FSK, 72 h after replating), are indicated. Representative results from four independent experiments are shown.

9. Ectopic Expression of SPCN_SH3 Recruits VASP and Promotes Cortical Actin Formation

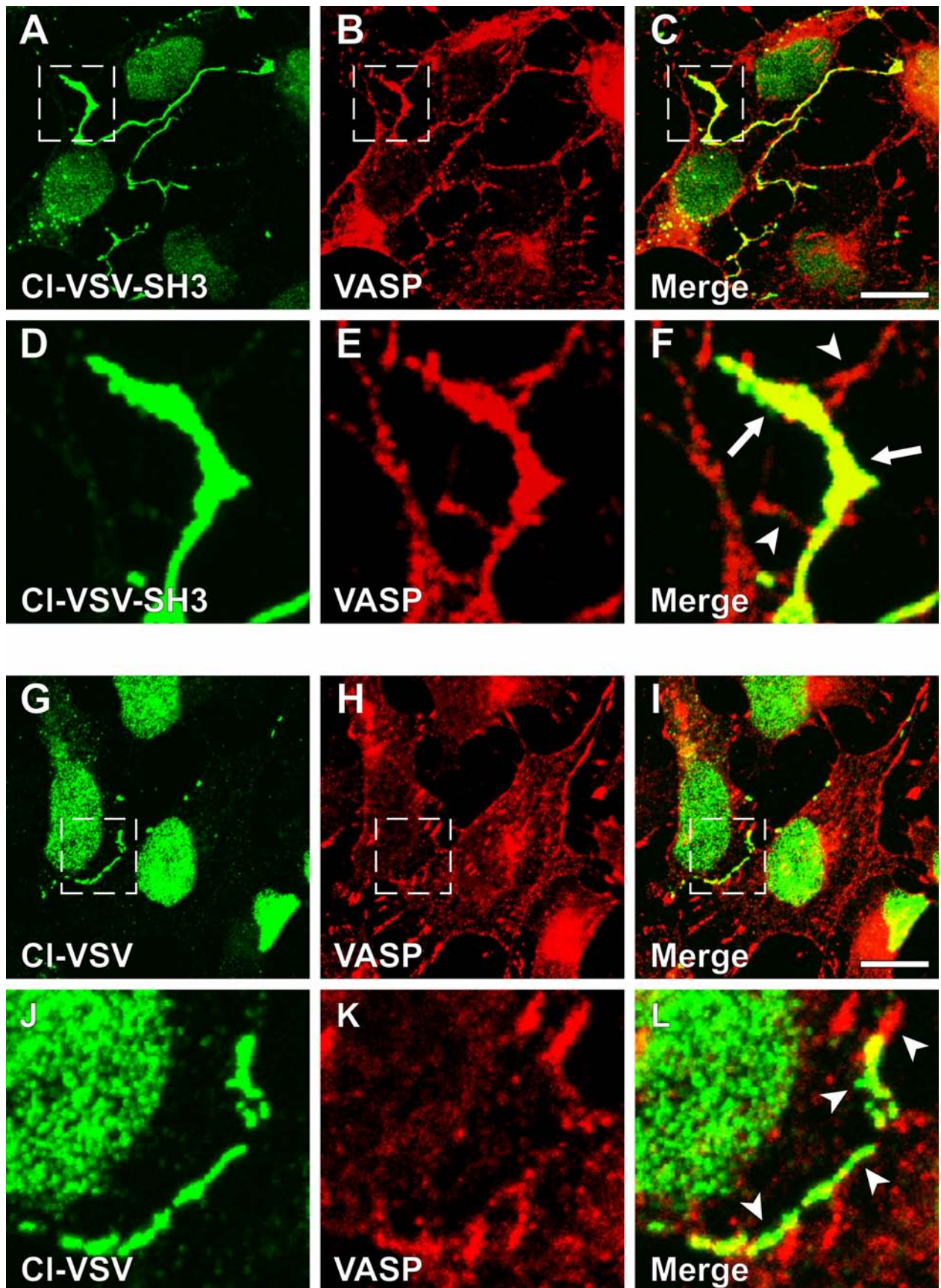
To analyze the function of the SPCN/VASP interaction for the formation of cell-cell contacts, we ectopically expressed the VASP-binding SPCN SH3 domain at endothelial junctions and investigated VASP distribution and cortical cytoskeleton formation. SPCN_SH3 was cloned to the C-terminus of claudin-5 (Cl), an integral membrane protein of tight junctions in endothelial cells (Tsukita et al., 2001), and a VSV-tag was inserted between Cl and the domain (Cl-VSV-SH3). We used a VSV-tagged Cl construct lacking SH3 as control (Cl-VSV). Expression of the constructs in ECV304 cells was confirmed by Western blotting with VSV-specific antibodies (Figure III-9A, inset). We analyzed the subcellular distribution of endogenous VASP in Cl-VSV and Cl-VSV-SH3 transfected ECV304 cells by confocal immunofluorescence microscopy. Tag-specific antibodies detected Cl-VSV-SH3 and Cl-VSV almost exclusively at the plasma membrane (Figure III-8A, D, G, and J). In Cl-VSV-SH3 expressing cells, VASP was enriched at the plasma membrane and the proteins colocalized in this compartment (Figure III-8B, C, E, and F). In contrast, VASP was not enriched at the plasma membrane of Cl-VSV expressing cells and overlap of Cl-VSV and VASP was minor (Figure III-8H, I, K, and L). Comparison of VASP localization in Cl-VSV-SH3 and Cl-VSV overexpressing cells suggests that the SPCN SH3 domain is sufficient to initiate VASP translocation (Figure III-8B and E vs. H and K). In Cl-VSV-SH3 transfected cells, VASP is taken away from stress fibers, recruited to cell-cell junctions, and colocalizes with SPCN_SH3. Notably, expression of Cl-VSV did not alter the subcellular VASP distribution as compared to mock-transfected cells (not shown).

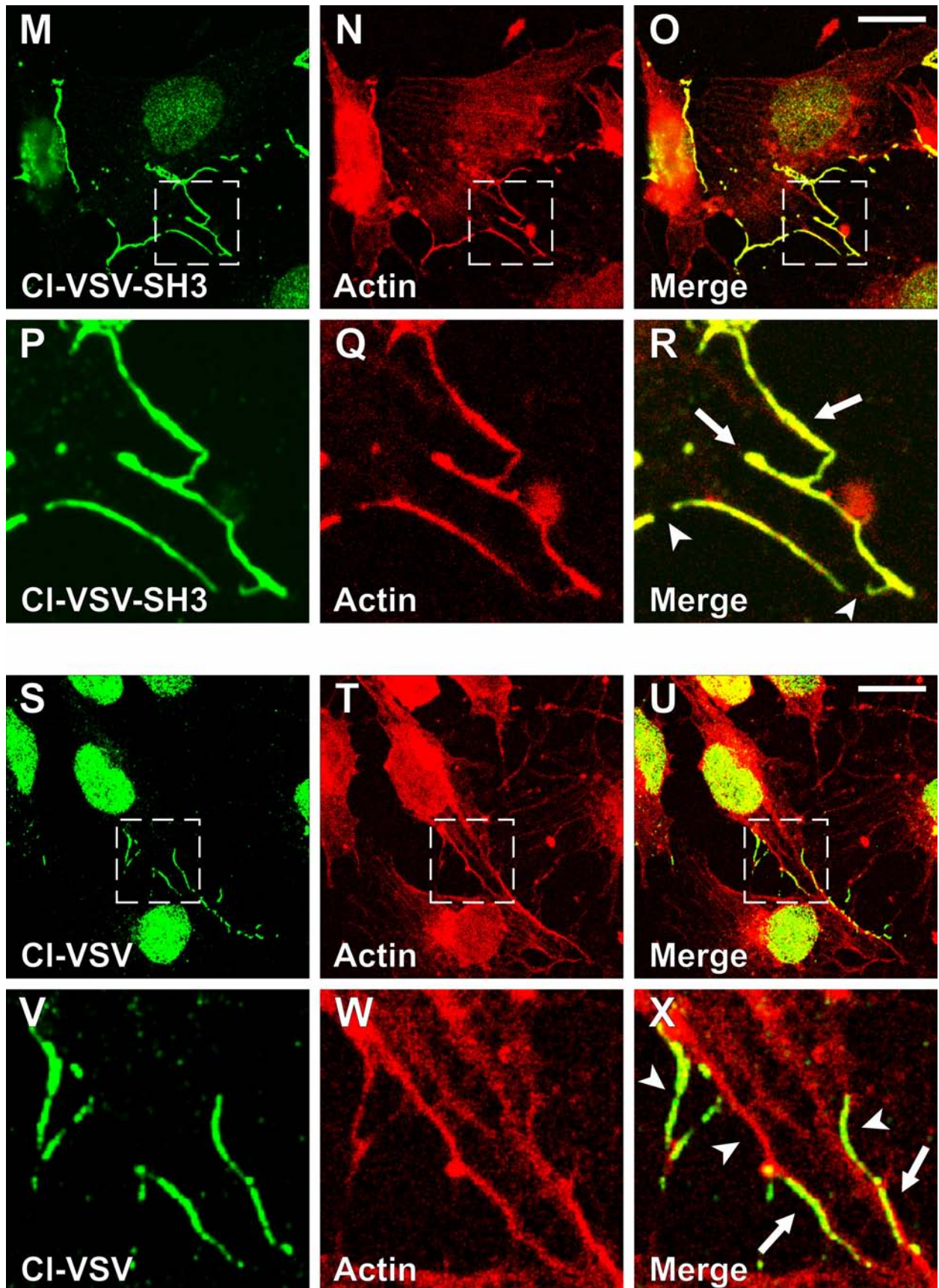
What is the consequence of SPCN/VASP complex formation for perijunctional actin filament assembly? Cl-VSV-SH3 expression substantially promoted cortical F-actin assembly, which was visualized with fluorescent phalloidine (Figure III-8N and Q). The formation of actin fibers was restricted to Cl-VSV-SH3 positive membrane sections (Figure III-8M, P, O, and R; arrows and arrowheads indicate Cl-VSV-SH3 positive or negative areas, respectively). In contrast, Cl-VSV overexpression did not initiate cortical actin cytoskeleton formation (Figure III-8S-X). These

results demonstrate that SPCN_SH3 recruits VASP to cell-cell contacts and that SPCN_SH3/VASP complexes promote cortical actin fiber formation in endothelial cells.

Figure III-8. Ectopic expression of SPCN_SH3 recruits VASP to the plasma membrane and promotes cortical actin formation (see next pages)

ECV304 cells were transfected with the SPCN SH3 domain fused to the C-terminus of VSV-tagged tight junction protein claudin-5 (Cl-VSV-SH3, A-F and M-R) or with VSV-tagged claudin-5 alone (Cl-VSV, G-L and S-X). Confocal microscopy images and overlays of overexpressing cells stained for Cl-VSV-SH3 (A, D M, and P; green), Cl-VSV (G, J, S, and V; green), VASP (B, E, H, and K; red), and actin (N, Q, T, and W; red). Images D-F, J-L, P-R, and V-X are magnified views of the indicated areas in the preceding images. 100 x objective, arrows (arrowheads) indicate sites with (without) colocalization. Scale bars 15 μ m.





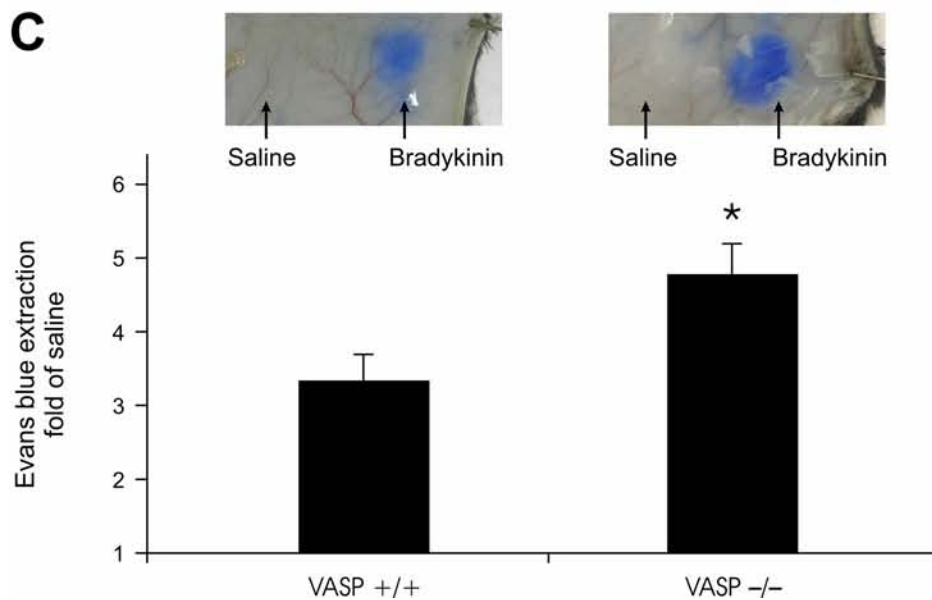
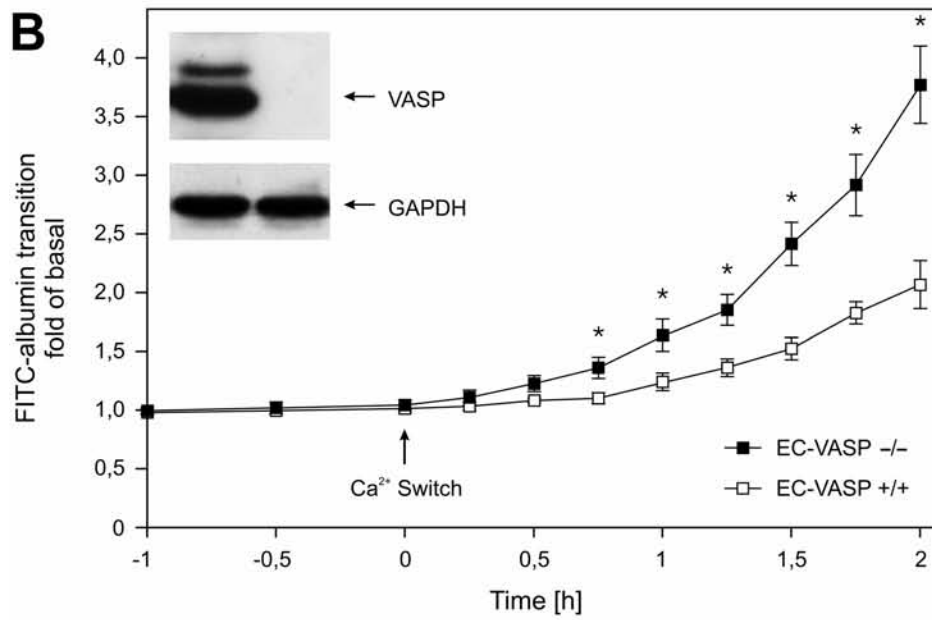
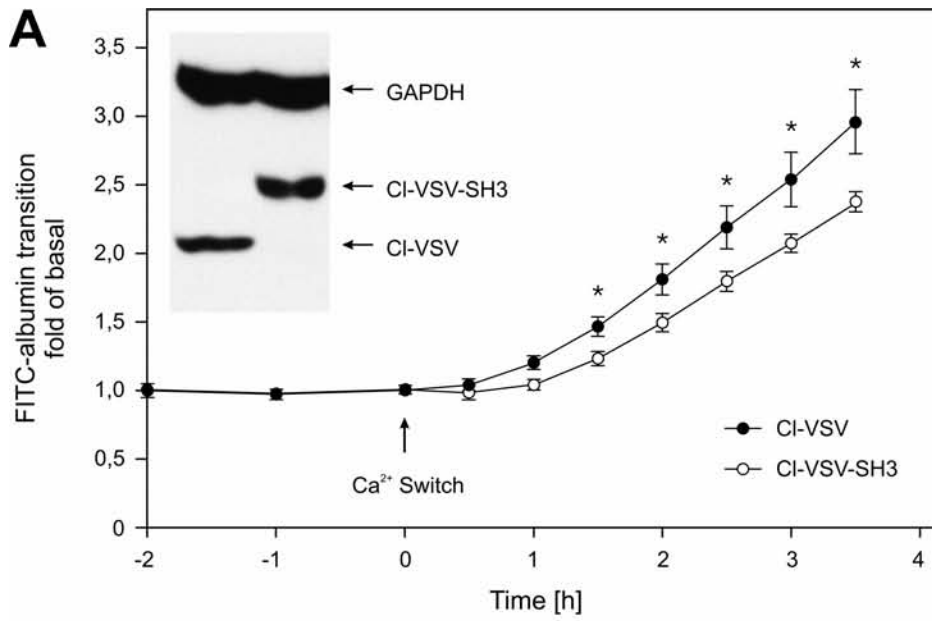
10. Function of SPCN/VASP Complexes for Endothelial Barrier Function

We investigated the function of SPCN/VASP interaction for permeability control in endothelial cells and mouse models. Stability of IEJs was analyzed in confluent cells with the calcium-switch model. In this model, complexation of extracellular calcium ions disrupts cell-cell contacts in confluent monolayers. Opening of IEJs is followed by transition of macromolecular tracers (Citi, 1992; Klingler et al., 2000). ECV304 cells were seeded on porous filters and transfected with CI-VSV-SH3 or CI-VSV (transfection rates 30-37% as determined by FACS analyses) before FITC-albumin addition to the apical chambers. Western blot analyses confirmed equal expression levels of the claudin-5 constructs (Figure III-9A, inset). Basal permeability of monolayers was recorded for 2 h. Following removal of extracellular calcium (4 mM EGTA, (Citi, 1992)) transition of fluorescent tracer into the lower chambers was determined for additional 3.5 h. FITC-albumin leakage through CI-VSV-SH3 overexpressing cell monolayers was significantly lower as compared to CI-VSV transfected cells (2.4 vs. 3.0 fold of basal, 3.5 h, $n=7$, $p<0.05$, Figure III-9A). To further analyze the function of SPCN/VASP-driven perijunctional actin formation for paracellular permeability, we employed microvascular endothelial cells from wild-type and VASP-deficient mice (EC-VASP^{+/+} and EC-VASP^{-/-}, respectively; Figure III-9B, inset). In the calcium-switch assay, permeability was significantly higher in EC-VASP^{-/-} as compared to EC-VASP^{+/+} (3.8 vs. 2.1 fold of basal, 2 h, $n=7$, $p<0.05$, Figure III-9B), suggesting that VASP deficiency interferes with the stability of IEJs. To test this hypothesis in whole animals, we analyzed VASP-null mice in a skin vascular leakage model. Edema formation was induced by subdermal application of the inflammatory mediator bradykinin, which increases paracellular permeability in mice (Han et al., 2002). Bradykinin dose-dependently initiated extravasation of Evans blue (10 nM - 5 mM tested in VASP^{-/-} and wild-type mice, not shown). Tracer measurements revealed that bradykinin-induced (100 μ M) vascular leakage was significantly increased in VASP^{-/-} over wild-type mice (4.8 vs. 3.3 fold of saline, $n=5$, $p<0.05$, Figure III-9C). Similarly, histamine-induced edema formation was increased in VASP-null mice over wild-type

animals (not shown). Together, the data suggest that SPCN/VASP complexes stabilize endothelial cell-cell contacts with implication for vascular barrier integrity.

Figure III-9. SPCN/VASP complexes seal endothelial cell-cell contacts and reduce vascular leakage (see next page)

Permeability of CI-VSV (filled circles) or CI-VSV-SH3 (open circles) overexpressing confluent ECV304 cells (A), or microvascular endothelial cells from VASP-deficient (EC-VASP^{-/-}, filled squares) or wild-type mice (EC-VASP^{+/+}, open squares) (B) was analyzed in the calcium switch model. Flux of FITC-albumin tracer into the basal chambers was measured before and after removal of extracellular calcium. Arrows indicate application of 4 mM EGTA. Means and SE are given (n=7, *p<0.05) relative to basal leakage. Insets: (A) Western blot of lysed CI-VSV or CI-VSV-SH3 transfected cells, probed with anti-VSV tag antibodies. (B) EC-VASP^{-/-} or EC-VASP^{+/+} cells analyzed with anti-VASP antibodies. Glyceraldehyde-3-phosphate dehydrogenase (GAPDH) served as loading control in the immunoprint analyses. (C) Comparison of bradykinin-induced vascular leakage in VASP-deficient and wild-type mice skin. Mice were anesthetized and injected with 0.2 ml of 0.25% Evans blue in retroorbital veins. Ten minutes after injection, bradykinin (100 μM) or saline (50 μl, each) was injected intradermally in the skin. Mice were killed 10 min later, and the skin was removed, turned over, mounted and photographed. For quantification, Evans blue was extracted from the tissues and quantified photometrically. Values are blotted relative to saline injection (n=5, *p<0.05).



IV DISCUSSION

The endothelial lining of the vessel wall acts as a permeable filter, which allows selective transition of water, solutes, macromolecules, and cells from the luminal to the abluminal side of the barrier. Paracellular endothelial permeability is regulated by a complex interplay of cellular adhesive and counteradhesive forces, generated by transmembrane adhesion molecules, actin filament assembly, actinomyosin molecular motors, and integrin receptor binding to the extracellular matrix. The present study links the spectrin-based submembranous skeleton to remodeling of the actin filament network. PKA-controlled SPCN/VASP interaction is sufficient for perijunctional stress fiber formation and implicated in regulation of paracellular vascular permeability. We propose that SPCN/VASP interactions control endothelial cell-cell adhesion by modulating cortical actin turnover in response to cAMP levels.

1. Spectrin/VASP Assemble Perijunctional Multi-Protein Complexes

Originally, VASP was identified in platelets and VASP activity participates in a variety of actin-based processes such as adhesion or spreading in these cells. Subsequently, the importance of VASP driven actin assembly was established in other cell lines including leucocytes (Lawrence and Pryzwansky, 2001), fibroblasts (Bear et al., 2002), smooth muscle (Chen et al., 2004), epithelial (Lawrence et al., 2002), and endothelial cells (Smolenski et al., 2000), and *in vivo* in vessels of animal models, and in humans (reviewed in (Munzel et al., 2003)). In confluent epithelial and keratinocyte monolayers, proteins of the Ena/VASP family participate in cell-cell adhesion and formation of adhesion zippers by a mechanism that requires α -catenin (Vasioukhin et al., 2000) and cadherin (Scott et al., 2006). Ena/VASP proteins promote actin polymerization and assembly and several models of VASP-mediated F-actin control have been proposed, including the regulation of nucleation, bundling, branching, and capping (Barzik et al., 2005; Schirenbeck et al., 2006). It is the interaction with α -spectrin that may give the spacing for VASP-driven plasma membrane-associated actin filament assembly. Spectrins form a

network, which is predominantly composed of heterotetramers [in non-erythroid cells (α II/βII)₂ (Bennett and Baines, 2001)] with approximately six filaments (≈250 nm in length (Bennett et al., 1982)) joining at each intersection. The two-dimensional planar lattice offers multiple VASP binding sites with defined interspaces. Bound to SPCN, the adaptor protein VASP assembles multi-protein complexes with IEJ components. VASP and the tight junction protein ZO-1 co-immunoprecipitate from lysates of endothelial cells (Comerford et al., 2002). However, the interaction appears to be indirect (Lawrence et al., 2002). SPCN interactions with VASP (Figures III-1 - III-3) and with ZO-1 (Tsukamoto et al., 1997) could bridge the molecules. α-catenin appears to be another component of SPCN/VASP multi-protein complexes. In α-catenin-deficient keratinocytes, VASP localization to cell-cell borders is impaired, suggesting that α-catenin interacts with VASP at sites of intercellular adhesion (Vasioukhin et al., 2000). Evidence for a direct interaction of α-catenin and VASP is missing and adaptors might link the proteins. Since α-catenin directly binds to spectrins (Pradhan et al., 2001), which in turn interact with VASP (Figure III-2), lack of α-catenin/SPCN interaction in α-catenin-null cells might account for defective recruitment of VASP to cell-cell contacts. Consistently, spectrin tetramer assembly at the plasma membrane has been shown to be diminished in cells expressing an α-catenin mutant that fails to associate with the plasma membrane (Pradhan et al., 2001). Together the data argue for large complexes of junctional proteins, actin, spectrin, and VASP at cell-cell contacts as hypothesized in a recent review (Mehta and Malik, 2006) (Figure IV-1).

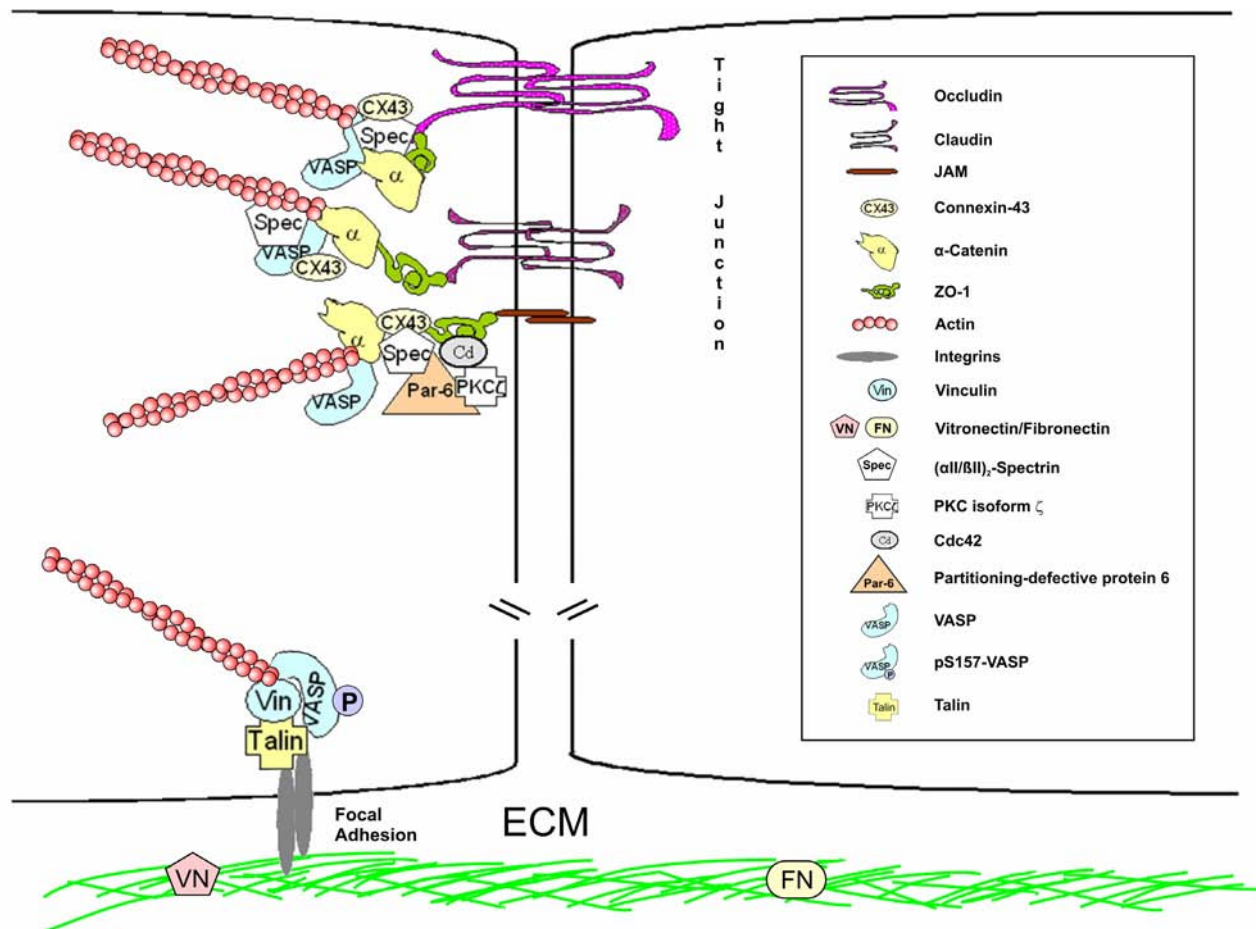


Figure IV-1. Spectrin/VASP Assembled Perijunctional Multi-Protein Complexes

Spectrin and VASP assemble multi-protein complexes at IEJs such as tight junctions (upper panel) and adherens junctions (not shown) which link transmembrane adhesion molecules to the actin cytoskeleton. Spectrin binds to VASP, α -catenin, and ZO-1, which in turn binds to the cytoplasmic domains of occludins, claudins, and JAMs. ZO-1 also binds to α -catenin and connexin-43, which facilitate communication between tight, adherens, and gap junctions. JAMs, by binding partitioning-defective protein 6, Cdc42, and the atypical PKC isoform ζ recruit these signaling molecules to tight junctions. The actin-binding protein VASP regulates distinct modes of actin organization at different subcellular compartments and VASP recruitment to these sites is balanced by PKA activity. When VASP is PKA-phosphorylated at S157 (e.g. in sparse ECs, where actin dynamics are focussed on cell adhesion and cell motility) interaction with spectrin is blocked and VASP exerts interactions that are not impaired by PKA, e.g. the EVH1-mediated interactions with vinculin, zyxin, and migfilin, which target VASP to integrin-based focal adhesions where it modulates actin-based motility. While ECs establish cell-cell junctions, VASP pS157 gradually declines and is absent in confluent cells. This allows SPCN/VASP interaction and recruits VASP to the cytoplasmic face of IEJs where it participates in the formation of a cortical actin ring. Figure modified from (Mehta and Malik, 2006).

2. SPCN SH3 Domain Mediates Interaction with VASP

One of the key findings of this study is that the spectrin SH3 domain, which is unique to α -spectrins and not found in other isoforms, specifically interacts with VASP. PKA-mediated phosphorylation controls SPCN_SH3/VASP interaction (Figure III-5). Consistently, binding of VASP and the Ena/VASP protein family member EVL to SH3 domains of Abl and Src is dependent on PKA activity (Ahern-Djamali et al., 1999; Howe et al., 2002; Lambrechts et al., 2000). Yeast two-hybrid screens indicated EVL and Tes (a tumor suppressor and actin-binding protein) interaction with SPCN SH3 domain (Rotter et al., 2005) supporting the coupling of spectrin-based membrane skeletons with proteins involved in actin dynamics. In the yeast nucleus VASP did not to bind to the bait SPCN_SH3 (Bournier et al., 2006). Because active PKA holoenzymes account for high kinase activity in the yeast nucleus (Griffioen and Thevelein, 2002), PKA could phosphorylate VASP at the preferred site S157 (Butt et al., 1994) and inhibit SPCN_SH3/VASP interaction. In contrast, other VASP domains mediate protein-protein interactions, which are not sensitive for phosphorylations such as the EVH1-driven binding to Tes, vinculin, and zyxin (Garvalov et al., 2003), PRR binding to profilin or the Lyn SH3 domain (Lambrechts et al., 2000; Reinhard et al., 1995a), or EVH2-mediated VASP homotetramerization (Harbeck et al., 2000).

Within the VASP PRR peptide scans identified sequences comprising the triple GP₅ (F2, P¹⁶⁵PAGGPPPPPGPPPP¹⁷⁹; F8, P¹⁷¹PPPGPPPPPGPPPP¹⁸⁵; Figure III-4C) as important for SPCN_SH3 binding. It is not clear, whether both peptide sequences contribute equally to SPCN/VASP complex formation or whether one harbors the preferred SH3 binding site of full-length VASP. Possibly, the two peptides together form a surface for SPCN_SH3 docking. Co-operative binding is known for other proline recognition domains (Li, 2005). SH3 domains bind to proline-rich ligands with the consensus sequence +xΦPxΦP (class I ligands) or ΦPxΦPx+ (class II ligands), where x is any, Φ a hydrophobic, and + a positively charged amino acid, respectively. Ligands adopt a left-handed polyproline type II (PPII) helix and interaction with the SH3 domain is mediated by the ΦP dipeptides and the positively charged residue, which occupy

two hydrophobic grooves or the "specificity" pocket of the SH3 domain, respectively (Kay et al., 2000; Li, 2005; Mayer, 2001). Since peptides F2 and F8 do not contain positively charged amino acid residues, SPCN_SH3 appears to belong to the atypical SH3 domains, which do not bind to classical class I or class II motifs. Atypical SH3 domains prefer ligands, in which hydrophobic residues contact the specificity pocket (Mayer, 2001). Consistently, SPCN SH3 domain was shown to interact with the peptide PPLALTAPPPA at the C-terminus of rat amiloride-sensitive epithelial Na⁺ channel alpha subunit (α ENaC), which also lacks a positively charged amino acid (Rotin et al., 1994). Furthermore, Abl SH3 domain, which binds to VASP (Howe et al., 2002), is also an atypical SH3 domain (Mayer, 2001). Using alanine substitution scans and VASP point mutants, we identified three prolines in the core of the triple GP₅ motif, which are important for the SPCN/VASP interaction (P177-P179) (Figure III-4D and E). Substitution of any of these residues abrogated the SPCN-SH3/VASP interaction. The PPII conformation is highly stable and typically resistant to single amino acid substitutions (Li, 2005). Therefore, the loss of binding seen with the point mutants is probably not resulting from a distortion of the PPII helix but from the loss of important prolines. Consistently, substitution of three consecutive prolines in the α ENaC peptide, which mediates SPCN-SH3 binding also abrogates interaction with SPCN (Rotin et al., 1994).

In addition to the PRR, VASP EVH2 domain appears to contribute to SPCN/VASP complex formation (compare VSV-VASP and VSV-EVH1-PRR binding to SPCN_SH3, Figure III-4A and B). In line, the EVH2 domain of *Drosophila* Ena participates in binding to Abl SH3 domain (Ahern-Djamali et al., 1998). Our peptide scans did not identify SH3 binding motifs within the EVH2 domain (data not shown), suggesting that EVH2 might indirectly modulate complex formation. Because EVH2 mediates VASP tetramerization, the parallel arrangement of the four VASP monomers ("bouquet-like" structure) (Kuhnel et al., 2004) could be the prerequisite for the binding of a single SPCN SH3 domain to two VASP proteins. Such a trimeric complex was previously described for the Pex13p SH3 domain, which binds two ligands at two independent binding sites (Douangamath et al., 2002). Clearly, structural analysis of SH3 domains bound to

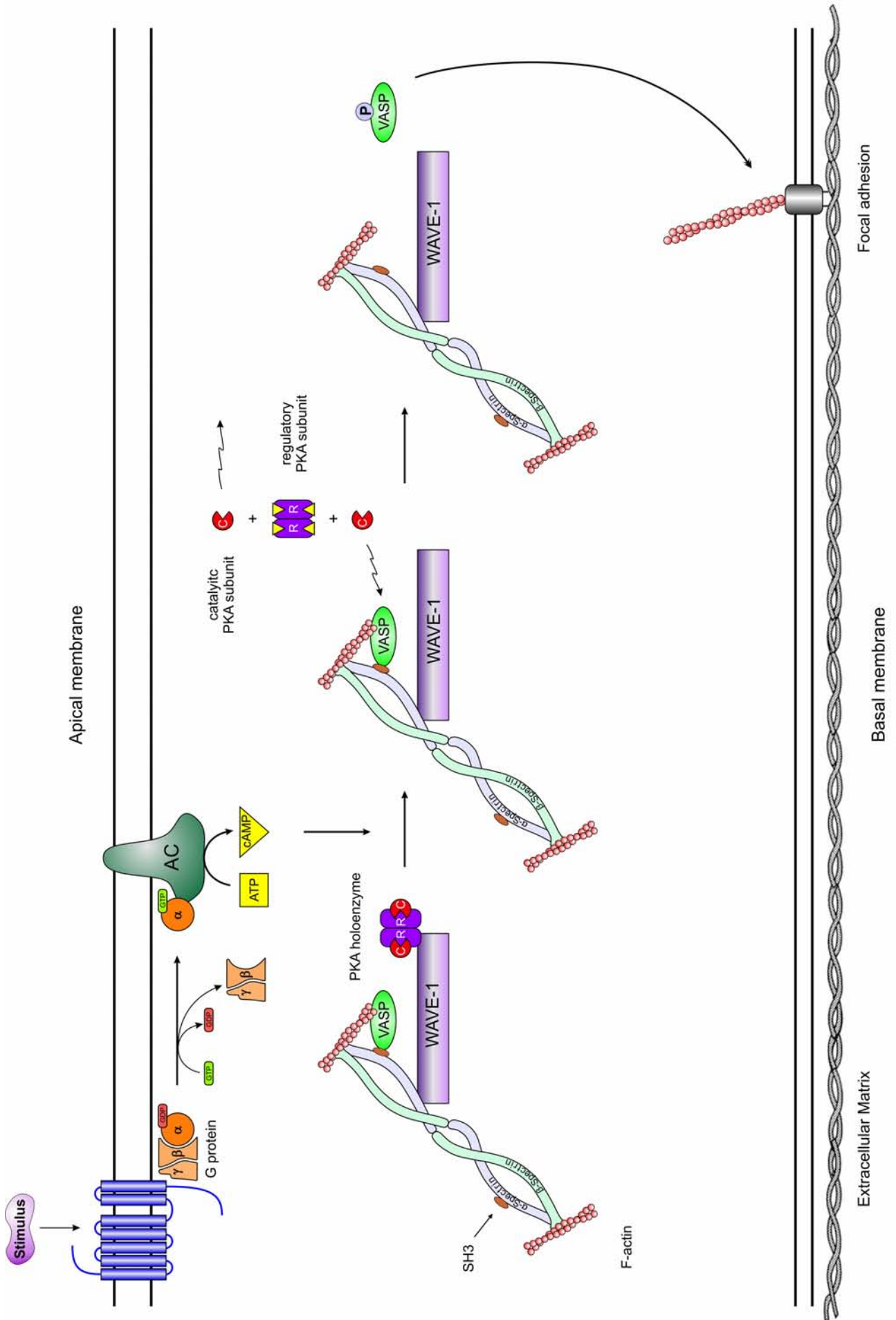
Ena/VASP proteins is a major challenge in the field.

3. Regulation and Functional Importance of SPCN/VASP Complexes

cAMP/PKA signaling is tightly controlled at several levels to maintain specificity in the multitude of signal inputs. An important regulatory mechanism in this cascade is subcellular targeting of PKA-holoenzymes through association with A-kinase-anchoring proteins (AKAPs) (Tasken and Aandahl, 2004). AKAPs participate in actin dynamics and couple signaling events to cytoskeleton turnover (Scott, 2003). WAVE-1, a member of the Wiskott-Aldrich syndrome protein (WASP) family, is an AKAP that coordinates cytoskeleton dynamics by coupling the small GTPase Rac to the actin filament nucleation activity of the Arp2/3 complex (Westphal et al., 2000). SPCN was recently identified as WAVE-1-binding protein in signaling complexes from rat brain (Scott, 2003). Together, the data suggest a multi-protein complex of WAVE-1, SPCN, VASP, and PKA. PKA-mediated VASP phosphorylation appears to be spatially regulated (Howe et al., 2005) and S157 phosphorylation could rapidly break up the SPCN/VASP interaction in response to cAMP-elevating stimuli (Figure IV-2).

Figure IV-2. PKA-mediated regulation of SPCN/VASP binding in WAVE-1 containing complexes (see next page)

In response to extracellular first messengers, cAMP-levels are elevated. cAMP binding to the regulatory PKA subunit, which is anchored to the AKAP WAVE-1, dissociates the holoenzyme, thereby liberating the catalytic PKA subunits in close proximity to the SPCN/VASP complex. PKA-mediated VASP phosphorylation at S157 abrogates SPCN/VASP binding and pS157 VASP exerts protein-protein interactions, which are insensitive to phosphorylation. E.g. binding to focal adhesion complexes via EVH1-mediated interactions with vinculin and zyxin.



Binding to SPCN is sufficient to initiate translocation of VASP from stress fibers to the cytoplasmic face of cell-cell contacts. At the plasma membrane, VASP initiates cortical actin assembly (Figure III-8). In contrast, VASP that is ectopically targeted to mitochondria surfaces does not induce F-actin assembly (Bear et al., 2000), indicating that clustering of endogenous VASP is not sufficient for actin assembly. VASP-driven actin assembly appears to be critically dependent on additional actin-modulating proteins that are present at the plasma membrane but absent on mitochondrial surfaces. Indeed, VASP that is targeted to the inner leaflet of the plasma membrane by EVH1 domain-binding motifs led to actin assembly (Bear et al., 2000; Drees et al., 2000; Lebrand et al., 2004).

Our study provides evidence that VASP regulates actin formation in defined subcellular compartments. Targeting of VASP to these sites is regulated by PKA activity. In sparse endothelial cells, VASP is PKA-phosphorylated at S157 and not bound to SPCN at the plasma membrane (Figures III-6 and III-7). S157-phosphorylated protein is enriched at focal adhesions and could interact with vinculin, zyxin, and migfilin at these sites (Drees et al., 2000; Hoffman et al., 2006; Holt et al., 1998; Zhang et al., 2006). When ECs establish cell-cell junctions, pS157 levels decrease. This is the prerequisite for SPCN/VASP complex formation and recruits VASP to IEJs (Figure III-6, III-7, IV-1, and IV-2). At the plasma membrane, VASP participates in the formation of a cortical actin ring (Mehta and Malik, 2006). The cortical actin cytoskeleton is pivotal for the integrity and stability of IEJs, which in turn is essential for proper EC barrier function (Ermer et al., 1995; Lai et al., 2005; Waschke et al., 2005). Consistently, vascular leakage (which depends on interendothelial adhesion) is increased VASP-deficient mice (Figure III-9) supporting previous observations that indicated a role of VASP for actin assembly at cell-cell contact sites in cultured endothelial cells (Comerford et al., 2002).

4. Concluding Remarks and Future Perspectives

In the present study, we have identified a new mechanism for formation of cortical actin cytoskeletons. SPCN/VASP complexes trigger perijunctional actin filament assembly and PKA-driven VASP phosphorylation at S157 inhibits this process. SPCN/VASP interactions improve cell-cell adhesion with implications for endothelial permeability and vascular leakage in mice. Therefore, our data provide a rational concept for earlier studies, which hypothesized a role of VASP in the cAMP-dependent regulation of epithelial junctional reassembly (Lawrence et al., 2002).

The SPCN SH3 domain interacts with the PRR of VASP. However, the stoichiometric composition of the complexes, the affinity constants of the binding, and the molecular mechanism, by which PKA-mediated VASP phosphorylation regulates SPCN/VASP complex formation are still unknown. To answer these questions, surface plasmon resonance and isothermal titration calorimetry experiments and structure analyses are in progress.

SPCN interacts with EVL and VASP, but an interaction with the third member of the protein family, Mena, has not been described so far and future studies should address this question. Besides it is of crucial importance to investigate, whether the interactions of EVL (and Mena) with SPCN are also sensitive to PKA phosphorylation. Interestingly, the PRR of Ena/VASP proteins is the most divergent region within the family and thus could account for differences in SPCN-binding.

Permeability of VASP-deficient endothelial cells and vascular leakage of VASP-deficient mice is elevated suggesting that SPCN/VASP complexes stabilize vascular barrier integrity. It will be interesting to see, whether this phenotype is conserved in EVL- and Mena-deficient cell lines and mice, especially because Ena/VASP proteins have been suggested to compensate for each other *in vivo*.

V SUMMARY

Directed cortical actin assembly is the driving force for intercellular adhesion. Vasodilator-stimulated phosphoprotein (VASP) participates in actin-fiber formation and VASP activity is regulated by phosphorylations. We screened for endothelial cell proteins, which bind to VASP dependent on its phosphorylation status. Differential proteomics identified α II-spectrin as novel VASP-interacting protein. α II-spectrin binds to the triple GP₅-motif in VASP via its SH3 domain. cAMP-dependent protein kinase-mediated VASP phosphorylation at Ser157 inhibits α II-spectrin/VASP complex formation. VASP becomes dephosphorylated upon formation of cell-cell contacts and in confluent but not in sparse endothelial cells α II-spectrin colocalizes with non-phosphorylated VASP at cell-cell junctions. Ectopic expression of the α II-spectrin SH3 domain fused to claudin-5 translocates VASP to cell-cell contacts and is sufficient to initiate the formation of cortical actin cytoskeletons. α II-spectrin SH3 domain overexpression stabilizes cell-cell contacts and decreases endothelial permeability. Conversely, permeability of VASP-deficient endothelial cells is elevated. In a skin edema model, microvascular leakage is increased in VASP-deficient over wild-type mice. We propose that α II-spectrin/VASP complexes regulate cortical actin cytoskeleton assembly with implications for formation of endothelial cell-cell contacts and regulation of vascular permeability.

VI ZUSAMMENFASSUNG

Der zielgerichtete Aufbau eines kortikalen Aktin-Zytoskeletts ist die treibende Kraft für die interzelluläre Adhäsion. Vasodilator-stimulated phosphoprotein (VASP) ist maßgeblich an der Bildung von Aktin-Fasern beteiligt und die VASP Aktivität wird durch seine Phosphorylierung geregelt. Wir haben in einem systematischen Ansatz nach endothelialen Proteinen gesucht, die an VASP, abhängig von seinem Phosphorylierungszustand, binden. Mit Hilfe differenzieller Massenspektrometrie konnte α II-Spectrin als neuer VASP Interaktionspartner identifiziert werden. Dabei bindet die α II-Spectrin SH3 Domäne an die drei GP₅-Motive in VASP. Die Phosphorylierung von VASP durch die cAMP-abhängige Protein Kinase hemmt die α II-Spectrin/VASP Komplexbildung. Bei der Bildung von Zell-Zell Kontakten wird VASP dephosphoryliert und in konfluenten - nicht aber in vereinzelt Endothelzellen - kolokalisieren α II-Spectrin und nicht-phosphoryliertes VASP an Zell-Zell Kontakten. Die ektopische Expression der α II-Spectrin SH3 Domäne als Fusionsprotein mit Claudin-5 führt zu einer Translokation von VASP an Zell-Zell Kontakte und ist hinreichend um die Bildung von kortikalen Aktin-Fasern einzuleiten. Funktionell stabilisiert die Überexpression der α II-Spectrin SH3 Domäne Zell-Zell Kontakte und führt zu einer Abnahme der Endothelzellpermeabilität. Dementsprechend ist die Permeabilität von VASP-defizienten Zellen erhöht. In einem Hautödem-Modell zeigt sich nach Bradykinin-Stimulation eine Erhöhung der mikrovaskuläre Permeabilität von VASP-defizienten Mäusen gegenüber wild-typ Tieren. Unsere Forschungsergebnisse legen nahe, dass α II-Spectrin/VASP Komplexe den Aufbau des kortikalen Aktin-Zytoskeletts regulieren und damit für die Bildung von endothelialen Zell-Zell Kontakten und die Regulation der vaskulären Permeabilität eine Rolle spielen.

VII ABBREVIATIONS

2D, two-dimensional; **ABP**, actin-binding protein; **AC**, adenylyl cyclase; **ADF**, actin-depolymerizing factor; **ADP**, adenosine 5`-diphosphate; **AJ**, adherens junction; **AKAP**, A-kinase anchoring protein; **AMPK**, AMP-activated protein kinase; **Arp**, actin-related protein; **ATP**, adenosine 5`-triphosphate; **BSA**, bovine serum albumin, **cAMP**, cyclic adenosine monophosphate; **CAP**, cyclase-associated protein; **Cl**, claudin-5; **CREB**, cAMP response element binding protein; **EC**, endothelial cell; **ECM**, extracellular matrix; **Ena**, Enabled; **EPAC**, guanine nucleotide-exchange proteins activated by cAMP; **EVH**, Ena/VASP homology; **EVL**, Ena-VASP-like; **FBS**, fetal bovine serum; **FITC**, fluoresceine isothiocyanate; **FSK**, forskolin; **Fyb**, Fyn-binding protein; **G-protein**, guanine nucleotide-binding protein; **GAPDH**, glyceraldehyde-3-phosphate dehydrogenase; **GPCR**, G-protein coupled receptor; **GST**, glutathione-S-transferase; **HUVEC**, human umbilical vein endothelial cells; **IEJ**, interendothelial junction; **IF**, immunofluorescence; **IP**, immunoprecipitation; **IP₃**, inositol 1,4,5-trisphosphate; **IPG**, immobilized pH gradient; **JAM**, junctional adhesion molecule; **MAD**, membrane association domain; **MALDI**, matrix-assisted laser desorption ionization; **Mena**, mammalian Ena; **PAGE**, polyacrylamide gel electrophoresis; **PDE**, phosphodiesterase; **PH**, pleckstrin homology; **PKA**, cAMP-dependent protein kinase; **PKG**, cGMP-dependent protein kinase; **PMF**, peptide mass finger printing; **PRR**, proline-rich region; **SH3**, Src homology 3; **SLAP**, SLP-76-associated protein; **SP**, suspension; **SPCN**, all-spectrin; **TJ**, tight junction; **TOF**, time-of-flight; **TRITC**, tetramethyl rhodamine iso-thiocyanate; **VASP**, vasodilator-stimulated phosphoprotein; **VSV**, vesicular stomatitis virus; **WASP**, Wiskott-Aldrich syndrome protein; **WAVE**, WASP family Verprolin-homologous protein; **WB**, western blot; **ZO-1**, zonula occludens protein-1.

VIII REFERENCES

- Adams, C.L., Chen, Y.T., Smith, S.J. and Nelson, W.J. (1998) Mechanisms of epithelial cell-cell adhesion and cell compaction revealed by high-resolution tracking of E-cadherin-green fluorescent protein. *J Cell Biol*, 142, 1105-1119.
- Ahern-Djamali, S.M., Bachmann, C., Hua, P., Reddy, S.K., Kastenmeier, A.S., Walter, U. and Hoffmann, F.M. (1999) Identification of profilin and src homology 3 domains as binding partners for Drosophila enabled. *Proc Natl Acad Sci U S A*, 96, 4977-4982.
- Ahern-Djamali, S.M., Comer, A.R., Bachmann, C., Kastenmeier, A.S., Reddy, S.K., Beckerle, M.C., Walter, U. and Hoffmann, F.M. (1998) Mutations in Drosophila enabled and rescue by human vasodilator-stimulated phosphoprotein (VASP) indicate important functional roles for Ena/VASP homology domain 1 (EVH1) and EVH2 domains. *Mol Biol Cell*, 9, 2157-2171.
- Bachmann, C., Fischer, L., Walter, U. and Reinhard, M. (1999) The EVH2 domain of the vasodilator-stimulated phosphoprotein mediates tetramerization, F-actin binding, and actin bundle formation. *J Biol Chem*, 274, 23549-23557.
- Ball, L.J., Kuhne, R., Hoffmann, B., Hafner, A., Schmieder, P., Volkmer-Engert, R., Hof, M., Wahl, M., Schneider-Mergener, J., Walter, U., Oschkinat, H. and Jarchau, T. (2000) Dual epitope recognition by the VASP EVH1 domain modulates polyproline ligand specificity and binding affinity. *EMBO J*, 19, 4903-4914.
- Barzik, M., Kotova, T.I., Higgs, H.N., Hazelwood, L., Hanein, D., Gertler, F.B. and Schafer, D.A. (2005) Ena/VASP proteins enhance actin polymerization in the presence of barbed end capping proteins. *J Biol Chem*, 280, 28653-28662.
- Bear, J.E., Loureiro, J.J., Libova, I., Fassler, R., Wehland, J. and Gertler, F.B. (2000) Negative regulation of fibroblast motility by Ena/VASP proteins. *Cell*, 101, 717-728.
- Bear, J.E., Svitkina, T.M., Krause, M., Schafer, D.A., Loureiro, J.J., Strasser, G.A., Maly, I.V., Chaga, O.Y., Cooper, J.A., Borisy, G.G. and Gertler, F.B. (2002) Antagonism between Ena/VASP proteins and actin filament capping regulates fibroblast motility. *Cell*, 109, 509-521.
- Bennett, V. and Baines, A.J. (2001) Spectrin and ankyrin-based pathways: metazoan inventions for integrating cells into tissues. *Physiol Rev*, 81, 1353-1392.
- Bennett, V., Davis, J. and Fowler, W.E. (1982) Brain spectrin, a membrane-associated protein related in structure and function to erythrocyte spectrin. *Nature*, 299, 126-131.
- Bennett, V. and Gilligan, D.M. (1993) The spectrin-based membrane skeleton and micron-scale organization of the plasma membrane. *Annu Rev Cell Biol*, 9, 27-66.
- Blume, C., Benz, P.M., Walter, U., Ha, J., Kemp, B.E. and Renne, T. (2007) AMP-activated Protein Kinase Impairs Endothelial Actin Cytoskeleton Assembly by Phosphorylating Vasodilator-stimulated Phosphoprotein. *J Biol Chem*, 282, 4601-4612.
- Bournier, O., Kroviarski, Y., Rotter, B., Nicolas, G., Lecomte, M.C. and Dhermy, D. (2006) Spectrin interacts with EVL (Enabled/vasodilator-stimulated phosphoprotein-like protein), a protein involved in actin polymerization. *Biol Cell*, 98, 279-293.

- Brannetti, B., Via, A., Cestra, G., Cesareni, G. and Helmer-Citterich, M. (2000) SH3-SPOT: an algorithm to predict preferred ligands to different members of the SH3 gene family. *J Mol Biol*, 298, 313-328.
- Butt, E., Abel, K., Krieger, M., Palm, D., Hoppe, V., Hoppe, J. and Walter, U. (1994) cAMP- and cGMP-dependent protein kinase phosphorylation sites of the focal adhesion vasodilator-stimulated phosphoprotein (VASP) in vitro and in intact human platelets. *J Biol Chem*, 269, 14509-14517.
- Chen, L., Daum, G., Chitaley, K., Coats, S.A., Bowen-Pope, D.F., Eigenthaler, M., Thumati, N.R., Walter, U. and Clowes, A.W. (2004) Vasodilator-stimulated phosphoprotein regulates proliferation and growth inhibition by nitric oxide in vascular smooth muscle cells. *Arterioscler Thromb Vasc Biol*, 24, 1403-1408.
- Citi, S. (1992) Protein kinase inhibitors prevent junction dissociation induced by low extracellular calcium in MDCK epithelial cells. *J Cell Biol*, 117, 169-178.
- Colledge, M. and Scott, J.D. (1999) AKAPs: from structure to function. *Trends Cell Biol*, 9, 216-221.
- Comerford, K.M., Lawrence, D.W., Synnestvedt, K., Levi, B.P. and Colgan, S.P. (2002) Role of vasodilator-stimulated phosphoprotein in PKA-induced changes in endothelial junctional permeability. *FASEB J*, 16, 583-585.
- De Matteis, M.A. and Morrow, J.S. (2000) Spectrin tethers and mesh in the biosynthetic pathway. *J Cell Sci*, 113 (Pt 13), 2331-2343.
- Dejana, E. (2004) Endothelial cell-cell junctions: happy together. *Nat Rev Mol Cell Biol*, 5, 261-270.
- Diviani, D. and Scott, J.D. (2001) AKAP signaling complexes at the cytoskeleton. *J Cell Sci*, 114, 1431-1437.
- Douangamath, A., Filipp, F.V., Klein, A.T., Barnett, P., Zou, P., Voorn-Brouwer, T., Vega, M.C., Mayans, O.M., Sattler, M., Distel, B. and Wilmanns, M. (2002) Topography for independent binding of alpha-helical and PPII-helical ligands to a peroxisomal SH3 domain. *Mol Cell*, 10, 1007-1017.
- Drees, B., Friederich, E., Fradelizi, J., Louvard, D., Beckerle, M.C. and Golsteyn, R.M. (2000) Characterization of the interaction between zyxin and members of the Ena/vasodilator-stimulated phosphoprotein family of proteins. *J Biol Chem*, 275, 22503-22511.
- Edgell, C.J., McDonald, C.C. and Graham, J.B. (1983) Permanent cell line expressing human factor VIII-related antigen established by hybridization. *Proc Natl Acad Sci U S A*, 80, 3734-3737.
- Ermekova, K.S., Zambrano, N., Linn, H., Minopoli, G., Gertler, F., Russo, T. and Sudol, M. (1997) The WW domain of neural protein FE65 interacts with proline-rich motifs in Mena, the mammalian homolog of Drosophila enabled. *J Biol Chem*, 272, 32869-32877.
- Ermert, L., Bruckner, H., Walmrath, D., Grimminger, F., Aktories, K., Suttorp, N., Duncker, H.R. and Seeger, W. (1995) Role of endothelial cytoskeleton in high-permeability edema due to botulinum C2 toxin in perfused rabbit lungs. *Am J Physiol*, 268, L753-761.

- Garvalov, B.K., Higgins, T.E., Sutherland, J.D., Zettl, M., Scaplehorn, N., Kocher, T., Piddini, E., Griffiths, G. and Way, M. (2003) The conformational state of Tes regulates its zyxin-dependent recruitment to focal adhesions. *J Cell Biol*, 161, 33-39.
- Gertler, F.B., Niebuhr, K., Reinhard, M., Wehland, J. and Soriano, P. (1996) Mena, a relative of VASP and *Drosophila Enabled*, is implicated in the control of microfilament dynamics. *Cell*, 87, 227-239.
- Golenhofen, N., Ness, W., Wawrousek, E.F. and Drenckhahn, D. (2002) Expression and induction of the stress protein alpha-B-crystallin in vascular endothelial cells. *Histochem Cell Biol*, 117, 203-209.
- Griffioen, G. and Thevelein, J.M. (2002) Molecular mechanisms controlling the localisation of protein kinase A. *Curr Genet*, 41, 199-207.
- Grosse, R., Copeland, J.W., Newsome, T.P., Way, M. and Treisman, R. (2003) A role for VASP in RhoA-Diaphanous signalling to actin dynamics and SRF activity. *EMBO J*, 22, 3050-3061.
- Haffner, C., Jarchau, T., Reinhard, M., Hoppe, J., Lohmann, S.M. and Walter, U. (1995) Molecular cloning, structural analysis and functional expression of the proline-rich focal adhesion and microfilament-associated protein VASP. *EMBO J*, 14, 19-27.
- Halbrugge, M., Friedrich, C., Eigenthaler, M., Schanzenbacher, P. and Walter, U. (1990) Stoichiometric and reversible phosphorylation of a 46-kDa protein in human platelets in response to cGMP- and cAMP-elevating vasodilators. *J Biol Chem*, 265, 3088-3093.
- Halbrugge, M. and Walter, U. (1989) Purification of a vasodilator-regulated phosphoprotein from human platelets. *Eur J Biochem*, 185, 41-50.
- Han, E.D., MacFarlane, R.C., Mulligan, A.N., Scafidi, J. and Davis, A.E., 3rd. (2002) Increased vascular permeability in C1 inhibitor-deficient mice mediated by the bradykinin type 2 receptor. *J Clin Invest*, 109, 1057-1063.
- Harbeck, B., Huttelmaier, S., Schluter, K., Jockusch, B.M. and Illenberger, S. (2000) Phosphorylation of the vasodilator-stimulated phosphoprotein regulates its interaction with actin. *J Biol Chem*, 275, 30817-30825.
- Hauser, W., Knobloch, K.P., Eigenthaler, M., Gambaryan, S., Krenn, V., Geiger, J., Glazova, M., Rohde, E., Horak, I., Walter, U. and Zimmer, M. (1999) Megakaryocyte hyperplasia and enhanced agonist-induced platelet activation in vasodilator-stimulated phosphoprotein knockout mice. *Proc Natl Acad Sci U S A*, 96, 8120-8125.
- Herwald, H., Dedio, J., Kellner, R., Loos, M. and Muller-Esterl, W. (1996) Isolation and characterization of the kininogen-binding protein p33 from endothelial cells. Identity with the gC1q receptor. *J Biol Chem*, 271, 13040-13047.
- Hoffman, L.M., Jensen, C.C., Kloeker, S., Wang, C.L., Yoshigi, M. and Beckerle, M.C. (2006) Genetic ablation of zyxin causes Mena/VASP mislocalization, increased motility, and deficits in actin remodeling. *J Cell Biol*, 172, 771-782.
- Holt, M.R., Critchley, D.R. and Brindle, N.P. (1998) The focal adhesion phosphoprotein, VASP. *Int J Biochem Cell Biol*, 30, 307-311.

- Horstrup, K., Jablonka, B., Honig-Liedl, P., Just, M., Kochsiek, K. and Walter, U. (1994) Phosphorylation of focal adhesion vasodilator-stimulated phosphoprotein at Ser157 in intact human platelets correlates with fibrinogen receptor inhibition. *Eur J Biochem*, 225, 21-27.
- Howe, A.K., Baldor, L.C. and Hogan, B.P. (2005) Spatial regulation of the cAMP-dependent protein kinase during chemotactic cell migration. *Proc Natl Acad Sci U S A*, 102, 14320-14325.
- Howe, A.K., Hogan, B.P. and Juliano, R.L. (2002) Regulation of vasodilator-stimulated phosphoprotein phosphorylation and interaction with Abl by protein kinase A and cell adhesion. *J Biol Chem*, 277, 38121-38126.
- Imamura, Y., Itoh, M., Maeno, Y., Tsukita, S. and Nagafuchi, A. (1999) Functional domains of alpha-catenin required for the strong state of cadherin-based cell adhesion. *J Cell Biol*, 144, 1311-1322.
- Kay, B.K., Williamson, M.P. and Sudol, M. (2000) The importance of being proline: the interaction of proline-rich motifs in signaling proteins with their cognate domains. *FASEB J*, 14, 231-241.
- Kennelly, P.J. and Krebs, E.G. (1991) Consensus sequences as substrate specificity determinants for protein kinases and protein phosphatases. *J Biol Chem*, 266, 15555-15558.
- Klingler, C., Kniesel, U., Bamforth, S.D., Wolburg, H., Engelhardt, B. and Risau, W. (2000) Disruption of epithelial tight junctions is prevented by cyclic nucleotide-dependent protein kinase inhibitors. *Histochem Cell Biol*, 113, 349-361.
- Koradi, R., Billeter, M. and Wuthrich, K. (1996) MOLMOL: a program for display and analysis of macromolecular structures. *J Mol Graph*, 14, 51-55, 29-32.
- Krause, M., Bear, J.E., Loureiro, J.J. and Gertler, F.B. (2002) The Ena/VASP enigma. *J Cell Sci*, 115, 4721-4726.
- Krause, M., Dent, E.W., Bear, J.E., Loureiro, J.J. and Gertler, F.B. (2003) Ena/VASP proteins: regulators of the actin cytoskeleton and cell migration. *Annu Rev Cell Dev Biol*, 19, 541-564.
- Kreis, T. and Vale, R. (1999) Spectrins. In *Cytoskeletal and Motor Proteins*. Oxford University Press, pp. 138-141.
- Krugmann, S., Jordens, I., Gevaert, K., Driessens, M., Vandekerckhove, J. and Hall, A. (2001) Cdc42 induces filopodia by promoting the formation of an IRSp53:Mena complex. *Curr Biol*, 11, 1645-1655.
- Kuhnel, K., Jarchau, T., Wolf, E., Schlichting, I., Walter, U., Wittinghofer, A. and Strelkov, S.V. (2004) The VASP tetramerization domain is a right-handed coiled coil based on a 15-residue repeat. *Proc Natl Acad Sci U S A*, 101, 17027-17032.
- Lai, C.H., Kuo, K.H. and Leo, J.M. (2005) Critical role of actin in modulating BBB permeability. *Brain Res Brain Res Rev*, 50, 7-13.

- Lambrechts, A., Kwiatkowski, A.V., Lanier, L.M., Bear, J.E., Vandekerckhove, J., Ampe, C. and Gertler, F.B. (2000) cAMP-dependent protein kinase phosphorylation of EVL, a Mena/VASP relative, regulates its interaction with actin and SH3 domains. *J Biol Chem*, 275, 36143-36151.
- Lawrence, D.W., Comerford, K.M. and Colgan, S.P. (2002) Role of VASP in reestablishment of epithelial tight junction assembly after Ca²⁺ switch. *Am J Physiol Cell Physiol*, 282, C1235-1245.
- Lawrence, D.W. and Pryzwansky, K.B. (2001) The vasodilator-stimulated phosphoprotein is regulated by cyclic GMP-dependent protein kinase during neutrophil spreading. *J Immunol*, 166, 5550-5556.
- Lebrand, C., Dent, E.W., Strasser, G.A., Lanier, L.M., Krause, M., Svitkina, T.M., Borisy, G.G. and Gertler, F.B. (2004) Critical role of Ena/VASP proteins for filopodia formation in neurons and in function downstream of netrin-1. *Neuron*, 42, 37-49.
- Li, S.S. (2005) Specificity and versatility of SH3 and other proline-recognition domains: structural basis and implications for cellular signal transduction. *Biochem J*, 390, 641-653.
- Loureiro, J.J., Rubinson, D.A., Bear, J.E., Baltus, G.A., Kwiatkowski, A.V. and Gertler, F.B. (2002) Critical roles of phosphorylation and actin binding motifs, but not the central proline-rich region, for Ena/vasodilator-stimulated phosphoprotein (VASP) function during cell migration. *Mol Biol Cell*, 13, 2533-2546.
- Matter, K. and Balda, M.S. (2003) Signalling to and from tight junctions. *Nat Rev Mol Cell Biol*, 4, 225-236.
- Mayer, B.J. (2001) SH3 domains: complexity in moderation. *J Cell Sci*, 114, 1253-1263.
- Mehta, D. and Malik, A.B. (2006) Signaling mechanisms regulating endothelial permeability. *Physiol Rev*, 86, 279-367.
- Munzel, T., Feil, R., Mulsch, A., Lohmann, S.M., Hofmann, F. and Walter, U. (2003) Physiology and pathophysiology of vascular signaling controlled by guanosine 3',5'-cyclic monophosphate-dependent protein kinase [corrected]. *Circulation*, 108, 2172-2183.
- Musacchio, A. (2002) How SH3 domains recognize proline. *Adv Protein Chem*, 61, 211-268.
- Musacchio, A., Noble, M., Pauptit, R., Wierenga, R. and Saraste, M. (1992) Crystal structure of a Src-homology 3 (SH3) domain. *Nature*, 359, 851-855.
- Nelson, W.J., Shore, E.M., Wang, A.Z. and Hammerton, R.W. (1990) Identification of a membrane-cytoskeletal complex containing the cell adhesion molecule uvomorulin (E-cadherin), ankyrin, and fodrin in Madin-Darby canine kidney epithelial cells. *J Cell Biol*, 110, 349-357.
- Neuhoff, V., Arold, N., Taube, D. and Ehrhardt, W. (1988) Improved staining of proteins in polyacrylamide gels including isoelectric focusing gels with clear background at nanogram sensitivity using Coomassie Brilliant Blue G-250 and R-250. *Electrophoresis*, 9, 255-262.

- Nicholson-Dykstra, S., Higgs, H.N. and Harris, E.S. (2005) Actin dynamics: growth from dendritic branches. *Curr Biol*, 15, R346-357.
- Niebuhr, K., Ebel, F., Frank, R., Reinhard, M., Domann, E., Carl, U.D., Walter, U., Gertler, F.B., Wehland, J. and Chakraborty, T. (1997) A novel proline-rich motif present in ActA of *Listeria monocytogenes* and cytoskeletal proteins is the ligand for the EVH1 domain, a protein module present in the Ena/VASP family. *EMBO J*, 16, 5433-5444.
- Pace, C.N., Vajdos, F., Fee, L., Grimsley, G. and Gray, T. (1995) How to measure and predict the molar absorption coefficient of a protein. *Protein Sci*, 4, 2411-2423.
- Pinder, J.C. and Baines, A.J. (2000) A protein accumulator. *Nature*, 406, 253-254.
- Pollard, T.D. and Borisy, G.G. (2003) Cellular motility driven by assembly and disassembly of actin filaments. *Cell*, 112, 453-465.
- Pradhan, D., Lombardo, C.R., Roe, S., Rimm, D.L. and Morrow, J.S. (2001) alpha -Catenin binds directly to spectrin and facilitates spectrin-membrane assembly in vivo. *J Biol Chem*, 276, 4175-4181.
- Profirovic, J., Gorovoy, M., Niu, J., Pavlovic, S. and Voyno-Yasenetskaya, T. (2005) A novel mechanism of G protein-dependent phosphorylation of vasodilator-stimulated phosphoprotein. *J Biol Chem*, 280, 32866-32876.
- Reinhard, M., Giehl, K., Abel, K., Haffner, C., Jarchau, T., Hoppe, V., Jockusch, B.M. and Walter, U. (1995a) The proline-rich focal adhesion and microfilament protein VASP is a ligand for profilins. *EMBO J*, 14, 1583-1589.
- Reinhard, M., Jouvenal, K., Tripier, D. and Walter, U. (1995b) Identification, purification, and characterization of a zyxin-related protein that binds the focal adhesion and microfilament protein VASP (vasodilator-stimulated phosphoprotein). *Proc Natl Acad Sci U S A*, 92, 7956-7960.
- Reinhard, M., Rudiger, M., Jockusch, B.M. and Walter, U. (1996) VASP interaction with vinculin: a recurring theme of interactions with proline-rich motifs. *FEBS Lett*, 399, 103-107.
- Renne, T., Schuh, K. and Muller-Esterl, W. (2005) Local bradykinin formation is controlled by glycosaminoglycans. *J Immunol*, 175, 3377-3385.
- Revenu, C., Athman, R., Robine, S. and Louvard, D. (2004) The co-workers of actin filaments: from cell structures to signals. *Nat Rev Mol Cell Biol*, 5, 635-646.
- Rotin, D., Bar-Sagi, D., O'Brodovich, H., Merilainen, J., Lehto, V.P., Canessa, C.M., Rossier, B.C. and Downey, G.P. (1994) An SH3 binding region in the epithelial Na⁺ channel (alpha rENaC) mediates its localization at the apical membrane. *EMBO J*, 13, 4440-4450.
- Rotter, B., Bournier, O., Nicolas, G., Dhermy, D. and Lecomte, M.C. (2005) AlphaII-spectrin interacts with Tes and EVL, two actin-binding proteins located at cell contacts. *Biochem J*, 388, 631-638.
- Rottner, K., Behrendt, B., Small, J.V. and Wehland, J. (1999) VASP dynamics during lamellipodia protrusion. *Nat Cell Biol*, 1, 321-322.

- Rousseau, S., Houle, F. and Huot, J. (2000) Integrating the VEGF signals leading to actin-based motility in vascular endothelial cells. *Trends Cardiovasc Med*, 10, 321-327.
- Schirenbeck, A., Arasada, R., Bretschneider, T., Stradal, T.E., Schleicher, M. and Faix, J. (2006) The bundling activity of vasodilator-stimulated phosphoprotein is required for filopodium formation. *Proc Natl Acad Sci U S A*, 103, 7694-7699.
- Schwartz, J.H. (2001) The many dimensions of cAMP signaling. *Proc Natl Acad Sci U S A*, 98, 13482-13484.
- Scott, J.A., Shewan, A.M., den Elzen, N.R., Loureiro, J.J., Gertler, F.B. and Yap, A.S. (2006) Ena/VASP proteins can regulate distinct modes of actin organization at cadherin-adhesive contacts. *Mol Biol Cell*, 17, 1085-1095.
- Scott, J.D. (2003) A-kinase-anchoring proteins and cytoskeletal signalling events. *Biochem Soc Trans*, 31, 87-89.
- Sechi, A.S. and Wehland, J. (2004) ENA/VASP proteins: multifunctional regulators of actin cytoskeleton dynamics. *Front Biosci*, 9, 1294-1310.
- Shaywitz, A.J. and Greenberg, M.E. (1999) CREB: a stimulus-induced transcription factor activated by a diverse array of extracellular signals. *Annu Rev Biochem*, 68, 821-861.
- Shevchenko, A., Wilm, M., Vorm, O. and Mann, M. (1996) Mass spectrometric sequencing of proteins silver-stained polyacrylamide gels. *Anal Chem*, 68, 850-858.
- Sleep, J., Wilson, D., Simmons, R. and Gratzer, W. (1999) Elasticity of the red cell membrane and its relation to hemolytic disorders: an optical tweezers study. *Biophys J*, 77, 3085-3095.
- Smolenski, A., Poller, W., Walter, U. and Lohmann, S.M. (2000) Regulation of human endothelial cell focal adhesion sites and migration by cGMP-dependent protein kinase I. *J Biol Chem*, 275, 25723-25732.
- Takahashi, K., Sawasaki, Y., Hata, J., Mukai, K. and Goto, T. (1990) Spontaneous transformation and immortalization of human endothelial cells. *In Vitro Cell Dev Biol*, 26, 265-274.
- Tang, S., Morgan, K.G., Parker, C. and Ware, J.A. (1997) Requirement for protein kinase C theta for cell cycle progression and formation of actin stress fibers and filopodia in vascular endothelial cells. *J Biol Chem*, 272, 28704-28711.
- Tasken, K. and Aandahl, E.M. (2004) Localized effects of cAMP mediated by distinct routes of protein kinase A. *Physiol Rev.*, 84, 137-167.
- Tsukamoto, T., T, T. and Nigam, S.K. (1997) Tight junction proteins form large complexes and associate with the cytoskeleton in an ATP depletion model for reversible junction assembly. *J Biol Chem.*, 272, 16133-16139.
- Tsukita, S., Furuse, M. and Itoh, M. (2001) Multifunctional strands in tight junctions. *Nat Rev Mol Cell Biol*, 2, 285-293.
- Vasioukhin, V., Bauer, C., Yin, M. and Fuchs, E. (2000) Directed actin polymerization is the driving force for epithelial cell-cell adhesion. *Cell*, 100, 209-219.

- Vasioukhin, V. and Fuchs, E. (2001) Actin dynamics and cell-cell adhesion in epithelia. *Curr Opin Cell Biol*, 13, 76-84.
- Walders-Harbeck, B., Khaitlina, S.Y., Hinssen, H., Jockusch, B.M. and Illenberger, S. (2002) The vasodilator-stimulated phosphoprotein promotes actin polymerisation through direct binding to monomeric actin. *FEBS Lett*, 529, 275-280.
- Waschke, J., Curry, F.E., Adamson, R.H. and Drenckhahn, D. (2005) Regulation of actin dynamics is critical for endothelial barrier functions. *Am J Physiol Heart Circ Physiol*, 288, H1296-1305.
- Westphal, R.S., Soderling, S.H., Alto, N.M., Langeberg, L.K. and Scott, J.D. (2000) Scar/WAVE-1, a Wiskott-Aldrich syndrome protein, assembles an actin-associated multi-kinase scaffold. *EMBO J*, 19, 4589-4600.
- Winder, S.J. and Ayscough, K.R. (2005) Actin-binding proteins. *J Cell Sci*, 118, 651-654.
- Wong, W. and Scott, J.D. (2004) AKAP signalling complexes: focal points in space and time. *Nat Rev Mol Cell Biol*, 5, 959-970.
- Yeaman, C., Grindstaff, K.K. and Nelson, W.J. (1999) New perspectives on mechanisms involved in generating epithelial cell polarity. *Physiol Rev*, 79, 73-98.
- Zhang, Y., Tu, Y., Gkretsi, V. and Wu, C. (2006) Migfilin interacts with vasodilator-stimulated phosphoprotein (VASP) and regulates VASP localization to cell-matrix adhesions and migration. *J Biol Chem*, 281, 12397-12407.

IX CURRICULUM VITAE**Personal Data**

Name B e n z, Peter Michael
Time and place of birth February 7th, 1977; Scherzingen/Switzerland
Citizenship German
Marital Status Married
Address Thüngersheimer-Str.121
97209 Veitshöchheim, Germany
Tel.: 0179-5272792, E-Mail: peterbenz@gmx.de

Schools

Sept. 1987 to July 1991 Siebold-Gymnasium, Würzburg
Sept. 1991 to June 1996 Deutschhaus-Gymnasium, Würzburg
June 1996 University-Entrance Diploma (Abitur)

Civilian Service

Oct. 1996 to Oct.1997 Civilian Service at the Bavarian Red Cross,
Würzburg

Course of Studies

Nov. 1997 to Dec. 2003 Chemistry study (Diploma), University of Würzburg
Sept. 1998 to July 2000 Research Assistant at the Fraunhofer Institut
Silicatforschung, Universität Würzburg
Apr. 2000 Intermediate Examination (Diplom-Vorprüfung)
Feb./Mar. 2001 Internship at the Bayer[®] Pharmaceutical Research
Center, Wuppertal
Oct. 2001 to Mar. 2002 Internship in the lab of Prof. Dr. Robert S. Molday,
Department of Biochemistry and Molecular Biology,
University of British Columbia,
Vancouver, BC, Canada
Oct. 2001 to Mar. 2002 Funding by the "Fonds Hochschule International" of
the Bavarian Department of Education
Jan. 2003 to Dec. 2003 Diploma Thesis in the Dept. of Biochemistry,
University Würzburg
"Identification of a novel transmembrane protein
family and characterization of a retina-specific
member, C12orf3"

Dec. 2003

Final examination (Diplomprüfung)

Since Feb. 2004

PhD Thesis at the Institute of Clinical
Biochemistry and Pathobiochemistry,
University of Würzburg
"Cytoskeleton assembly at endothelial cell-cell
contacts is regulated by α II-spectrin/VASP
complexes"